



**Fakultät für Medizin**

**II. Medizinische Klinik und Poliklinik**

# **Cell fate decisions of common dendritic cell progenitors characterized by continuous live cell imaging at the single cell level**

**Ezgi Dursun**

Vollständiger Abdruck der von der Fakultät für Medizin der Technischen Universität München zur Erlangung des akademischen Grades eines

**Doctor of Philosophy (Ph.D.)**

genehmigten Dissertation.

**Vorsitzender: Univ.-Prof. Dr. Jürgen Ruland**

**Betreuerin: apl. Prof. Dr. Anne Krug**

**Prüfer der Dissertation:**

1. **Univ.-Prof. Dr. Markus Gerhard**
2. **Univ.-Prof. Dr. Thomas Korn**

Die Dissertation wurde am 09.06.2015 bei der Fakultät für Medizin der Technischen Universität München eingereicht und durch die Fakultät für Medizin am 12.08.2015 angenommen.



*“Raise your words, not voice. It is rain that grows  
flowers, not thunder.”*

*Rumi*

## Table of Contents

<b>LIST OF TABLES .....</b>	<b>III</b>
<b>LIST OF FIGURES .....</b>	<b>IV</b>
<b>LIST OF ABBREVIATIONS.....</b>	<b>V</b>
<b>1 Introduction .....</b>	<b>1</b>
<b>1.1 Dendritic cells are mediators of innate and adaptive immunity .....</b>	<b>1</b>
1.1.1 DC subsets in lymphoid tissues .....	2
1.1.2 DC subsets in non-lymphoid tissues .....	3
1.1.3 Plasmacytoid dendritic cells .....	5
<b>1.2 Origin of dendritic cells .....</b>	<b>7</b>
<b>1.3 Dendritic cell development .....</b>	<b>9</b>
1.3.1 Transcriptional regulation of DC development .....	9
1.3.2 Role of cytokines in DC development .....	11
<b>1.4 Novel tools to define lineage relationships between DC subsets .....</b>	<b>12</b>
<b>2 Aims of the study .....</b>	<b>15</b>
<b>3 Material and Methods .....</b>	<b>16</b>
<b>3.1 Material.....</b>	<b>16</b>
3.1.1 Reagents.....	16
3.1.2 Kits .....	17
3.1.3 Enzymes .....	17
3.1.4 Antibodies .....	18
3.1.5 Media and Buffers .....	19
3.1.6 PCR Primers for genotyping .....	21
3.1.7 Mice .....	21
3.1.8 Cell lines .....	22
<b>3.2 Methods.....</b>	<b>22</b>
3.2.1 PCR genotyping of Id2 <sup>eGFP/eGFP</sup> reporter mice .....	22
3.2.2 Cell culture .....	23
3.2.3 Cell isolation from primary tissues .....	25
3.2.4 Flow Cytometry .....	25
3.2.5 Cell sorting for in vivo and in vitro experiments .....	26
3.2.6 Internalization of Siglec H and confocal microscopy.....	28
3.2.7 Cytokine ELISA protocols .....	29

3.2.8	In vivo mouse experiments .....	30
3.2.9	Time-lapse imaging and long-term antibody staining of CDP cultures .....	32
3.2.10	Single cell tracking of CDP progeny .....	33
3.2.11	Statistical analysis.....	36
<b>4</b>	<b>Results .....</b>	<b>38</b>
<b>4.1</b>	<b>Continuous observation of CDP differentiation into DCs on the single cell level</b> .....	<b>38</b>
4.1.1	Differentiation of CDPs into pDCs and cDCs is supported by co-culture with a stromal cell line derived from embryonic liver cells.....	38
4.1.2	The EL08 stromal cell line has supportive but not instructive effect on CDPs....	41
4.1.3	Analysis of individual CDP differentiation by continuous single cell tracking.....	41
4.1.4	CDP differentiation into CCR9 <sup>+</sup> pDCs and CCR9 <sup>low</sup> pDC-like cells .....	49
4.1.5	CDPs are heterogeneous and imprinted to give rise to pDCs or cDCs .....	51
4.1.6	Analysis of transcription factor Id2 expression during differentiation of individual CDPs into pDCs and cDCs .....	54
4.1.7	Internalization of recombinant antibodies .....	66
<b>4.2</b>	<b>Plasticity of CCR9<sup>+</sup> pDCs and CCR9<sup>low</sup> pDC-like precursors in inflammation... 68</b>	
4.2.1	Accumulation of CCR9 <sup>+</sup> pDCs and CCR9 <sup>low</sup> pDC-like cells in CNS under inflammatory conditions .....	70
4.2.2	B220 <sup>low</sup> CCR9 <sup>low</sup> pDC-like cells differentiate into cDCs in the inflamed CNS .....	72
<b>5</b>	<b>Discussion .....</b>	<b>77</b>
<b>5.1</b>	<b>EL08 co-culture system to study DC development .....</b>	<b>77</b>
<b>5.2</b>	<b>Graded commitment of CDPs to CCR9<sup>low</sup> pDC-like cells and to CCR9<sup>+</sup> pDCs ..</b>	<b>79</b>
<b>5.3</b>	<b>Id2-GFP mouse model to study the role of intrinsic regulators in DC development .....</b>	<b>81</b>
<b>5.4</b>	<b>In vitro live cell imaging as a tool to study cell fate decisions .....</b>	<b>82</b>
<b>5.5</b>	<b>Plasticity of pDC precursors under inflammatory conditions .....</b>	<b>84</b>
<b>6</b>	<b>Summary .....</b>	<b>87</b>
	<b>REFERENCES.....</b>	<b>89</b>
	<b>ACKNOWLEDGEMENT .....</b>	<b>98</b>
	<b>CURRICULUM VITAE .....</b>	<b>100</b>

## LIST OF TABLES

Table 1: Phenotype of murine DC subsets .....	4
Table 2: Antibodies used in this study.....	18
Table 3: PCR primers used in this study.....	21
Table 4: Mouse strains used in this study .....	21
Table 5: Cell lines used in this study .....	22
Table 6: EAE Clinical Score .....	31
Table 7: Fluorescently labelled antibodies used in time-lapse imaging experiments.....	33
Table 8: Definition of DC subsets in time-lapse imaging experiments performed with cells from C57BL/6 mice.....	43
Table 9: Definition of DC subsets in time-lapse imaging experiments performed with cells from Id2-GFP reporter mice .....	59

## LIST OF FIGURES

Fig. 1: Sorting strategy of CDPs.....	27
Fig. 2: Sorting strategy of CCR9 subsets.....	28
Fig. 3: Cell filters created for time-lapse imaging of C57BL/6 wildtype CDP cultures.....	35
Fig. 4: Cell filters created for time-lapse imaging of ID2 <sup>eGFP/eGFP</sup> CDP cultures.....	36
Fig. 5: Phenotype of DCs generated from CDPs in EL08 culture system in the presence of Flt3L .....	40
Fig. 6: Phase contrast images of sorted CDPs on stromal cells .....	42
Fig. 7: Quantitative analysis of the progeny by single cell tracking.....	43
Fig. 8: Detection of surface molecules using fluorescently labelled antibodies in living cells	44
Fig. 9: The time point of occurrence of fluorescent markers .....	46
Fig. 10: Number of generations and cell cycle times of CDP progenies .....	48
Fig. 11: Results of cell filter analysis of CDP and its progeny.....	50
Fig. 12: End point FACS analysis of CDP .....	53
Fig. 13: Id2-GFP expression in DCs .....	55
Fig. 14: Id2-GFP expression in BM derived DC subsets.....	56
Fig. 15: Id2-GFP expression in DCs derived from CDP .....	58
Fig. 16: Results of cell filter analysis of ID2-GFP CDP and its progeny.....	60
Fig. 17: Quantitative analysis of Id2 <sup>eGFP/eGFP</sup> CDP and its progeny by single cell tracking....	61
Fig. 18: Detection of surface molecules using fluorescently labelled antibodies in ID2 <sup>eGFP/eGFP</sup> CDP.....	62
Fig. 19: The time point of occurrence of fluorescent markers .....	63
Fig. 20: End point analysis of Id2 <sup>eGFP/eGFP</sup> CDP and its progeny .....	65
Fig. 21: Internalization of Siglec H antibody.....	67
Fig. 22: Outline of EAE experiment setup and FACS sorting of pDC subsets from BM .....	69
Fig. 23: The frequency of CD45.1 <sup>+</sup> infiltrates in CNS.....	70
Fig. 24: The percentage of BST2 <sup>+</sup> pDCs in CCR9 <sup>low</sup> B220 <sup>high</sup> and CCR9 <sup>high</sup> B220 <sup>high</sup> transferred groups .....	71
Fig. 25: Staining of pre-DCs and pDCs in the BM.....	72
Fig. 26: Sorting strategy of pDC subsets .....	73
Fig. 27: CNS gating exemplified in EAE induced mice .....	74
Fig. 28: Composition of CD45.1 <sup>+</sup> infiltrates in CNS.....	76

## LIST OF ABBREVIATIONS

°C	Celsius
33D1	Dendritic cell inhibitory receptor 2
ABST	2,2'-azino-bis(3-ethylbenzothiazoline-6-sulphonic acid)
AGM	Aorta-gonad-mesonephros
APC	Antigen presenting cells
Batf3	Basic leucine zipper transcription factor ATF-like 3
BBB	Brain blood barrier
BM	Bone marrow
bp	Base pair
BST2	Bone marrow stromal antigen 2
CD	Cluster of differentiation
cDC	Conventional dendritic cell
CDP	Common dendritic cell progenitor
CFA	Complete Freund's adjuvant
CLP	Common lymphoid progenitor
CMP	Common myeloid progenitor
CNS	Central nervous system
CO <sub>2</sub>	Carbondioxyde
CpG	CpG oligodeoxynucleotides
DC	Dendritic cell
DMEM	Dulbecco's Modified Eagle's Medium
DMSO	Dimethyl sulfoxide
e.g.	For example
E2-2	E-protein 2-2
EAE	Experimental autoimmune encephalomyelitis
EDTA	Ethylenediaminetetraacetic acid
ETS	E-twenty-six
FACS	Fluorescently activated cell sorting
FCS	Fetal calf serum
Flt3	FMS-like tyrosin kinase 3
Flt3L	FMS-like tyrosin kinase 3 Ligand
GFP	Green fluorescence protein
GM-CSF	Granulocyte macrophage colony stimulating factor
h	Hour



HBSS	Hank's Balanced Salt Solution
HCl	Hydrochloric acid
HI	Heat inactivated
HLH	Helix loop helix protein
HS	Horse serum
HSC	Hematopoietic stem cells
HSV	Herpes simplex virus
i.v	Intravenous
ICSBP	Interferon consensus sequence-binding protein
Id2	Inhibitor of DNA binding 2
IFN	Interferon
IFN- $\alpha$	Interferon-alpha
IFN- $\beta$	Interferon-beta
IFNAR	IFN- $\alpha/\beta$ receptor
IL	Interleukine
IRF	Interferon regulatory factor
kb	Kilobase
kbp	Kilobase pair
LC	Langerhans cell
LCMV	Lymphocytic choriomeningitis virus
Lin	Lineage
LN	Lymph nodes
M	Molar
M-CSF	Macrophage colony stimulating factor
M-CSFR	Macrophage colony stimulating factor receptor
MACS	Magnetically activated cell sorting
MCMV	Murine cytomegalovirus
MDP	Macrophage dendritic cell progenitor
MEM	Minimum Essential Medium
mg	Milligram
MHC	Major histocompatibility complex
MHV	Mouse hepatitis virus
min	Minute
mM	Millimolar
MOG	Myelin oligodendrocyte glycoprotein
n	Number of replicates

N	Normal
NaOH	Sodium hydroxide solution
NEAA	Non-essential amino acids
ng	Nanogram
NK	Natural killer cell
nm	Nanometer
P/S	Penicilin and streptomycin
PBS	Phosphate buffered saline
PCR	Polymerase chain reaction
pDC	Plasmacytoid dendritic cell
PE	Phycoerythrin
PTx	Pertussis toxin
PU.1	Spleen focus forming virus proviral integration oncogene spi1
qRT-PCR	Quantitative real time PCR
rpm	Revolutions per minute
RPMI	Roswell Park Memorial Institute Medium
s.c.	Subcutaneous
sec	Seconds
Sh-RNA	Short hairpin RNA
Siglec H	Sialic acid binding Ig-like lectin H
STAT	Signal transducer and activator of transcription
TAE	Tris-acetate-EDTA
TBST	Tris buffered saline with Tween-20
TGF- $\beta$ 1	Transforming growth factor beta 1
Th	T helper cell
TLR	Toll like receptor
TNF- $\alpha$	Tumor necrosis factor alpha
Treg	Regulatory T cell
TRIS	Tris hydroxymethyl amonmethane
v/v	Volume/volume
VSV	Vesicular stomatitis virus
w/v	Mass/volume
XBP-1	X-box binding protein 1
Zbtb46	Zinc finger and BTB domain containing 46
$\alpha$	Anti
$\mu$ g	Microgram

# 1 Introduction

Since the beginning of life there is a constant war between all living beings and a vast numbers of microbial invaders. This holds true from the simplest organism to the most complex one. As a result, even simple living organisms like bacteria are equipped with an internal defense system called the immune system that is dedicated to cope with pathogens. Innate immune responses are quite rapid and result in controlling invaders quickly, and are called “innate immunity”. In contrast, adaptive immune responses, which developed later in evolution, are specifically directed against the invading pathogens and generate immunological memory. Dendritic cells (DCs) are sentinels of the immune system, which detect foreign invaders and initiate innate immune responses. Furthermore, DCs play a pivotal role in regulating adaptive immune responses, which will be clarified in the following chapters.

## 1.1 Dendritic cells are mediators of innate and adaptive immunity

DCs are professional antigen presenting cells that reside in lymphoid and non-lymphoid tissues. Their main functions are to process and present antigens to T lymphocytes. After the initial discovery of DCs (Steinman and Cohn 1973) intensive research was conducted to understand DCs and their function in the innate and adaptive immune system. DCs are a heterogeneous group of cells composed of several distinct subpopulations and can be divided into two main subsets: plasmacytoid DCs (pDCs) and conventional DCs (cDCs), which have specialized functions in adaptive and innate responses. Below, functionally distinct DC subsets that have been identified in lymphoid and non-lymphoid tissues will be discussed. Since this study was performed in mice, I will mainly focus on mouse DCs.

### 1.1.1 DC subsets in lymphoid tissues

DCs are defined by their distinct phenotypes, functions and surface marker expressions. All mature DCs in the mouse express CD11c and major histocompatibility complex (MHC) class II molecules. Additional surface molecules such as CD8 $\alpha$ , CD4, CD11b (known also as Mac-1), CD103, 33D1 and CD205 are currently used to define DC subsets in lymphoid and non-lymphoid compartments of mice.

The mouse spleen, where DCs were initially discovered, consists of two major subpopulations. The CD8<sup>+</sup> CD205<sup>+</sup> DC subset, which is localized in marginal and T cell zones (Idoyaga, Suda et al. 2009) and the CD8<sup>-</sup> 33D1<sup>+</sup> DC subset, which resides in the red pulp. Upon activation, CD8<sup>+</sup> and CD8<sup>-</sup> subsets can migrate via efferent lymphatic vessels into the T cell zones of secondary lymphoid organs to initiate adaptive immune responses (De Smedt, Pajak et al. 1996, Idoyaga, Suda et al. 2009). These two subsets differ also in their ability to present antigens. For instance, CD8<sup>+</sup> CD205<sup>+</sup> DCs can capture and cross present antigens to CD8<sup>+</sup> T cells (den Haan, Lehar et al. 2000, Idoyaga, Suda et al. 2009), whereas the CD8<sup>-</sup> 33D1<sup>+</sup> subset is more efficient in processing and presenting antigens on MHCII to induce CD4<sup>+</sup> T cell responses (Dudziak, Kamphorst et al. 2007).

Other lymphoid tissue DCs are found in lymph nodes and known as CD11c<sup>high</sup> MHCII<sup>+</sup> lymphoid tissue resident DCs, which contain two subsets of cells: CD8<sup>+</sup> CD205<sup>+</sup> and CD8<sup>-</sup> CD11b<sup>+</sup> DCs which are phenotypically and functionally equivalents of spleen CD8<sup>+</sup> CD205<sup>+</sup> and CD8<sup>-</sup> CD11b<sup>+</sup> 33D1<sup>+</sup> DCs (Belz, Behrens et al. 2002, Shortman and Liu 2002, Allan, Waithman et al. 2006). Moreover, non-lymphoid tissue DCs can migrate to the lymph nodes from the periphery through afferent lymphatics upon activation in a CCR7 dependent fashion (Ohl, Mohaupt et al. 2004). Migratory DC can be distinguished from resident DCs by higher MHCII expression and lower CD11c expression but only in the steady state conditions. It is known that migratory DCs can also transfer and cross present antigens to CD8<sup>+</sup> DCs in the lymph nodes (Allan, Waithman et al. 2006).

### 1.1.2 DC subsets in non-lymphoid tissues







Long after the discovery of Langerhans cells (LCs) by Paul Langerhans, the notion that LCs have immunogenic properties similar to DCs was recognized (Schuler, Romani et al. 1985). The finding led to the idea that more than one type of DCs exists and subpopulations, which have similar phenotype but distinct functions are present in non-lymphoid tissues.

The mammalian skin is composed of two layers: the epidermis and the dermis. The epidermal layer of the skin is home to LCs, which can respond to stimuli and acquire DC morphology; surface antigens and functions such as stimulating MHCII restricted T cells. Compared to dermal DCs, epidermal DCs exhibit intermediate expression levels of CD11c, low MHCII and high expression of Langerin. In addition, LCs express CD11b, F4/80 and lack CX<sub>3</sub>CR<sub>1</sub> (Merad, Ginhoux et al. 2008). However the function of LCs is not fully understood. LCs differ from other DCs regarding their unique ontogeny. Unlike DCs, LCs do not originate from pre-DCs but derive from embryonic hematopoietic precursors that have migrated to the skin and are self-renewing cells (Merad, Manz et al. 2002).

DCs which reside in the dermal layers of the skin contain two major subsets: CD103<sup>+</sup> CD11b<sup>low</sup> Langerin<sup>+</sup> and CD103<sup>-</sup> CD11b<sup>high</sup> Langerin<sup>-</sup> DCs (Merad, Ginhoux et al. 2008). It has been reported that CD103<sup>+</sup> CD11b<sup>low</sup> Langerin<sup>+</sup> cells migrate to skin draining lymph nodes and cross present antigens, however the functions of CD103<sup>-</sup> CD11b<sup>high</sup> Langerin<sup>-</sup> DCs are not clear (Bedoui, Whitney et al. 2009).

Three populations of DCs have been identified in the intestine based on their CD103 and CD11b expression: CD103<sup>+</sup> CD11b<sup>-</sup>, CD103<sup>-</sup> CD11b<sup>high</sup> and CD103<sup>+</sup> CD11b<sup>+</sup> DCs. CD103<sup>+</sup> CD11b<sup>-</sup> DCs are phenotypically and functionally similar to the CD8α<sup>+</sup> DCs in lymphoid tissues. They have superior cross presentation and crosspriming potential and participate in regulatory T cell (Treg) induction. CD103<sup>+</sup> CD11b<sup>+</sup> DCs can take up bacteria from the intestinal tract and transport them to mesenteric lymph nodes (Bogunovic, Ginhoux et al. 2009, Varol, Vallon-Eberhard et al. 2009). CD103<sup>+</sup> CD11b<sup>+</sup> DC subpopulation is involved in Th17 cell homeostasis in the intestine and Th17 response to infection (Scott, Tfp et al. 2014). CD103<sup>+</sup> CD11b<sup>+</sup> and CD103<sup>-</sup> CD11b<sup>high</sup> DCs can be found in other non-lymphoid tissues such as lung, liver and kidney (Ginhoux, Liu et al. 2009). Intestinal macrophages, which express high levels of MHCII and low levels of CD11c can be distinguished from CD11b<sup>+</sup> DCs by expression of CD64 (Tamoutounour, Henri et al. 2012).

Recently, the human counterparts of murine CD8 $\alpha$ <sup>+</sup> cDCs and CD8 $\alpha$ <sup>-</sup> cDCs were identified on CD141<sup>+</sup> BDCA3<sup>+</sup> cDCs and BDCA1<sup>+</sup> CD1c<sup>+</sup> cDCs by their common gene expression signature and similar function (Breton, Lee et al. 2015, Lee, Breton et al. 2015). Table 1 recapitulates members of the DC family in the murine lymphoid and non-lymphoid tissue on the basis of surface marker expressions.

Phenotypical marker	Lymphoid tissue cDC		Non-lymphoid tissue cDC			
						
	CD8 <sup>+</sup> cDC	CD11b <sup>+</sup> cDC	CD103 <sup>+</sup> CD11b <sup>-</sup> cDC	CD103 <sup>+</sup> CD11b <sup>+</sup> intestinal cDC	CD103 <sup>-</sup> CD11b <sup>+</sup> cDC	Langerhans cells
CD11c	+++	+++	++	++	++	++
MHC II	++	++	++	++	++	++
CD8	+	-	-	-	-	-
CD4	-	+/-	-	-	-	ND
CD11b	-	+	-	+	+	+
CD103	subset	-	++	++	-	-
Langerin	subset	-	+	-	-	++
B220	-	-	-	-	-	-
Clec9a (DNGR1)	++	-	++	-	-	-
CD205	++	+	++	ND	ND	++
CX <sub>3</sub> CR <sub>1</sub>	subset	-	-	-	++	+

**Table 1: Phenotype of murine DC subsets**

The expression level of different surface markers by DCs is denoted as - and +. ND corresponds to not determined (Table is adapted from (Merad, Sathe et al. 2013)).

### 1.1.3 Plasmacytoid dendritic cells

Plasmacytoid DCs (pDCs) are a unique subset of DCs that are morphologically and functionally distinct from cDCs. Unlike cDCs, pDCs have a morphology characteristic of antibody producing plasma cells with abundant endoplasmic reticulum. PDCs are rare cells that can be found in blood and in lymphoid and non-lymphoid organs and in murine bone marrow (BM). In the steady state, pDCs primarily circulate in the blood but can enter lymphoid organs via high endothelial venules (Randolph, Ochando et al. 2008, Sozzani, Vermi et al. 2010).

In terms of surface markers, pDCs are segregated from cDCs by their low expression of CD11c and MHCII and by the expression of B220, sialic acid binding Ig-like lectin H (Siglec H) and bone marrow stromal antigen 2 (BST2) on the surface. Some other useful albeit less specific surface markers used to define murine pDCs are Ly6C and Ly49Q (Tai, Goulet et al. 2008). Furthermore, pDCs can further divided into CCR9<sup>+</sup> and CCR9<sup>-/low</sup> pDCs in BM and in lymphoid tissues (Schlitzer, Loschko et al. 2011). Both CCR9<sup>+</sup> and CCR9<sup>-/low</sup> pDCs that reside in the BM express CD9 but downregulate expression of CD9 upon entry to lymphoid organs. PDCs can also be found in other lymphoid tissues in mice such as spleen, lymph nodes and thymus. Unlike their counterparts in the BM, these pDCs lack expression of CD9 (Bjorck, Leong et al. 2011).

The main function of pDCs is to secrete vast amounts of type I interferons (IFNs) in response to foreign nucleic acids e.g. during viral infection, mainly interferon alpha (IFN- $\alpha$ ) and interferon beta (IFN- $\beta$ ) and they are therefore known as the most efficient interferon producers (Liu 2005). In addition to being an interferon source, pDCs play a role in differentiation of B cells to plasma cells by secreting interleukin 6 (IL-6) and type I interferon (Jego, Palucka et al. 2003). PDCs express toll-like receptors (TLRs) 7 and 9; hence they sense endosomal and viral nucleic acids and also respond to the respective ligands, single stranded RNA and unmethylated CpG-containing DNA (CpG). Unlike cDCs, which stabilize peptide MHCII complex on their surface for a long time, pDCs can continuously form peptide MHCII complexes and present endogenous antigens following stimulation with TLR9 ligands such as CpG DNA (Young, Wilson et al. 2008).

In the steady state, pDCs express low levels of MHCII and exhibit secretory morphology similar to plasma cells. Upon stimulation with TLR7 and 9 agonists, pDCs undergo DC maturation, increase MHCII and costimulatory molecule expression and develop a cDC-like

morphology, factors that allow them to act as antigen presenting cells (APC). Activation of pDCs leads to IFN- $\alpha$  secretion as well as other cytokines such as tumor necrosis factor alpha (TNF- $\alpha$ ), IL-12 and IL-6. Moreover, upon stimulation pDCs can attract other immune cell types and acquire the capacity to prime T cells (Krug, Uppaluri et al. 2002). The secretory function of pDCs is regulated by X-box binding protein 1 (XBP-1) and required for development and survival of both pDCs and cDCs in mice (Iwakoshi, Pypaert et al. 2007).

Being a major effector cell type in immunity, pDCs have been associated with immune tolerance as well as immune responses in humans and mice. For instance, pDCs can promote Treg differentiation in human thymus (Martin-Gayo, Sierra-Filardi et al. 2010, Hadeiba, Lahl et al. 2012) and induce Treg mediated tolerance in mouse draining lymph nodes (Sharma, Baban et al. 2007) and in experimental autoimmune encephalomyelitis (EAE) model (Irla, Kupfer et al. 2010). The role of pDCs in antiviral responses was also well studied in mice lymphocytic choriomeningitis virus (LCMV) models, mouse hepatitis virus (MHV) models, herpes virus infection models and in mucosal viral infections (Lund, Linehan et al. 2006). PDCs produce type I interferon in response to nearly all enveloped viruses and contribute to virus clearance. The contribution of pDCs to antiviral responses has been reported by using pDC-depleted mice (BDCA2-DTR) in mouse cytomegalovirus (MCMV) and vesicular stomatitis virus (VSV) infection. PDC depletion led to reduced early IFN-I production by pDCs in response to MCMV infection as well as impaired survival and accumulation of CD8<sup>+</sup> T cells (Swiecki, Gilfillan et al. 2010).

PDCs have also been associated with induction of autoimmune responses. It has been shown that pDCs are involved in some diseases in humans: psoriasis and systemic lupus erythematosus. In both cases, patients show decreased numbers of pDCs in circulation and massive accumulation of IFN producing pDCs in the affected tissues (Nestle, Conrad et al. 2005). Recently, it has been shown that targeting myelin oligodendrocyte glycoprotein (MOG) peptide to pDCs via Siglec H dampened the EAE onset (Loschko, Heink et al. 2011). It was also shown that, ablation of MHCII on pDCs exacerbated the course of the EAE (Irla, Kupfer et al. 2010).

In conclusion, pDCs make an important contribution to tolerance and immunity.



## 1.2 Origin of dendritic cells

DCs can originate from both myeloid and lymphoid lineages within the BM niche. Monocytes, macrophages, granulocytes, megakaryocytes and erythrocytes are all derived from common myeloid progenitors (CMP), whereas common lymphoid progenitors (CLP) give rise to lymphocytes and natural killer (NK) cells. The identification of DC progenitors is based on adoptive transfer experiments in mice. Adoptive transfer of CLPs as well as CMPs into irradiated mice gave rise to pDCs and cDCs *in vivo*. This holds true for *in vitro* culture experiments of human CLPs and CMPs as well (Chicha, Jarrossay et al. 2004). Although CLPs and CMPs showed a similar potential to give rise to CD8<sup>+</sup> and CD8<sup>-</sup> splenic DCs as well as CD8<sup>+</sup> thymic DCs, CMPs are more efficient at generating splenic and lymph node cDCs whereas CLPs were more potent at producing thymic DCs (Manz, Traver et al. 2001).

In the steady state distinguishing DCs from monocytes and macrophages can be achieved by fluorescently activated cell sorting (FACS) staining of specific markers. However, the hypothesis that DCs share a common origin with monocytes and macrophages is hard to prove especially under inflammatory conditions. Several groups have attempted to prove that DCs develop from monocytes by direct adoptive transfer experiments in mice in steady state and under inflammatory conditions (Naik, Metcalf et al. 2006). However, adoptively transferred monocytes do not produce classical lymphoid organ DCs.

Macrophage DC progenitors (MDP) are described based on their surface markers as Lin<sup>-</sup> ckit<sup>+</sup> CX<sub>3</sub>CR<sub>1</sub><sup>+</sup> CD11b<sup>-</sup> CD115<sup>+</sup> CD135<sup>+</sup> (Fogg, Sibon et al. 2006). MDPs account for 0.5% of all BM mononuclear cells in mice (Serbina, Salazar-Mather et al. 2003). When cultured with granulocyte macrophage colony stimulating factor (GM-CSF) *in vitro* or upon adoptive transfer into mice, MDPs produce lymphoid-resident cDCs, some pDCs (Fogg, Sibon et al. 2006) and non-lymphoid tissue resident cDCs (Bogunovic, Ginhoux et al. 2009). Thus, MDPs are more restricted to develop into DCs and macrophages than early myeloid progenitors. Recent studies defining human DC progenitors support the evidence of a distinct macrophage DC progenitor stage (Lee, Breton et al. 2015).

A DC-restricted progenitor called common DC progenitor (CDP), giving rise exclusively to cDCs and pDCs was identified in the murine BM (Naik, Sathe et al. 2007, Onai, Obata-Onai et al. 2007). CDPs comprise 0.1-0.3% of all BM mononuclear cells. CDPs were identified as Lin<sup>-</sup> ckit<sup>low</sup> CD135<sup>+</sup> CD115<sup>+</sup> and shown to give rise at clonal levels to cDCs and pDCs in FMS-like tyrosin kinase 3 ligand (Flt3L) supplemented cultures (Naik, Sathe et al. 2007).

Moreover, several adoptive transfer experiments showed that CDPs give rise to CD8<sup>+</sup> and CD11b<sup>+</sup> DCs and pDCs in spleen (Onai, Obata-Onai et al. 2007), CD103<sup>+</sup> CD11b<sup>-</sup> and CD11b<sup>+</sup> DCs in liver and kidney, and intestinal cDCs (Bogunovic, Ginhoux et al. 2009, Varol, Vallon-Eberhard et al. 2009). Although, these DC restricted progenitors have been identified as Lin<sup>-</sup> ckit<sup>low</sup> CD135<sup>+</sup> CD115<sup>+</sup>, evidence was found for a new DC progenitor (Lin<sup>-</sup> ckit<sup>low</sup> CD135<sup>+</sup>), which lacks CD115 and has prominent pDC differentiation capacity (Onai, Kurabayashi et al. 2013). cDC committed precursors have been identified in the BM, blood and lymphoid tissues. These CD11c<sup>+</sup> MHCII<sup>-</sup> precursors called pre-cDCs derive from CDPs and have the ability to differentiate into CD8<sup>+</sup> and CD11b<sup>+</sup> cDCs as well as CD103<sup>+</sup> and CD103<sup>-</sup> non-lymphoid tissue cDCs, but not pDCs upon transfer experiments (Ginhoux, Liu et al. 2009, Liu, Victora et al. 2009).

BM contains high numbers of pDCs (2-3%), which are thought to develop directly from CDP in the BM with a minor contribution from CLP-derived progenitors, which are not defined (Chen, Chen et al. 2013). A DC precursor with pDC-like phenotype but expressing low levels of CCR9 was identified in the BM, which upon transfer can give rise to pDCs and cDC subsets depending on the tissue microenvironment (Schlitzer, Loschko et al. 2011). Recently, human counterparts of murine MDP, CDP and pre-cDC were identified (Breton, Lee et al. 2015, Lee, Breton et al. 2015). Even so, final commitment to pDC and cDC subpopulations is influenced by multiple factors and is still a highly debated question in the field.

## 1.3 Dendritic cell development

As discussed previously, DCs are a very heterogeneous population in the immune system. Although they share common features, such as processing and presenting antigens to T cells, they vary a lot in surface marker expression, localization, origin, migratory patterns and functional specialization. Indeed, the development of DC subsets is differentially regulated by intrinsic and extrinsic mechanisms. Regulation of DC development is discussed in the following chapters.

### 1.3.1 Transcriptional regulation of DC development

The diversity of the DC lineage has been shown in many studies. These findings raised one of the most important questions in the field namely, how to delineate distinct DC lineages and identify the developmental steps during DC commitment. Studies on the role of transcription factors partially answered these questions.

The interferon regulatory factor (IRF) family consists of 9 members in mammals, which are involved in cellular differentiation of hematopoietic stem cells (HSC), apoptosis and cell cycle regulation. Some of the IRF family members have been associated with DC development in humans and mice. Mice lacking the IRF2 or IRF4 genes showed defects in the development of CD4<sup>+</sup> subset of CD8<sup>-</sup> cDCs and IRF8 deficient mice showed defects in CD8 $\alpha$ <sup>+</sup> cDCs and pDC subsets in spleen (Suzuki, Honma et al. 2004). On the other hand, IRF8, also known as interferon consensus sequence-binding protein (ICSBP), plays a critical role in myeloid cell differentiation. IRF8 deficient animals develop myeloproliferative disease and are unable to generate sufficient numbers of monocytes. IRF8 deficient mice also lack pDCs and CD8<sup>+</sup> cDCs in lymphoid tissues and CD103<sup>+</sup> cDCs in non-lymphoid tissues (Tsuji-mura, Tamura et al. 2003, Edelson, Kc et al. 2010). In addition to its function in DC development, IRF8 plays a role in regulation of DC function. It has been shown that IRF8 deficient mice do not just lack CD8<sup>+</sup> DCs in lymphoid tissues; in fact, IRF8 controls CD8<sup>+</sup> cDC maturation as well as IL-12 production (Schiavoni, Mattei et al. 2002). Further studies showed that IRF4 and IRF8 double deficiency leads to defects in all DC populations indicating an indispensable role of both factors in the development of DCs (Tamura, Taylor et al. 2005). It has been reported that in humans, IRF8 deficient patients lack circulating monocytes and DCs, moreover have a selective loss of BDCA-1<sup>+</sup> CD1c<sup>+</sup> CD11c<sup>+</sup> circulating DCs (Hambleton, Salem et al. 2011).

Inhibitor of DNA-binding 2 (Id2) is a member of the helix-loop-helix (HLH) transcription factor family that works as an antagonist of the HLH family-E protein 2-2 (E2-2). Id2 is upregulated during DC development and is required for the development of LC and CD8<sup>+</sup> cDCs (Hacker, Kirsch et al. 2003). Overexpression of Id2 in HSCs inhibited the development of pDCs, but left cDCs unaffected, implying that Id2 acts as an inhibitor of pDC development (Spits, Couwenberg et al. 2000). In contrast, mice lacking Id2 have reduced numbers of CD8<sup>+</sup> and CD103<sup>+</sup> DCs (Ginhoux, Liu et al. 2009).

E2-2, another member of HLH transcription factor family, has a non-redundant role in pDC development and pDC-mediated responses in humans and in mice. Cisse et.al. have shown that E2-2 is expressed specifically in pDCs but not in cDCs and can directly induce expression of transcriptional regulators such as SpiB and IRF8 which are associated with pDC development. Moreover, it has been shown that, in E2-2 knock out mice pDC development is greatly impaired and pDCs from E2-2<sup>+/-</sup> mice have reduced pDC specific gene expressions and abolished IFN secretion upon TLR stimulation (Cisse, Caton et al. 2008). Recently, it has been shown that loss or reduction of E2-2 in mature peripheral pDCs caused pDCs to acquire a cDC-like phenotype and showed increased expression of cDC markers such as CD8, CD11c and MHCII (Ghosh, Cisse et al. 2010). These studies show that E2-2 acts in a dose-dependent manner and is essential for pDC development and maintenance.

The zinc finger transcription factor (Zbtb46) is one of the transcription factors expressed specifically in the cDC lineage. Zbtb46 expression begins at the pre-cDC stage and is maintained in developing CD8<sup>+</sup> and CD11b<sup>+</sup> cDCs in lymphoid tissues and in CD103<sup>+</sup> cDCs in non-lymphoid organs. Zbtb46 expression on pDCs, monocytes and macrophages is not reported (Meredith, Liu et al. 2012, Satpathy, Kc et al. 2012).

The E-twenty-six (ETS) family is one of the largest transcription factor families. It is involved in a wide variety of functions such as regulation of cellular differentiation, cell cycle control, migratory patterns and proliferation. One of the ETS family members, PU.1, has multiple roles in hematopoiesis and lineage selection. Within the DC lineage, PU.1 is expressed at low levels in pDCs and at high levels in cDCs. In a recent study, it has been shown that PU.1 is a critical regulator in DC development, which regulates FMS-like tyrosin kinase 3 (Flt3) expression in a dose dependent manner. Therefore, it is a good candidate to study DC development (Carotta, Dakic et al. 2010). The role of PU.1 in DC development was investigated in mice with germ line deficiency of PU.1. PU.1 deficient mice showed impaired

development of cDCs from the hematopoietic progenitors in the embryo or in neonatal mice (Anderson, Perkin et al. 2000). It is known that PU.1 interacts with other transcription factors such as IRF 4 and 8 and SpiB. SpiB, also a member of the ETS transcription factor family, is expressed by pDCs, B cells and CD34<sup>+</sup> hematopoietic progenitor cells but not by cDCs. Human studies using knockdown of SpiB by short hairpin-RNA (sh-RNA) showed that SpiB functions as a key regulator in pDC survival (Karrich, Balzarolo et al. 2012).

The basic leucine zipper transcription factor ATF-like (Batf3) is expressed in all cDCs such as the CD8<sup>+</sup> cDCs, CD103<sup>+</sup> cDCs as well as CD11b<sup>+</sup> cDCs and has non-redundant subset specific functions in DC development. Mice deficient for Batf3 in the 129S6/SvEv strain lack selectively CD8<sup>+</sup> and CD103<sup>+</sup> cDCs (Edelson, Kc et al. 2010). It has been reported that Batf3 is essential for development of CD103<sup>+</sup> cDCs, and for the maintenance of CD8<sup>+</sup> cDC development (Jackson, Hu et al. 2011). Moreover, many other intrinsic regulators such as signal transducer and activator of transcriptions (STATs) and Ikaros have indispensable roles in the development of DC subsets. In addition to intrinsic factors, several cytokines and growth factor promote the differentiation of DC subsets. These will be introduced further in the following chapter.

### **1.3.2 Role of cytokines in DC development**

The differentiation of DCs relies on the activity of cytokines. The cytokine Flt3L is one of the key mediators in DC development. Flt3L can be produced by endothelial cells, stroma cells and activated T cells (Schmid, Kingston et al. 2010). The receptor of Flt3L, Flt3 also known as CD135, is expressed on many HSCs, progenitors such as CLPs, a subset of CMPs, CDPs and MDPs (Adolfsson, Borge et al. 2001). Furthermore, Flt3 is also expressed downstream of DC precursors and DC subpopulations, and it is absent in other circulating and tissue-resident leucocytes (Karsunky, Merad et al. 2003).

The importance of Flt3L in DC development has been shown in many studies. Mice lacking Flt3 or its ligand showed defects in hematopoiesis resulting in reduced numbers of HSCs, pDCs and cDCs (McKenna, Stocking et al. 2000). In contrast, studies conducted in humans and mice revealed that, in vivo treatment with or over expression of Flt3L leads to increased numbers of pDCs and cDCs in vivo (Maraskovsky, Daro et al. 2000, Manfra, Chen et al. 2003). In addition to its role in DC differentiation, it has been reported that Flt3L is an important regulator of homeostatic DC division in the periphery in vivo (Waskow, Liu et al. 2008).

Another well-studied cytokine is GM-CSF that promotes the differentiation of monocytes to myeloid DCs that resemble splenic cDCs (Inaba, Inaba et al. 1992). Although Flt3L and GM-CSF both play critical roles in differentiation of pDCs and cDCs, GM-CSF favors cDC development rather than pDCs, which are tightly regulated by Flt3L *in vivo* and *in vitro* (Greter, Helft et al. 2012).

Csf-1, also known as macrophage colony stimulating factor (M-CSF), regulates the survival and proliferation of macrophages. M-CSF receptor (CD115) is expressed on MDPs, monocytes and macrophages as well as on CDPs. It has been postulated that the strength of Flt3 versus M-CSF receptor signals determines the diversion of MDPs to CDPs instead of monocyte macrophages (Schmid, Kingston et al. 2010). M-CSF receptor partially regulates CD11b<sup>+</sup> cDCs but is also required for epidermal LC development (Ginhoux, Tacke et al. 2006). In addition to its role in monocyte and macrophage development, M-CSF is involved in pDC and cDC development *in vitro* and *in vivo*. It has been shown that M-CSF can drive pDC and cDC development *in vitro* from BM precursors independently of Flt3L. M-CSF when administered *in vivo*, is able to increase DC numbers in mice (Fancke, Suter et al. 2008).

In conclusion, homeostasis of DC development is dynamically regulated by several growth factors, cytokines as well as transcription factors. However, the role of further signals emerging from local tissues and other immune cells in the steady state and under inflammatory conditions remain to be investigated.

#### **1.4 Novel tools to define lineage relationships between DC subsets**

Hematopoiesis is orchestrated by intrinsic and extrinsic mechanisms and existing heterogeneity within progenitor cells can influence cell fate decisions. Many DC subtypes and DC progenitors share similar surface markers. Therefore, the identification of unique surface molecules that mark distinct lineages is critical.

Beyond surface markers, several methods such as transcription factor based approaches have been used to define DCs from other immune cell types. Zbtb46 was identified for its prominent expression in mouse preDCs and cDCs, and absence in pDCs. Despite being a good candidate for studying DC development, Zbtb46 is downregulated after DC stimulation and is also expressed in non-immune cells (Meredith, Liu et al. 2012), which can dampen analysis. Recently, an *in vivo* fate-mapping model of CDP progenitors has been proposed by the Reis e Sousa group. Scharml and colleagues have identified DNNGR-1 (Clec9a) as a

unique surface marker, which is specifically expressed in DC-restricted progenitors, CDPs and pre-DCs but not in MDPs. By tracing DNNGR-1 expression through the progeny, spleen ESAM<sup>lo</sup> CD11b<sup>+</sup> DCs were found to be derived from DC precursors and not from macrophages (Schraml, van Blijswijk et al. 2013).

Comparative gene expression analyses have shed light on developmental studies by identifying gene expression signatures, which characterize distinct DC subtypes (Gautier, Shay et al. 2012). However, reliability of such analyses depends on the homogeneity of the target population. More importantly, gene expression profiles not always provide hints for cell ontogeny. More precise approaches at the single cell level such as single cell transcriptome analysis and epigenetic analysis might circumvent these problems (Paul and Amit 2014).

Another powerful tool termed cellular barcoding is used to address individual cell fates on a large scale in vivo (Schepers, Swart et al. 2008). In principle, cellular barcoding involves tagging of individual cells of interest with heritable cellular barcodes. The barcode library is created using semirandom noncoding DNAs and can be delivered to the progenitor cells using lentiviral or retroviral vectors. (Naik, Schumacher et al. 2014).

Understanding dynamic processes in HSC are challenging due to the heterogeneity of the populations. To gain insights into behaviors of HSCs, cell cycle times, adherence status and cell-cell interactions as well as progeny of the single cells have to be observed during a suitable time period. So far, with traditional methods, populational-based analysis was carried out by looking at the populations by FACS analysis at different time points. Working with heterogeneous populations such as HSCs requires long-term observations at the single cell level, which can be achieved by continuous single cell imaging. This approach allows the simultaneous quantification of cell cycle times, cell death and differentiation events. Even more, effects of cytokines on cell survival and differentiation can be observed over time (Eilken, Nishikawa et al. 2009, Rieger, Hoppe et al. 2009).

Long-term single cell imaging is typically fluorescence imaging. In contrast to in vivo two-photon fluorescence imaging, it does not require invasive methods. Progenitor cells can be cultured up to a few weeks under constant CO<sub>2</sub> and at 37°C. Time-lapse imaging of living cells is done by microscopes equipped with motorized compartments. Single cell tracking and analysis of the resulting data can be done with custom-made softwares.

Markers for live cell imaging can be genetically encoded fluorescent proteins or fluorescently labeled antibodies (Rothbauer, Zolghadr et al. 2006). For instance, transgenic cells and animal lines in which the marker of interest is fused to fluorescent proteins such as green fluorescent protein (eGFP) are currently being used (Kueh, Champhekar et al. 2013).

Although the required technology for single cell time-lapse imaging is quite complex, the number of studies using single cell imaging and tracking is increasing.



## 2 Aims of the study

The aim of this study was, to investigate cell fate decisions of dendritic cell progenitors and precursors during their development into DC subpopulations focussing on pDC development. Fully differentiated pDCs were shown to develop directly from CDPs in the BM, while cDC subpopulations differentiate in the tissue from cDC-precursors, which are generated from CDPs in the BM.

Recently, a pDC-like DC precursor, which retains flexibility to differentiate into mature pDCs as well as cDCs was identified in murine BM and was also found at low frequencies in peripheral tissues and blood (Schlitzer, Loschko et al. 2011). These CCR9<sup>low</sup> pDC-like cells, which resemble pDCs in phenotype and function, are CDP-derived precursors, which upon entry into peripheral tissues differentiate into pDCs as well as cDCs. It was known, that, in the presence of Flt3L, CDPs give rise to both pDC-like precursors and pDCs. However, it was not clear, if CDPs in the BM give rise to pDCs via the CCR9<sup>low</sup> pDC-like precursor stage, or, if pDCs develop directly from CDPs in the BM in parallel with pDC-like precursors. The question, whether the sequential or parallel development model is correct, cannot be answered by cell population analyses. **The first aim of this study** was therefore, to develop a method to adress this question on the single cell level. The objective was to establish a cell culture system, which allows imaging and following CDPs and their progeny continuously during their developmental steps towards differentiated pDC.

It has been shown, that, similar to the differentiation of cDC precursors into cDC subtypes, the final differentiation of pDC-like precursors into functionally distinct pDC and cDC subpopulations is shaped by the tissue microenvironment (Schlitzer, Heiseke et al. 2012). This plasticity decreases with further differentiation into distinct DC subpopulations. Under inflammatory conditions, the tissue microenvironment changes drastically, which may also influence the differentiation of precursor cells and the phenotype and function of DC subsets. **The second aim of the study** was therefore, to investigate the phenotypic changes of CCR9<sup>low</sup> pDC-like cells and CCR9<sup>+</sup> pDCs under local inflammatory conditions in vivo. For this purpose a well-established model of central nervous system (CNS) inflammation, MOG peptide induced EAE, was chosen. With adoptive transfer experiments, the fate and plasticity of the CCR9<sup>low</sup> pDC-like cells and CCR9<sup>+</sup> pDCs, which migrate to the inflamed CNS, was investigated.

## 3 Material and Methods

### 3.1 Material

#### 3.1.1 Reagents

Agarose	Biozym (Hess-Oldendorf, Germany)
$\beta$ -mercaptoethanol	Sigma-Aldrich (Seelze, Germany)
Biocoll	Merck (Darmstadt, Germany)
Complete Freund's Adjuvant (CFA)	Difco (Detroit, USA)
Dimethyl sulfoxide (DMSO)	Sigma-Aldrich (Seelze, Germany)
Dulbecco's Modified Eagle's Medium (DMEM)	Invitrogen (Karlsruhe, Germany)
DNA ladder (1 kbp)	NEB (Frankfurt, Germany)
dNTP mix	Promega (Mannheim, Germany)
EDTA (0.5 M, pH 8.0)	Invitrogen (Karlsruhe, Germany)
Ethidiumbromide	Invitrogen (Karlsruhe, Germany)
Fetal calf serum (FCS)	PAA (Pasching, Austria)
Flt3L	Produced in the lab
Gelatin	Sigma-Aldrich (Seelze, Germany)
Glacial acetic acid	Roth (Karlsruhe, Germany)
Glutamax-I (100X)	Invitrogen (Karlsruhe, Germany)
Hank's balanced salt solution (HBSS)	Invitrogen (Karlsruhe, Germany)
Hydrochloric acid (HCl)	Merck (Darmstadt, Germany)
Horse Serum	Stem cell technologies (Köln, Germany)
LysoTracker	Invitrogen (Karlsruhe, Germany)
MEM $\alpha$ Glutamax	Invitrogen (Karlsruhe, Germany)
Non-essential aminoacids (100X)	PAA (Pasching, Austria)
Penicilin/streptomycin (100X)	PAA (Pasching, Austria)
Pertussis Toxin (PTx)	Fluka (Seelze, Germany)
Phosphate buffered saline (PBS) without $\text{Ca}^{2+}\text{Mg}^{+2}$	Invitrogen (Karlsruhe, Germany)
Propidium iodide	Sigma-Aldrich (Seelze, Germany)
Red blood cell lysis buffer	Sigma-Aldrich (Seelze, Germany)
RPMI 1640	Invitrogen (Karlsruhe, Germany)
Sodium hydroxide solution (NaOH)	Merck (Darmstadt, Germany)
Sodium pyruvate solution (100 mM)	Invitrogen (Karlsruhe, Germany)
Tris (hydroxymethyl)aminomethane (TRIS)	Roth (Karlsruhe, Germany)
Tween-20	Sigma-Aldrich (Seelze, Germany)



### 3.1.4 Antibodies

Antigen	Clone	Conjugate	Manufacturer
CD3	145-2C11	FITC	BD Bioscience
CD19	1D3	FITC	BD Bioscience
B220	RA3-6B2	FITC, PE, Pe- Cy5	BD Bioscience
Gr1	1A8, RB6-8C5	FITC	Biolegend
NK1.1	PK136	FITC, efluor 450	BD Bioscience
CD11b	M1/70	FITC	eBioscience
CD135	A2F10	PE	eBioscience
CCR9	eBioCW.1.2.	PE, APC	eBioscience
Siglec H	440c	Alexa 488, Alexa 647	Produced in the lab
BST2	120G8	Alexa 647, FITC	Produced in the lab
CD11c	N418	Alexa 488, PE-Cy7, BV 421	eBioscience, Biolegend
MHCII	M5/114.15.2	efluor 450, efluor APC- 780, BV 421	eBioscience, Biolegend
CD117	ACK2	efluor APC- 780	eBioscience
CD115	AF598	APC	eBioscience
Sca1	D7	Per CP	eBioscience
Mouse hematopoietic lineage cocktail	17A2, RA3-6B2, M1/70, Ter119, RB6-8C5	efluor 450	eBioscience
CD8	53.6.7	PE	BD Bioscience
CD103	M290	PE	eBioscience
RatIgG2a	r2a-21B2	FITC	BD Bioscience
CD45.1	A20	Per CP-Cy5.5	eBioscience
CD45.2	104	V450	BD Bioscience
CD64	X54-5/7.1	APC	BD Bioscience
Streptavidin		APC	eBioscience

**Table 2: Antibodies used in this study**

### 3.1.5 Media and Buffers

#### 3.1.5.1 Cell culture media

##### DC medium

(For BM cells, CDPs, DCs)

RPMI 1640

10% FCS (HI)

1% (v/v) NEAA

1% (v/v) Glutamax

1% (v/v) sodium pyruvate

1% (v/v) P/S

0.05 mM  $\beta$ -mercaptoethanol

##### EL08 medium

(For EL08 stromal cell line)

MEM- $\alpha$  Glutamax

15% (v/v) FCS (HI)

5% (v/v) HS

1% (v/v) P/S

0.01 mM  $\beta$ -mercaptoethanol

##### RPMI complete medium

(For B16 melanoma cell line)

RPMI 1640

10% (v/v) FCS (HI)

1% (v/v) NEAA

1% (v/v) Glutamax

1% (v/v) P/S

##### Freezing medium

90% (v/v) FCS (HI)

10% (v/v) DMSO



### 3.1.6 PCR Primers for genotyping

PCR Primer	5' Sequence 3'
Id2_61	TGCCTATGTGGTAAGTCAAGCGG
Id2_65	CTCCAAGCTCAAGGAACTGG
Id2_67	GCGGAATTCATTTAATCACCCA

Table 3: PCR primers used in this study

### 3.1.7 Mice

Strain	Source	Application
<b>C57BL/6J</b>	Harlan, Paderborn Bred in SPF Facility	Adoptive transfer experiments In vitro culture experiments Live cell imaging Immunization experiments
<b>CD45.1</b>	Harlan, Paderborn Bred in SPF Facility	Adoptive transfer experiments In vitro culture experiments In vivo DC expansion
<b>Id2<sup>eGFP/eGFP</sup></b>	Gabrielle T. Belz, The Walter and Eliza Hall Institute of Medical Research, Melbourne, Australia (Jackson, Hu et al. 2011)	Live cell imaging In vitro culture experiments

Table 4: Mouse strains used in this study

### 3.1.8 Cell lines

Cell line	Species	Source	Application
<b>EL08</b>	Mouse	Robert AJ Oostendorp, III. Medical Clinic, Hematology and Oncology Department, Munich (Oostendorp, Medvinsky et al. 2002).	Feeder cells for CDP cultures
<b>B16-Flt3L melanoma</b>	Mouse	Carole Bourquin, University of Fribourg, Switzerland. Originally from G. Dranoff, Dana Farber Cancer Institute, Boston, MA, USA (Mach, Gillessen et al. 2000).	In vivo expansion of DCs

Table 5: Cell lines used in this study

## 3.2 Methods

### 3.2.1 PCR genotyping of $Id2^{eGFP/eGFP}$ reporter mice

Polymerase chain reaction (PCR) was used to amplify DNA fragments inserted into *Id2* locus. Founders of *Id2*-GFP reporter line, which is derived from an embryonic stem cell clone, lacked 5' Lox P site (Jackson, Hu et al. 2011). PCR genotyping of *Id2*-GFP reporter mice was performed using the primer combination described in Table 3. Agarose gel electrophoresis was used to separate DNA fragments. 1% agarose gel was prepared in 1 X TAE buffer and ethidium bromide was added at the concentration of 100 ng/ml to stain DNA fragments. For size determination, 1 kbp DNA ladder was used and DNA fragments were visualized with UV light at 254 nm.



**PCR REACTION**

ld2_61	0.5 µl
ld2_65	0.5 µl
ld2_67	0.5 µl
ddH <sub>2</sub> O	11 µl
Green Taq	12.5 µl
DNA	1 µl
	Σ= 26µl

**PCR CONDITIONS**

1) 94°C	4 min
2) 94°C	35 sec
3) 59.5°C	35 sec
4) 72°C	1 min
5) go to step 2	repeat 38 times
6) 72°C	10 min
7) 4 °C	Hold

**PRODUCT SIZE**

Wild Type	688 bp
Reporter	959 bp
Heterozygous	688 bp 959 bp

**3.2.2 Cell culture**

All cell cultures were maintained at 37°C with 5% CO<sub>2</sub> in humidified incubator with the respective media listed in 3.1.5.1. FCS was heat inactivated at 56°C for 45 min before used in culture mediums. DC medium for CDPs was filtered before used in time-lapse imaging experiments.

### **3.2.2.1 *Culturing EL08 stromal cell line***

EL08 stromal cells were thawed in EL08 medium and centrifuged at 1500 rpm at 4°C. Cells were resuspended at a ratio of  $5 \times 10^5$  cells/ml and cultured on 10 cm dishes coated with 0.1% gelatin as described before (Oostendorp, Harvey et al. 2002). After 2-3 days of expansion, cells were detached using Trypsin/EDTA at 37°C for 5 min. After centrifugation, cells were resuspended in EL08 medium and plated at a density of  $5 \times 10^4$  cells/cm<sup>2</sup> in gelatin-coated 12 well plates for co-culture experiments or on an ibidi  $\mu$ -slides (see 3.2.9).

### **3.2.2.2 *B16-Flt3L secreting melanoma cell line***

After thawing Flt3L-secreting B16 melanoma cells (B16-Flt3L) in RPMI complete medium, cells were cultured in 75 cm<sup>2</sup> cell culture flasks. After 2 days of culture, medium was aspirated and cells were washed once with PBS. Subsequently, 5 ml Trypsin/EDTA was added to culture flask and incubated for 5 min at 37°C. Cells were harvested by gentle pipetting and centrifuged at 1500 rpm 5 min at 4°C. Cells were then resuspended in RPMI complete medium and split at the ratio 1:15. After 3 days of additional culture, cells were harvested using Trypsin/EDTA. Subsequently, cells were spun down at 1500 rpm 5 min at 4°C and the pellet was resuspended in PBS for in vivo adoptive transfer experiments.

### **3.2.2.3 *In vivo expansion of DCs by Flt3L expressing B16 melanoma cells***

B16-Flt3L melanoma cells were cultured and harvested as described before 3.2.2.2. Cells were resuspended in PBS at a concentration of  $2,5 \times 10^7$  cells/ml and 200  $\mu$ L per animal, which equals  $5 \times 10^6$  cells/mouse were injected subcutaneously in the flank of mice under isoflurane anesthesia. 7 days after injection, mice were sacrificed.

### **3.2.2.4 *Generation of Flt3L derived murine BM cells***

6-8 weeks old mice were used for isolation of BM cells. Mice were euthanized by CO<sub>2</sub> asphyxia. To obtain BM cells, hind legs were removed and cleaned from muscle and fur. Femur and tibia were isolated and both bone extremities were cut. Bones were then flushed with RPMI using a 24G syringe in a 10 cm dish, to obtain a single cell suspension. Cells were centrifuged at 1500 rpm at 4°C for 5 min. After centrifugation, pellet was resuspended in 1 ml Red Blood Cell Lysis Buffer for lysing erythrocytes, and incubated at room temperature for 5

min. Reaction was stopped by adding 10 ml RPMI. Cells were centrifuged and pellet was resuspended in DC medium.  $1,5 \times 10^6$  cells/ml were seeded in 6 well plates in total volume of 3 ml/well and cultured for 7 days in the presence of 20ng/ml recombinant Flt3L to obtain Flt3L-derived DCs.

### **3.2.3 Cell isolation from primary tissues**

#### ***3.2.3.1 Isolation of cells from lymphoid organs in mice***

Mice were sacrificed as described in 3.2.2.4. The spleen was digested with DNase I (final concentration 100µg/ml) and Collagenase D (final concentration 500 µg/ml) in RPMI for 30 min at 37°C. After incubation, all organs were pushed through a 100µm cell strainer to obtain single cell suspensions. Cells were then centrifuged at 1500 rpm at 4°C and the cell pellet was resuspended in 1ml red blood cell lysis buffer to lyse erythrocytes. The lysis was stopped after 5 min of incubation by adding 10 ml of RPMI. After centrifugation, cells were resuspended in FACS buffer or DC medium for further analysis.

#### ***3.2.3.2 Isolation of mononuclear cells from brain and spinal cord***

On day 15 or 16, at peak EAE, mice were sacrificed by isoflurane anesthesia and before harvesting organs cardiac perfusion was performed through the left cardiac ventricle with ice cold PBS. Subcranial structures were dissected from cerebellum and spinal cord was flushed from spine by means of hydrostatic pressure with PBS. CNS tissue was cut in small pieces and digested with 2,5 mg/ml Collagenase D and 1 mg/ml DNase I at 37°C for 45 min. After incubation time, tissues were passed through a 70µm cell strainer and mononuclear cells were isolated by Percoll gradient (37% over 70%) centrifugation. Mononuclear cells were removed from the interphase, washed and then resuspended in FACS buffer for further analysis.

### **3.2.4 Flow Cytometry**

Flow cytometry allows separation of heterogeneous populations of cells by tagging them with antibodies linked to fluorescently labeled dyes. For FACS analysis, cells were stained with 1:200 dilutions (unless stated otherwise) of the respective antibodies in staining solution (FACS buffer, FcR blocking buffer, 1:1) for 20 min at 4°C. FcR blocking buffer is anti-

CD16/32 hybridoma supernatant, which blocks non-specific Fc receptor-mediated antibody binding. Afterwards, cells were washed twice with FACS buffer. Propidium iodide (2.5 µg/ml) was added to exclude dead cells from analysis. Cells were analyzed by FACS Gallios (Beckmann Coulter, Krefeld, Germany). FACS data were analyzed using Kaluza Software (Beckman Coulter, Krefeld, Germany) or Flow Jo Single Cell Analysis Software v10 (FlowJo LLC, Ashland, USA).

### 3.2.5 Cell sorting for in vivo and in vitro experiments

#### 3.2.5.1 CDP sorting for co-culture and in vitro imaging experiments

BM cell isolation was performed as described in 3.2.2.4. Before staining cells for CDP sorting, lineage depletion of total BM cells from mature hematopoietic cells such as B cells, granulocytes, monocytes/macrophages, T cells and their committed precursors was performed. BM cells were stained with FITC conjugated antibodies (1:200) against CD3, CD19, B220, CD11b, Gr1 and NK1.1 in FACS buffer for 20 min at 4°C. Subsequently, cells were separated with Anti-FITC Microbeads kit according to manufacturer's instructions, and the negative fraction (flow-through) was collected, centrifuged at 1500 rpm at 4°C for 5 min and used for sample staining for CDP sorting.

The cell pellet was resuspended in 400 µl of FACS buffer and FcR blocking buffer at the ratio of (1:1). For single stainings, 500.000 cells were kept aside for each single staining and control tube. The following murine antibodies were used for sample staining: Lineage cocktail containing CD3, CD19, Gr1, CD11b, NK1.1 and B220 antibodies, CD135, CD11c, CD115, CD117 and MHCII. Antibodies were used in 1:200 dilutions for sample staining except for the CD135 antibody (1:100). Cells were stained in a 50 ml Falcon tube and incubated with respective antibodies for 20 min at 4°C in the dark. Subsequently, cells were washed once with 30 ml FACS buffer and pellet was resuspended in FACS buffer for cell sorting. Cell sorting was performed with a BD Bioscience Aria III sorter into a 15 ml polystyrene tube containing 3 ml DC medium with 20 ng/ml Flt3L. CDP gating strategy is shown in Fig. 1.

In other experiments, 6-8 weeks old  $Id2^{eGFP/eGFP}$  reporter mice, which express GFP under the control of the Id2 promoter, were used for CDP sort. The following murine antibodies were used for sample staining: Lineage cocktail containing CD3, Ter119, Gr1, CD11b, B220, NK1.1 and MHCII antibodies and antibodies against CD135, CD11c, CD115, CD117 and Sca1. CDPs were gated as described before in Fig. 1 with the exception of Sca1 antibody instead of MHCII in final gate ( $Lin^- CD135^+ CD115^+ CD117^{low}$  and  $CD11c^- Sca1^-$ ). Purity was

assessed with a Beckman Coulter Gallios flow cytometer. Cells were sorted to greater than 90% of purity. Data were analyzed using Kaluza Software (Beckman Coulter, Krefeld, Germany) or Flow Jo Single Cell Analysis Software v10 (FlowJo LLC, Ashland, USA).

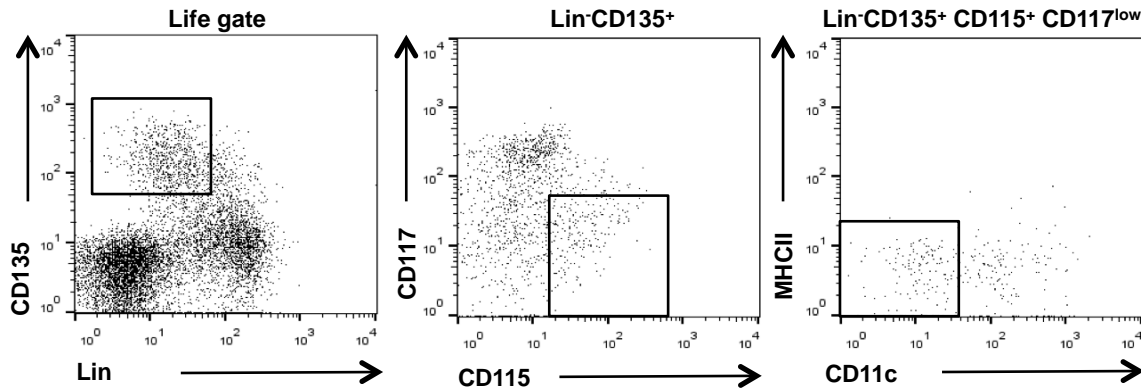


**Fig. 1: Sorting strategy of CDPs**

BM cells were isolated from 6-8 weeks old C57BL/6 mice and stained for cell sorting. BM cells were stained with fluorescently labeled antibodies Lin FITC, CD135 PE, CD115 APC, CD117 e780, CD11c PE-Cy7 and MHCII e450. CDPs were gated as  $\text{Lin}^- \text{CD135}^+ \text{CD115}^+ \text{CD117}^{\text{low}} \text{CD11c}^- \text{MHCII}^-$ . Gating strategy for sorting CDPs is shown.

### 3.2.5.2 Culturing sorted CDPs for *in vitro* experiments

*In vitro* co-culture experiments were performed in 12 well plates (unless stated otherwise). EL08 stromal cells were seeded into 0.1% gelatin coated wells. CDPs were sorted from total BM cells of C57BL/6 mice or  $\text{Id2}^{\text{eGFP/eGFP}}$  reporter mice as described in 3.2.5.1. Thereafter,  $\text{CD45.1}^- \text{CD45.2}^+$  sorted CDPs were cultured with  $2 \times 10^6$  total BM cells/well ( $\text{CD45.1}^+ \text{CD45.2}^-$ ) or with  $4 \times 10^4$  EL08 stromal cells/well in DC medium supplemented with 20ng/ml Flt3L for up to 5 days. One well with only total BM cells was used as a control. Culture medium was not replenished during experiment time. At day 3 and 5, cells were harvested by gentle pipetting and FACS analysis was performed to examine DC differentiation. CDPs were identified from feeder cells and from total BM cells by expression of congenic marker CD45.2.

### 3.2.5.3 pDC subsets sorting for in vivo transfer experiments

Prior to FACS sorting of pDC subsets, DCs were expanded in vivo as described in 3.2.2.3 and BM cells were isolated as described before in 3.2.2.4. Isolated BM cells were resuspended in 500  $\mu$ l staining solution (FACS buffer + FcR blocking buffer, 1:1) with antibodies against Siglec H, B220, CCR9, CD11c and BST2 for 20 min at 4°C in the dark. Subsequently, cells were washed with 30 ml of FACS buffer and resuspended in FACS buffer for cell sorting. BST2<sup>+</sup> Siglec H<sup>+</sup> CD11c<sup>+</sup> cells were sorted into B220<sup>high</sup> CCR9<sup>+</sup> pDCs and two populations of B220<sup>high</sup> and B220<sup>low</sup> CCR9<sup>low/-</sup> pDC-like cells (see Fig. 2, Fig. 22 and Fig. 26) with a Beckman Coulter MoFlow II sorter and collected into a polystyrene 15 ml tube containing DC medium and 20ng/ml Flt3L. Purity was assessed with a Beckman Coulter Gallios flow cytometer. Cells were sorted to greater than 90% of purity. Data were analyzed using Kaluza Software (Beckman Coulter, Krefeld, Germany) or Flow Jo Single Cell Analysis Software v10 (FlowJo LLC, Ashland, USA). Sorted cells were centrifuged at 1500 rpm for 10 min at 4°C and resuspended in PBS and filtered for further experiments.

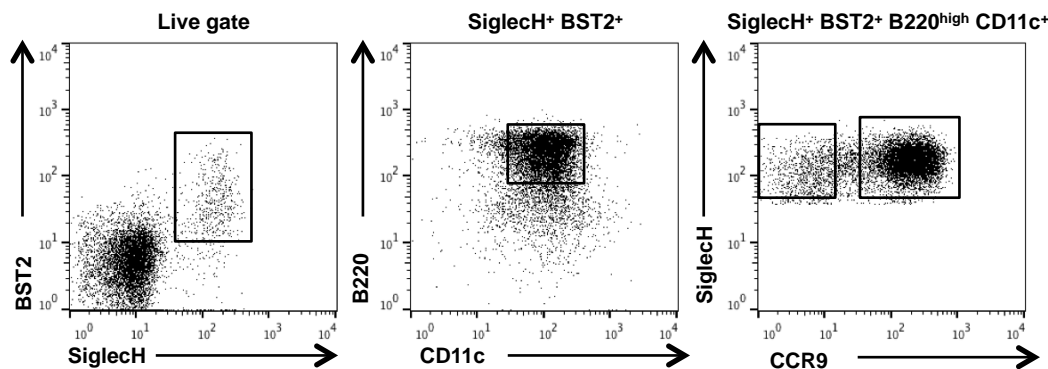


**Fig. 2: Sorting strategy of CCR9 subsets**

BM cells were isolated from CD45.1<sup>+</sup> wild type mice and stained with antibodies against Siglec H-A488, BST2-A647, CD11c-Pe-Cy7, B220 Per-CP and CCR9-PE. Siglec H<sup>+</sup> CD11c<sup>+</sup> BST2<sup>+</sup> cells were further segregated into B220<sup>high</sup> CCR9<sup>high</sup> and B220<sup>high</sup> CCR9<sup>low</sup> populations.

### 3.2.6 Internalization of Siglec H and confocal microscopy

To determine the kinetics of Siglec H internalization, splenocytes were incubated with biotinylated  $\alpha$ -Siglec H antibody (1:200) at 37°C for up to 3 hours. At the indicated time points, surface antibody staining was detected on pDCs (CD11c<sup>int</sup>, B220<sup>+</sup>) with Streptavidin-APC staining and FACS analysis.

For further investigation, Flt3L-cultured BM cells or CDPs were stained with Alexa Fluor 647-conjugated  $\alpha$ -Siglec H antibody (1:4000) at 37°C for 120 hours. Subsequently, cells were stained with LysoTracker Red DND-99, a red fluorescent dye for tracking acidic organelles in living cells, according to the manufacturer's instructions. Just before imaging, cells were placed on ice and FITC-conjugated  $\alpha$ -Siglec H antibody (1:200 dilution) was added to culture medium for detecting surface staining at the end point. Internalization of  $\alpha$ -Siglec H antibody was analyzed using a Leica TSP SP5 II confocal microscope and Leica AF-software. Images were analyzed with 20x magnification (Leica Microsystems, Wetzlar, Germany).

### **3.2.7 Cytokine ELISA protocols**

To detect murine M-CSF and GM-CSF, enzyme-linked immunosorbent assay (ELISA) was performed. M-CSF ELISA was performed by using Duo Set (R&D Systems, Catalog number DY416) and GM-CSF ELISA was performed with matched antibody pairs (capture antibody, 88-7334-CP; detection antibody, 88-7334-DT, eBioscience). ELISA plates were coated with the capture antibody (M-CSF capture 1:250, GM-CSF capture 1:250) in 100  $\mu$ l/well coating buffer and incubated overnight at 4°C. Afterwards, the plates were washed 3 times with wash buffer and incubated with 200  $\mu$ l blocking buffer for 1 h at room temperature. The blocking buffer was aspirated and 50  $\mu$ l/well of the 1:2 standard dilution series (GM-CSF, range from 500 pg/ml – 0,98 pg/ml; M-CSF range from 1000pg/ml – 7,81 pg/ml) and the diluted samples (M-CSF and GM-CSF ELISA, dilution factor 1:5, 1:10 and 1:20) were added and incubated for 3 h at room temperature. After the incubation, plates were washed 4 times, detection antibody was added (50  $\mu$ l/well) at the concentration of 1:250 for both ELISAs and the plates were incubated for 2 h at room temperature. Subsequently plates were washed 4 times, Streptavidin-HRP was diluted to 1:3000, 50  $\mu$ l was added to each well and incubated for 1 h at room temperature. Washing step was repeated after incubation and each well was filled with 100  $\mu$ l of the substrate solution and incubated for 5-10 min. To stop the reaction 100  $\mu$ l stop solution was added to each well. The optical density was measured by the ELISA reader at 405 nm and 495 nm. The resulting standard curve was assessed by point-to-point analysis and the respective cytokine concentrations in the samples were calculated accordingly. The detection limit of the ELISAs lay in the range of 15-30 ng/ml.

### **3.2.8 In vivo mouse experiments**

#### **3.2.8.1 EAE immunization protocol**

Experimental autoimmune encephalomyelitis (EAE) is a murine model of autoimmune disease directed against CNS autoantigens such as MOG peptide.

To induce EAE, mice were immunized by subcutaneous tail base injection (100  $\mu$ L per side) of an emulsion mixed 1:1 from CFA (5 mg/ml Mycobacterium tuberculosis H37Ra in a mineral oil mixture containing Paraffin oil and Arlacel A) and MOG35-55 peptide (final concentration of 2 mg/ml diluted in PBS, 100  $\mu$ g per side). At day 0 and day 2, pertussis toxin (PTx) (final concentration of 2 $\mu$ g/ml diluted in PBS) was injected intravenously (i.v.) (200 $\mu$ g per mouse, 100 $\mu$ g per side). Immunization of mice with MOG/CFA/Ptx resulted in the development of severe signs of illness (score > 2.5) between day 13 and 16. Disease progression and severity were assessed as previously described (Korn, Reddy et al. 2007). Clinical symptoms were scored as depicted in Table 6. These experiments were conducted in collaboration with the laboratory of Thomas Korn.



Score	Symptoms
0	No symptoms
0.5	Beginning of tail paralysis
1.0	Flaccid tail (tail paralysis)
1.5	Flaccid tail and impaired righting reflex
2.0	Paraparesis/hind limb weakness
2.5	Monoplegia (paralysis of one hind limb)
3.0	Paraplegia (paralysis of both hind limbs)
3.5	Paraplegia and weak front limb paralysis
4.0	Tetraplegia (front and hind limb paralysis)
5.0	Moribund

**Table 6: EAE Clinical Score**

### **3.2.8.2 Adoptive transfer of pDC subsets during EAE**

Adoptive transfer of CCR9<sup>+</sup> pDCs and CCR9<sup>low</sup> pDC-like precursor subsets was performed at peak disease, 16 days after EAE induction with MOG peptide. BM cells of mice previously injected with Flt3L melanoma were sorted as described in 3.2.5.3. After cell sorting, pDC subsets were resuspended in PBS and  $5-7 \times 10^5$  cells/mice injected i.v. into the tail vein using 1 ml insulin syringe (200  $\mu$ L per animal), 3 days after transfer, mice were sacrificed by CO<sub>2</sub> asphyxia and analyzed further.

### 3.2.9 Time-lapse imaging and long-term antibody staining of CDP cultures

CDPs were sorted from BM cells of 6-8 weeks old C57BL/6 or  $Id2^{eGFP/eGFP}$  mice as described before in 3.2.5.1. Sorted CDPs were cultured in Ibidi  $\mu$ -slides (I<sup>0.4</sup> Luer series, catalog number 80176) which are specifically designed for microscopic analysis of living cells. The plastic material of Ibidi  $\mu$ -slides has high optical quality similar to glass, which gives a better resolution than standard cell culture plastic dishes.

Ibidi  $\mu$ -slides used in this study are bought uncoated/untreated. One day prior to imaging experiments, Ibidi  $\mu$ -slides were coated with 0.1% gelatin. After 1 h incubation at room temperature,  $\mu$ -slides were washed with PBS once and dried. EL08 stromal cells were resuspended at the concentration of  $2 \cdot 10^5$ /ml and 100  $\mu$ l of cells ( $2 \cdot 10^4$ ) were seeded in Ibidi  $\mu$ -slides in EL08 medium and within 24 h, stromal cells reached 40-50% optical confluence. 24 h after seeding EL08 stromal cells, EL08 medium was removed and replaced with DC medium supplemented with 20 ng/ml Flt3L.

CDPs were sorted as described in 3.2.5.1 and resuspended in DC medium supplemented with 20 ng/ml Flt3L and  $2 \cdot 10^3$  CDPs were seeded on ibidi  $\mu$ -slides. Time-lapse imaging was performed with a cell observer system (Carl Zeiss) at constant 37°C and 5% CO<sub>2</sub>. Bright field images were taken at 2 min intervals and fluorescent images were taken at 3 h intervals with the exception of imaging panel wherein MHCII E450 was included (4 h intervals for MHCII E450) with an AxioCam-HRm camera (1338X1040 pixel resolution) with 10X objective (Carl Zeiss) Carl Zeiss AxioVision 4.5 Software was used in this study.

Long-term antibody staining in living cultures was achieved by „in culture staining“ as described before (Eilken, Nishikawa et al. 2009). Antibody concentration was titrated carefully in order to use the lowest possible concentration to avoid phototoxicity. Antibody concentrations used in this study gave good staining signals, which were detectable by fluorescence microscope (Table 7). During time-lapse imaging, culture medium was not replenished and no additional antibodies were added. For end point analysis, cells were recovered from  $\mu$ -slides by gentle pipetting and FACS analysis was performed directly after imaging, without additional staining.

Florescent Dye	Conjugate	Clone	Concentration (µg/ml)	Dilution
<b>MHCII</b>	BV421	M5/114.15.2	0.0125	1:4000
<b>CD11c</b>	BV421	N418	0.0125	1:4000
<b>MHCII</b>	efluor 450	M5/114.15.2	0.05	1:4000
<b>CCR9</b>	PE	eBioCW-1.2	0.05	1:4000
<b>Siglec H</b>	Alexa 647	440c	0.25	1:4000
<b>CD11c</b>	Alexa 488	N418	0.025	1:20.000

**Table 7: Fluorescently labelled antibodies used in time-lapse imaging experiments**

### 3.2.10 Single cell tracking of CDP progeny

#### 3.2.10.1 Colony creation and single cell tracking

CDPs and their progeny were tracked using TTT, non-commercial tracking software designed by Timm Schroeder, Department of Biosystems Science and Engineering (D-BSSE), ETH Zurich, Basel (Rieger, Hoppe et al. 2009).

For progeny tracking, every second bright field image and every fluorescent image were loaded. Bright field and fluorescent images were synchronized so that occurrence of fluorescent markers could be detected at the same time in multiple channels. Image contrast was optimized for each wavelength channel.

TTT software has two main windows: The movie editor and the cell editor window. In the movie editor window, colony creation was done in the bright field images at time point zero by selecting single CDPs to track. All CDPs in bright field were chosen in order to avoid bias in analysis. After colony creation, progeny of the CDP in the selected positions were observed and manually tracked at each time point. During tracking, all properties such as lost events, cell death, division and onset of fluorescent signals were logged to the pedigree information manually by the user. Cell division is displayed in the pedigree as branching into two daughter cells. Cell death is displayed with “X” symbol and cells lost to tracking are displayed with “?” in the pedigree. The occurrence of each fluorescent marker is denoted by wavelength specific colors. In addition, wavelength specific bold lines denote high expression of fluorescent markers. All relevant information saved during tracking was visualized in pedigree trees. Imaging data was further analyzed in apposite software called staTTTs.

### **3.2.10.2 Analysis of tracked colonies in staTTTs**

Pedigrees were loaded in staTTTs analysis software. Pedigrees, which were lost to tracking or apoptotic before 36 h of experiment time, were excluded from the analysis. To segregate the phenotype of the cells, cell filters were created with staTTTs.

### **3.2.10.3 Creating cell filters for the progeny**

When loading selected CDP pedigrees into staTTTs, all cells are automatically divided into three categories: Dividing, non-dividing and apoptotic.

For time-lapse experiments, wherein CDPs from C57BL/6 wildtype mice were used, all progeny, which were generated during the experiment time (1-120 h), were divided into two main categories by their CD11c and MHCII expression. CD11c<sup>+</sup>MHCII<sup>+</sup> cells consist of pDCs and cDCs, which can be distinguished by their Siglec H expression. CD11c<sup>+</sup>MHCII<sup>+</sup>Siglec H<sup>+</sup> cells include CCR9<sup>high</sup> pDCs and CCR9<sup>low</sup> pDC-like cells; CD11c<sup>+</sup>MHCII<sup>+</sup>Siglec H<sup>-</sup> cells include cDCs. The second main category, CD11c<sup>+</sup>MHCII<sup>-</sup> cells contain undifferentiated DC precursors (pre-DCs). Further categorization is shown in Fig. 3. Cell filters were created by using Boolean gates. To create Boolean gates, existing gates and AND/NOT functions were used.

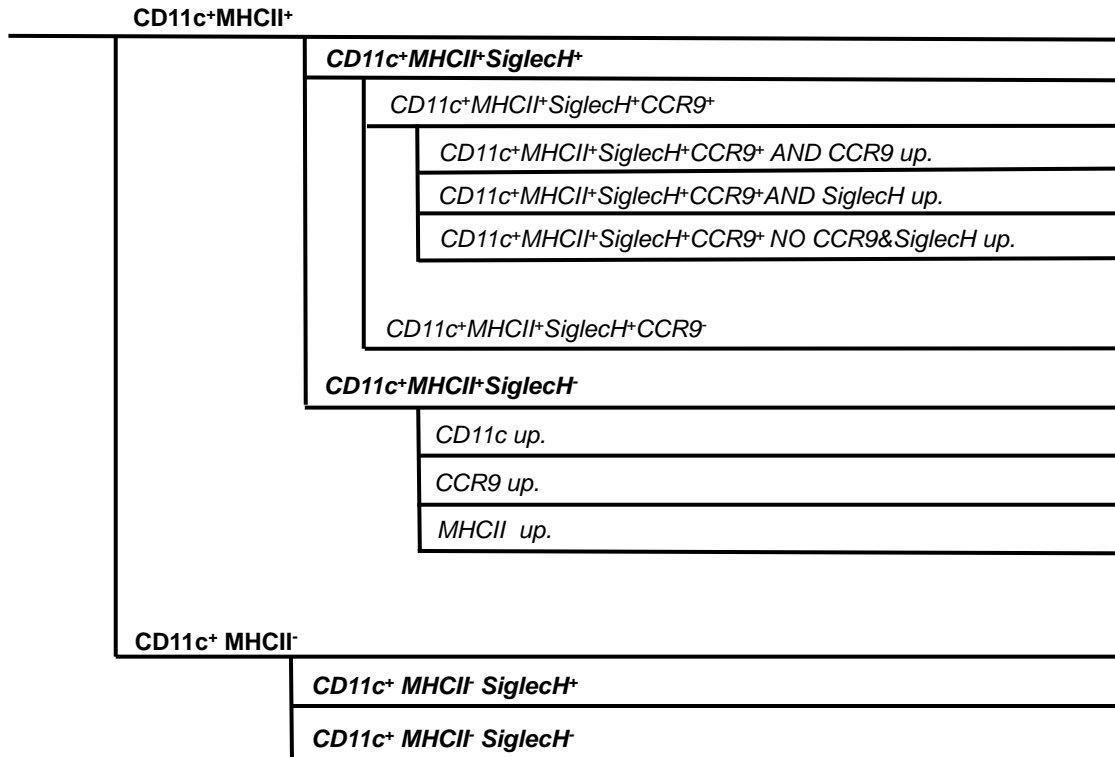


**Fig. 3: Cell filters created for time-lapse imaging of C57BL/6 wildtype CDP cultures**

For experiments in which CDPs from Id2<sup>eGFP/eGFP</sup> reporter mice were used, cells were first filtered by their CD11c expression. Thereafter, presence of GFP expression was used as second filter. CD11c<sup>+</sup> GFP<sup>+</sup> cells consist of pDCs and cDCs as well as undifferentiated DC precursors.

CD11c<sup>+</sup> GFP<sup>+</sup> cells were further divided into two main categories by their Siglec H expression. CD11c<sup>+</sup> GFP<sup>+</sup> Siglec H<sup>+</sup> cells include mostly CCR9<sup>high</sup> pDCs and CCR9<sup>low</sup> pDC-like cells. CD11c<sup>+</sup> GFP<sup>+</sup> Siglec H<sup>-</sup> cells include cDCs and some undifferentiated cells, which express CCR9 but not Siglec H. These cells were considered as undifferentiated cells, which were not further assessed. Within CD11c<sup>+</sup> GFP<sup>+</sup> Siglec H<sup>-</sup> cells, cells with high GFP expression (GFP up) were considered as cDCs. CD11c<sup>+</sup> GFP<sup>-</sup> cells were a minor population and they were not further assessed (Fig. 4).

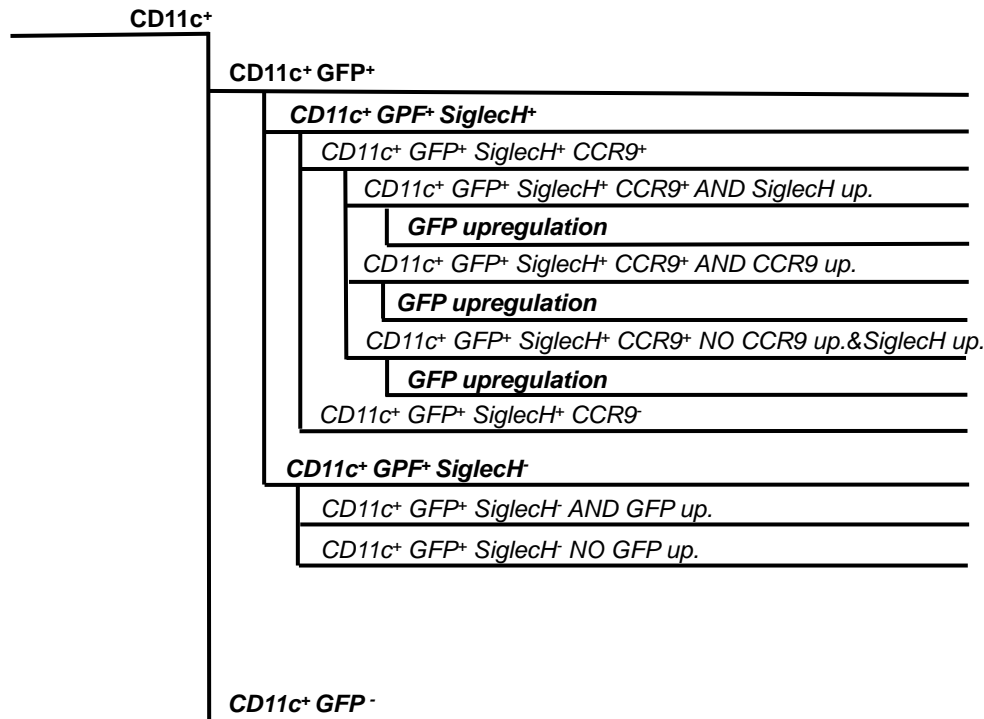


Fig. 4: Cell filters created for time-lapse imaging of ID2<sup>eGFP/eGFP</sup> CDP cultures

#### 3.2.10.4 Creating tree filters for analysis of the progeny

Similar to cell filters, tree filters can be created with staTTTs software based on number of generations, tree lifetime and occurrence of fluorescent markers. In addition, by looking at the end point phenotype of the CDP progeny in each pedigree, pedigrees can be filtered by their cell fate choices as: pedigree with CCR9<sup>+</sup> pDC fate, pedigree with CCR9<sup>low</sup> pDC-like fate, pedigree with both CCR9<sup>+</sup> pDC fate and CCR9<sup>low</sup> pDC-like fate, pedigree with cDC fate and pedigree with pre-DC fate. Trees that were not fulfilling given criteria were categorized as undifferentiated.

#### 3.2.11 Statistical analysis

Statistical analysis was performed using GraphPad Prism. Testing for Gaussian distribution was done using D'Agostino Pearson normality test. For two-group comparison of normally distributed variables unpaired two-tailed Student's t-test was used. For detecting differences in the time points of occurrence between several fluorescent markers, which did not show Gaussian distributions and equal variances, the non-parametric Kruskal-Wallis test followed

by Dunn's multiple comparison test was used. P values < 0.05 were considered significant and indicated with asterisks.

---

## 4 Results

### 4.1 Continuous observation of CDP differentiation into DCs on the single cell level

It has been shown that CCR9<sup>low</sup> pDC-like cells derived from murine BM have a common DC precursor function in vivo and retain the ability to differentiate into pDCs and cDCs (Schlitzer, Heiseke et al. 2012). It is still obscure at which developmental stage final commitment to the pDC lineage occurs. In this study, we postulated that CDPs are heterogeneous and within the progenitor pool, pre-committed cells exist, which can differentiate into pDCs or cDCs. My hypothesis was that CCR9<sup>+</sup> pDCs develop from CDPs via a distinct precursor stage characterized by expression of pDC markers (Siglec H, MHCII and CD11c) but low expression of CCR9. To test this, we set up an in vitro culture system to follow individual CDPs and their progeny continuously under the fluorescent microscope.

#### 4.1.1 Differentiation of CDPs into pDCs and cDCs is supported by co-culture with a stromal cell line derived from embryonic liver cells

Dishes coated with extracellular matrices, such as collagen and fibronectin, are commonly used for stem cell cultures. Some HSCs can grow on coated surfaces but some need feeder cells to differentiate. For CDPs, it was shown that they could differentiate into DCs in co-culture with feeder cells, such as total BM cells and the OP9 cell line.

The survival time of sorted CDPs in Flt3L containing medium was tested on fibronectin and gelatin coated surfaces without feeder cells but was less than 24 h (data not shown). It has been shown that stromal cells derived from Aorta-gonad-mesonephros (AGM) region can be used to support differentiation of HSCs (Oostendorp, Harvey et al. 2002). In this study, EL08 cell line, derived from mouse fetal embryonic liver cells was used as feeder cells for co-culture with CDPs due to their flat morphology which is suitable for imaging experiments.

The optimal seeding density, which resulted in 50% optical confluence, was established for EL08 cells and was found to be  $4 \times 10^4$  cells/well (data not shown).



To assess whether EL08 feeder cells support in vitro differentiation of CDPs in long-term cultures, CDPs were sorted from total BM cells and cultured as described previously (3.2.5.1).

DC subsets were defined based on surface marker expressions. pDCs were CD11c<sup>+</sup> Siglec H<sup>+</sup> and MHCII<sup>low</sup> whereas cDCs were CD11c<sup>+</sup> Siglec H<sup>-</sup> MHCII<sup>high</sup>. After 3 days of culture, CDPs co-cultured with feeder cells gave rise to both DC subtypes in vitro. In total BM co-cultures percentages of pDCs and cDCs generated were similar to those in EL08 co-cultures (Fig. 5A)

Furthermore, the frequency of CCR9<sup>+</sup> pDCs and CCR9<sup>low</sup> pDC-like cells generated from both co-culture systems was assessed. After 5 days of culture, differentiation efficiency of CDPs into CD11c<sup>+</sup> Siglec H<sup>+</sup> MHCII<sup>+</sup> CCR9<sup>+</sup> pDCs and CD11c<sup>+</sup> Siglec H<sup>+</sup> MHCII<sup>+</sup> CCR9<sup>low</sup> pDCs was comparable in both culture systems (Fig. 5B).

Thus, EL08 feeder cells support maintenance and the development of CDPs into both pDCs and cDCs in long-term cultures.

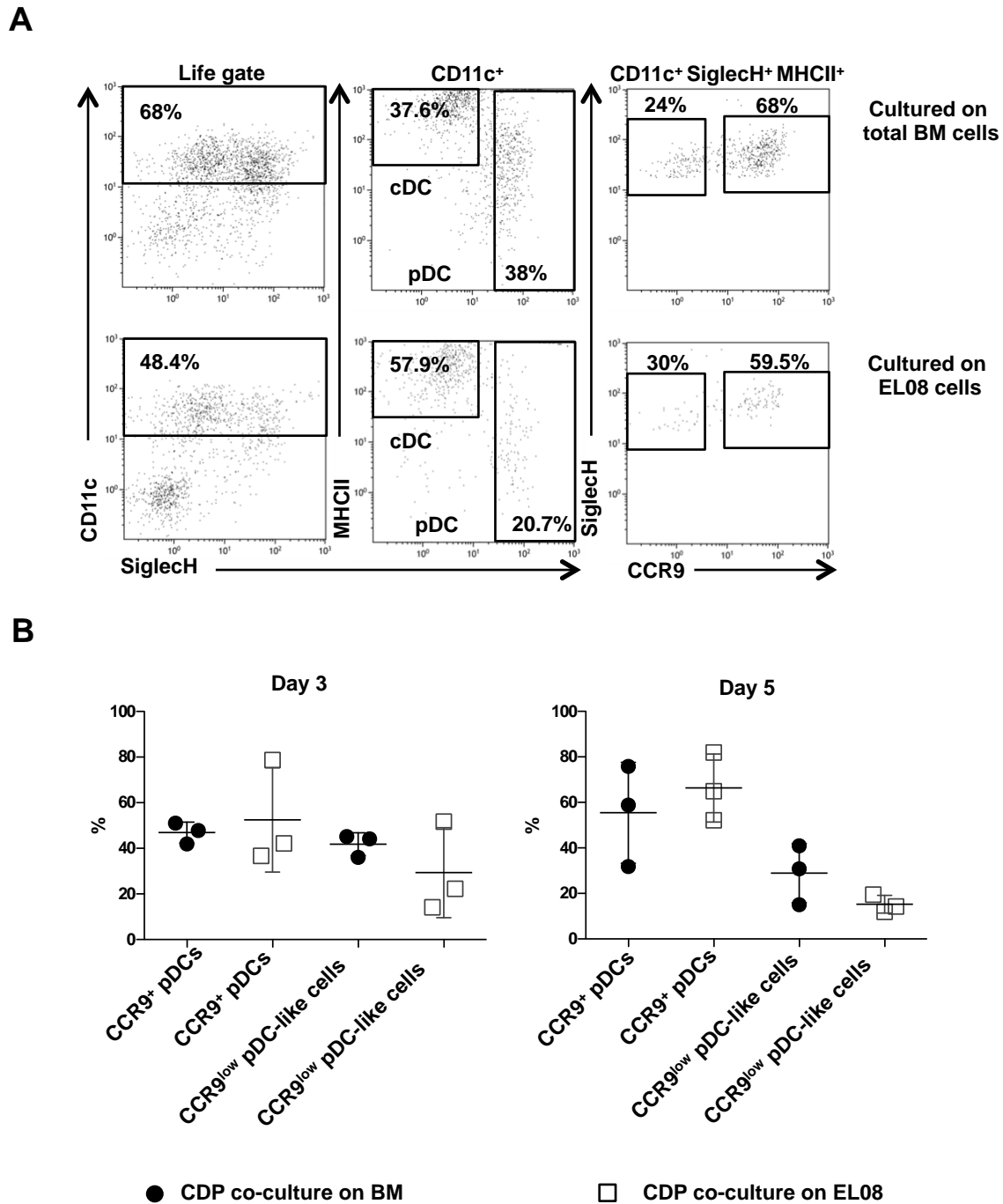


**Fig. 5: Phenotype of DCs generated from CDPs in EL08 culture system in the presence of Flt3L**  
**(A)** CDPs ( $CD45.2^+$ ) were co-cultured either with total BM cells ( $CD45.1^+$ ) or on EL08 feeder cells in the presence of 20ng/ml Flt3L for 3 days. The percentages of pDCs, cDCs and  $CCR9^+$  and  $CCR9^{low}$  pDC subtypes were determined by FACS analysis. Results of one representative of 3 experiments are shown. **(B)** CDPs were cultured on total BM cells or on EL08 feeder cells for 3 and 5 days. The percentages of  $CCR9^+$  and  $CCR9^{low}$  pDC subtypes as determined by FACS analysis are shown. The results of three independent experiments are shown. The mean values and standard deviations are indicated.

#### **4.1.2 The EL08 stromal cell line has supportive but not instructive effect on CDPs**

It is known that feeder cells do not just provide a microenvironment for survival; they also secrete cytokines, some of which are unknown. Since Flt3L was the only cytokine added in this culture system, the role of additional cytokine secretion by the stromal cells for the development of DCs remained unclear. It is known that EL08 stromal cells when cultured with human umbilical cord blood cells, secrete small amounts of murine cytokines (McCullar, Oostendorp et al. 2008)

To test whether the co-culture with EL08 stromal cells contains cytokines, which may have an additional effect on differentiation of CDPs, murine M-CSF and GM-CSF levels in co-culture supernatants were measured by high sensitivity ELISA. EL08 stromal cells did not secrete enough murine M-CSF or GM-CSF to be detected by ELISA in supernatants collected after 3 and 5 days of co-culture (data not shown). Hence, additional effects of M-CSF or GM-CSF produced by stromal cells can be excluded.

#### **4.1.3 Analysis of individual CDP differentiation by continuous single cell tracking**

In this study, EL08 stromal cells used as feeder layer provided a suitable milieu for development of CDPs in vitro. In addition, this flat morphology allowed us to easily distinguish sorted CDPs from feeder cells in microscopic images without using congenic markers. The increase in cell density in the culture indicated a strong proliferation capacity of the CDPs and their progeny in those culture conditions (**Fig. 6**).

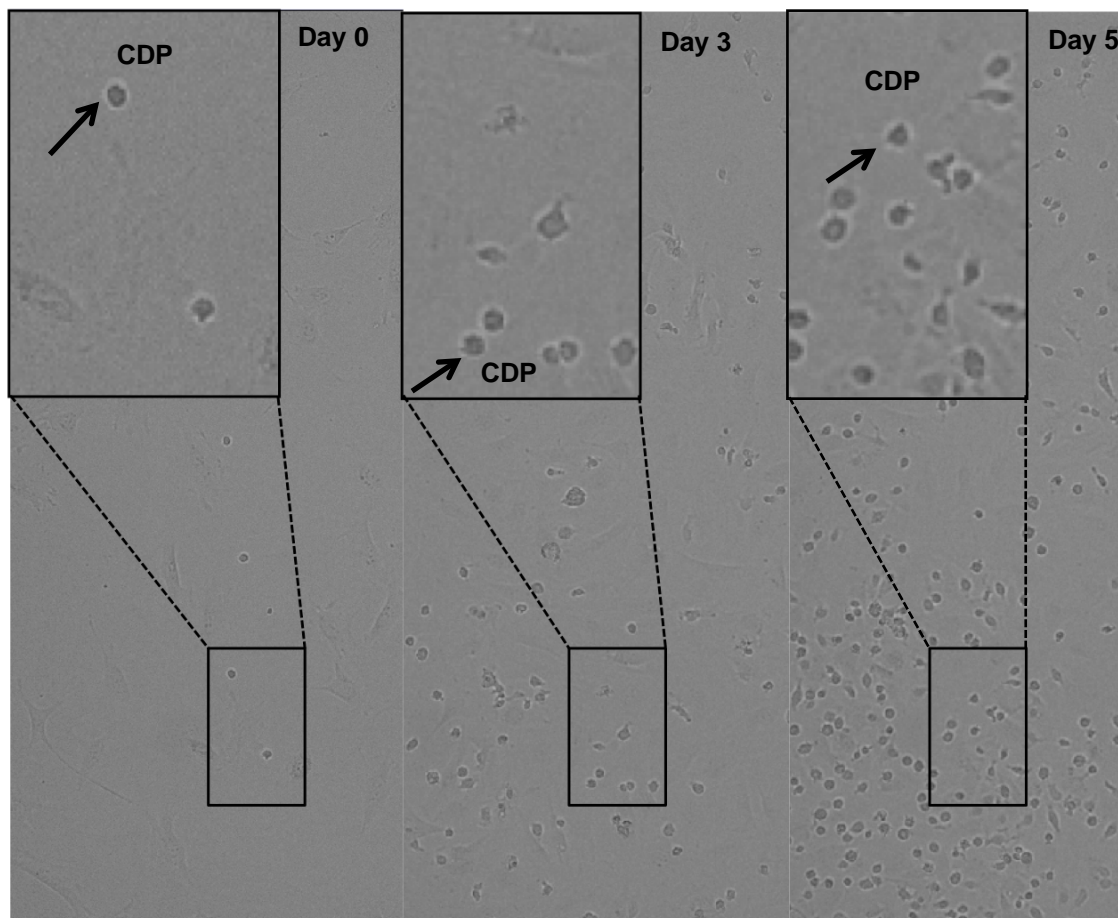


**Fig. 6: Phase contrast images of sorted CDPs on stromal cells**

Phase contrast images of CDPs and EL08 stromal cells in co-culture system are shown. Arrows indicate CDPs.

For live cell imaging experiments, CDPs were purified from BM cells of C57BL/6 wildtype mice and seeded at the density of  $2 \times 10^3$  cells in Ibidi  $\mu$ -slides. Live cell imaging was performed as described before in 3.2.9 up to 120 h.

A total of 650 cells were tracked in 40 different pedigrees. Pedigrees, which were lost to tracking or apoptotic before 36 h of experiment time were discarded. Although, some cells went under the stroma and were lost to tracking, the majority of the cells could be followed until the end of the experiment time (120 h). Even though culture medium was not replenished or Flt3L was not readded to the culture during imaging, the proliferation and differentiation capacity of progenitor cells were unimpaired. As shown in Fig. 7, only 4% of the cells were apoptotic and they were excluded from the analysis. 12% of the CDP progeny were lost during tracking and 84% of them were tracked without getting lost during their lifetime until the end of the experiment.

Among all the cells that were “not lost”, 56% of them were dividing and 44% of them were non-dividing cells indicating proliferative capacity of the CDP progeny. “Non-dividing” category also includes cells which are generated later during the experiment and which may have divided at later time points, if the experiment had not been finished after 120 h (Fig. 7B). Of the 40 pedigrees, which were generated, only 2 showed no division during the experiment time.

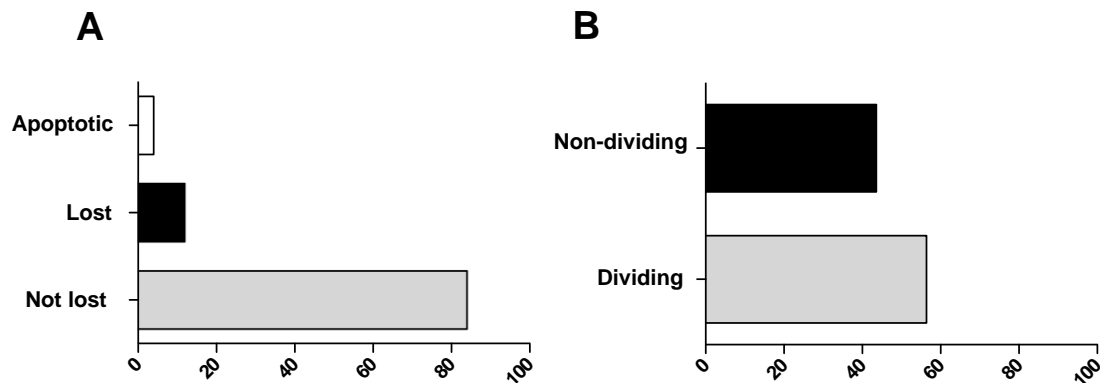


**Fig. 7: Quantitative analysis of the progeny by single cell tracking**

**(A)** CDPs were cultured on EL08 feeder cells for 5 days. CDP progeny was followed by time-lapse microscopy and single cell tracking. The percentage of apoptotic, lost and continuously tracked (not lost) is shown. **(B)** The percentage of dividing and non-dividing cells among “not lost” cells is shown.

The imaging system is limited by the number of lasers/detectors available, which led us to make a selection of surface markers. CD11c and MHCII, well known DC markers, were used to define DC of all types. Siglec H surface marker served as a marker for identifying pDCs and pDC-like cells. CCR9 and/or Siglec H high expression was used to define CCR9<sup>+</sup> pDCs. CCR9 and Siglec H presence but not high expression was used to define CCR9<sup>low</sup> pDC-like cells. Detection of surface molecules is exemplified in Fig. 8. Definition of DC subsets by combining fluorescently labeled antibodies in time-lapse imaging experiments is shown in Table 8.

Marker	CDP	Pre-DC	cDC	CCR9 <sup>+</sup> pDC	CCR9 <sup>low</sup> pDC-like cells
CD11c	-	+	+	+	+
MHCII	-	-	+	+	+
Siglec H	-	+/-	-	+ and/or high	+
CCR9	-	-	-	high	+

**Table 8: Definition of DC subsets in time-lapse imaging experiments performed with cells from C57BL/6 mice**

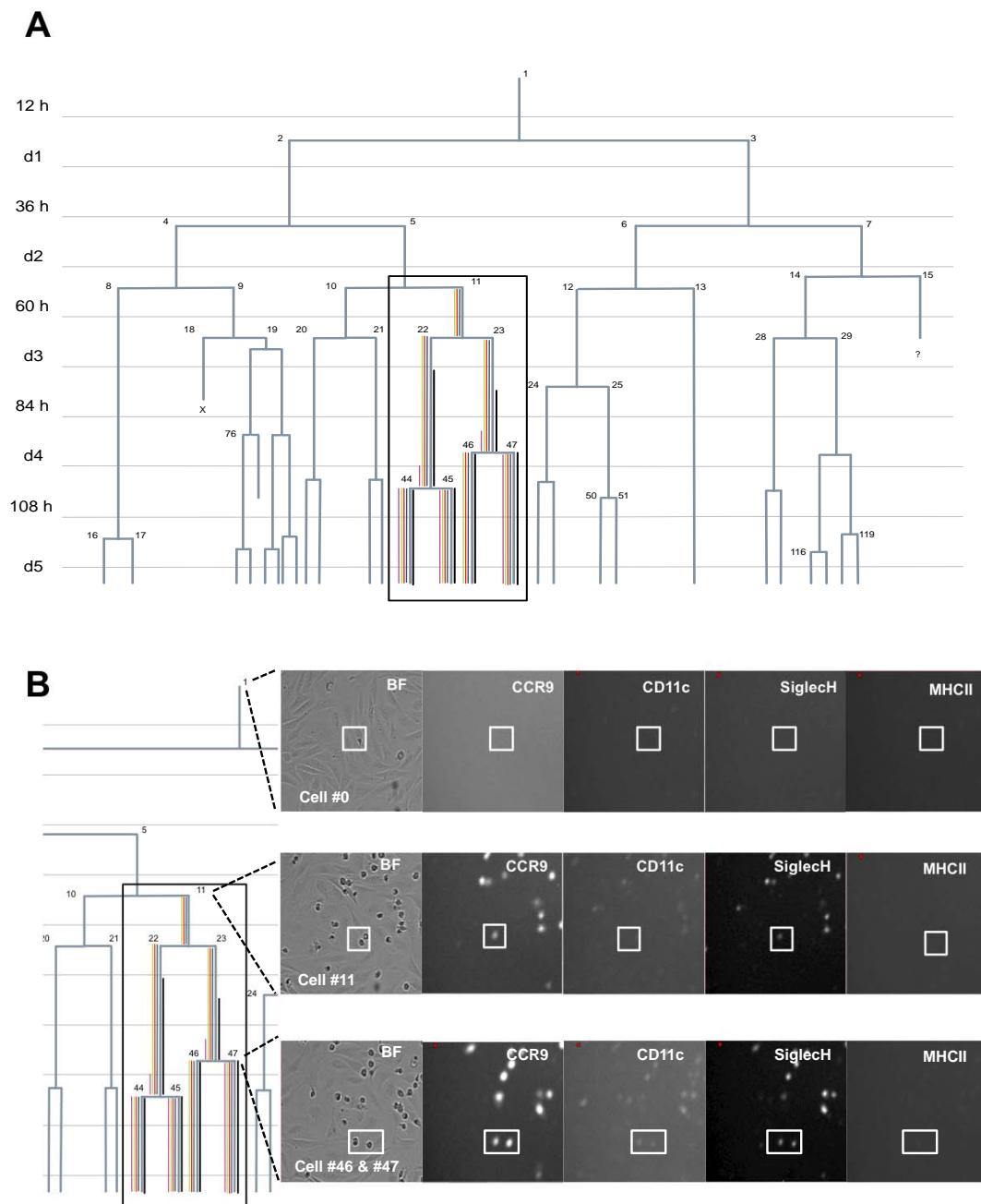


**Fig. 8: Detection of surface molecules using fluorescently labelled antibodies in living cells**

**(A)** A representative pedigree of a single CDP and its progeny is shown. CDPs were cultured on EL08 feeder cells for 5 days. Fluorescently labeled antibodies against Siglec H, CCR9, CD11c and MHCII were added at the start of the experiment. CDP and their progeny were monitored by time-lapse microscopy and single cell tracking. All relevant information was recorded and annotated in colored lines. Each colored line denotes one fluorescent marker (Green: CCR9; Red: CD11c; Blue: Siglec H; Pink: MHCII). Bold lines denote upregulation of certain fluorescent markers. Here for example bold black line indicated CCR9 upregulation. Apoptotic events marked with "X" whereas lost events are indicated with a question mark. **(B)** Bright field and fluorescent images of indicated cells are shown.

Continuous observation of CDPs over time provided insights into the onset of surface marker expressions in real time. In each pedigree the time point of first occurrence of each marker was recorded; CD11c expression onset happened generally earlier than onset of other fluorescent markers (mean  $\pm$  SD, 25h  $\pm$  13h) and was followed by Siglec H and CCR9 expression onset (Fig. 9A). The time point of first occurrence of each marker was recorded for all dividing cells in pedigrees. CD11c was the first marker that was expressed by dividing cells in all trees. Siglec H and CCR9 expression followed CD11c expression and occurrence of MHCII was delayed (Fig. 9B). This indicates that only onset of CD11c marks the pre-DC identity defined as CD11c<sup>+</sup> MHCII<sup>-</sup> at earlier time points.

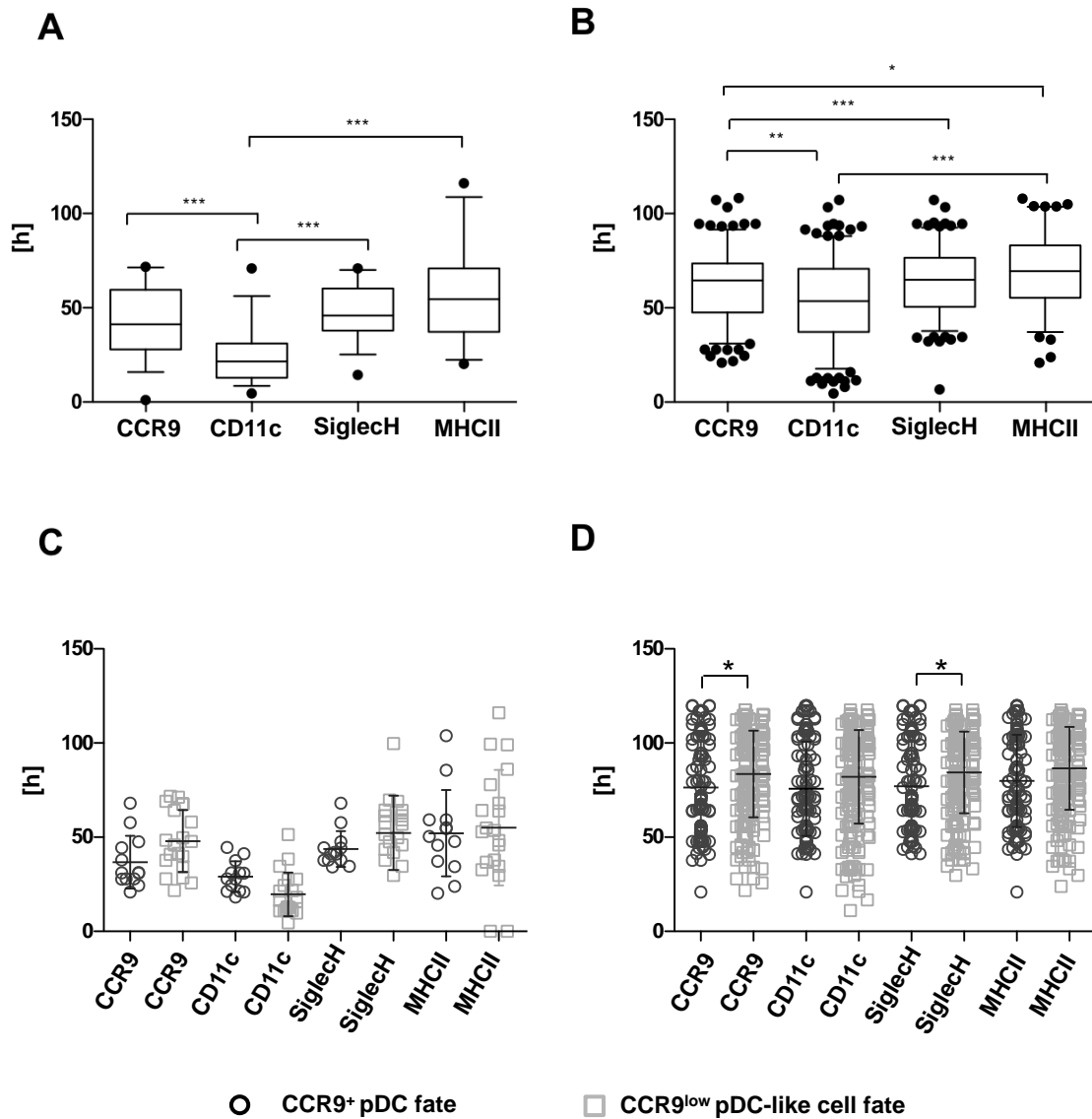


**Fig. 9: The time point of occurrence of fluorescent markers**

CDPs were cultured on EL08 cells for 5 days and tracked as described previously. The single cell tracking data was analyzed quantitatively using staTTT's software. **(A)** The time point of first occurrence of fluorescent markers in different pedigrees is shown (n=40 pedigrees) as box plots (bars indicate 5-95% percentile; dots represent outliers). **(B)** The time point of first occurrence of fluorescent markers in different cells is shown as box plots (CCR9, n=199; CD11c, n=256; Siglec H, n=182, MHCII, n=102) (bars indicate 5-95% percentile; dots represent outliers). **(C)** Pedigrees were separated according to their cell fate choices (CCR9<sup>+</sup> pDC fate and CCR9<sup>low</sup> pDC-like fate) and time point of first occurrence of the markers is shown for distinct pedigrees (CCR9<sup>+</sup> pDCs, n=13; CCR9<sup>low</sup> pDC-like cells, n=20). **(D)** Time point of first occurrence of fluorescent markers is shown in all cells in pedigrees with CCR9<sup>+</sup> pDC fate or pedigrees which only contained CCR9<sup>low</sup> pDC-like cells. Statistical analysis was performed using Kruskal-Wallis and Dunn's multiple comparison tests (\* p<0.05; \*\* p ≤ 0.01; \*\*\* p ≤ 0.001).



---

A similar analysis was performed in pedigrees, which have distinct cell fate choices. CDP and its progeny produced pedigrees with cDC fate, pre-DC fate and pDC fate, which were composed of pedigrees with CCR9<sup>+</sup> pDC fate and pedigrees with CCR9<sup>low</sup> pDC-like cell fate. Here, we focus only on pedigrees with CCR9<sup>+</sup> pDC fate and CCR9<sup>low</sup> pDC-like fate. As shown in Fig. 9C, there was a trend towards later onset of CCR9 and Siglec H expression in pedigrees with development of only CCR9<sup>low</sup> pDC-like cells but not in pedigrees with CCR9<sup>+</sup> pDCs. On the other hand, when individual cells were assessed in those pedigrees, CCR9 and Siglec H expression onset occurred earlier in pedigrees with CCR9<sup>+</sup> pDC fate than in pedigrees with CCR9<sup>low</sup> pDC-like cell fate (Fig. 9D). These results suggest that CCR9<sup>+</sup> pDCs, which were generated during 120 h of experiment time, were derived from CDP, which were already further differentiated from the beginning on.

In addition to onset of multiple fluorescent markers, division kinetics can be associated with cell fates. Pedigrees were segregated as described previously. CDPs that were generating fully differentiated CCR9<sup>+</sup> pDCs divided more often than CDPs that only gave rise to CCR9<sup>low</sup> pDC-like cells during the experiment time (Fig. 10A). To investigate whether the number of generations of a given pedigree has any correlation with cell cycle times, lifetime of dividing cells in pedigrees with CCR9<sup>+</sup> pDCs or CCR9<sup>low</sup> pDC-like cells were assessed, but no significant difference was found (Fig. 10B).

CDP lifetime until the first division was similar in CDPs giving rise CCR9<sup>+</sup> pDCs and CDPs giving rise to CCR9<sup>low</sup> pDC-like cells ( $14.8 \pm 6.7$  h vs  $13.2 \pm 7$  h). In contrast, CDP lifetime until first division was longer in CDP generating cDCs (33h, 43h).

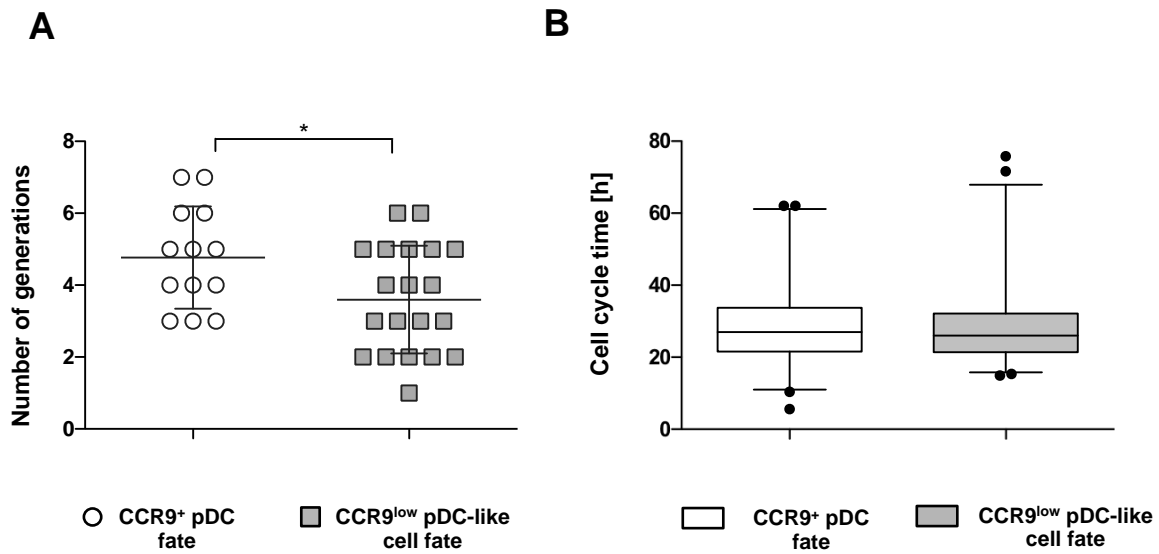


**Fig. 10: Number of generations and cell cycle times of CDP progenies**

**(A)** CDPs were cultured on EL08 feeder cells for 5 days and progenies of the CDP were tracked continuously. Pedigrees were segregated according to their cell fate choices. The number of generations in each pedigree shown in symbols (CCR9<sup>+</sup> pDCs, n=13; CCR9<sup>low</sup> pDC-like cells, n=20). **(B)** The cell cycle time is shown in all dividing cells in pedigrees with CCR9<sup>+</sup> pDC fate and CCR9<sup>low</sup> pDC-like cell fate (CCR9<sup>+</sup> pDCs, n=42; CCR9<sup>low</sup> pDC-like cells, n=56). Statistical analysis between groups was performed using t-test (\* indicates  $p < 0.05$ ).

#### 4.1.4 CDP differentiation into CCR9<sup>+</sup> pDCs and CCR9<sup>low</sup> pDC-like cells

In this study, we integrated the population-based approach into a single cell observation model to better link kinship between CDPs, CCR9<sup>+</sup> pDCs and CCR9<sup>low</sup> pDC-like cells.

Cell filters were created including all cells during the experiment time (1-120 h) with boolean gates. One or more cell properties can be implemented into one cell filter. Cells, which were fulfilling given criterias fell into the respective cell filters (see Fig. 11).

Almost one half of the CDP progeny generated within 1-120 h of experiment time, expressed CD11c and MHCII (49.5%) and were classified as „DC of all subtypes“. 38.2% of the progeny were CD11c<sup>+</sup> MHCII<sup>-</sup> suggesting that this population could contain some undifferentiated cells in the pre-DC stage or that MHCII expression was below detection limit. Subsequently, CD11c<sup>+</sup> MHCII<sup>-</sup> cells were further divided into two categories by their Siglec H expression. CD11c<sup>+</sup> MHCII<sup>-</sup> Siglec H<sup>-</sup> and CD11c<sup>+</sup> MHCII<sup>-</sup> Siglec H<sup>+</sup> fractions contained cells that expressed CCR9 but CCR9 upregulation was never observed. It is known that Siglec H is a surface marker, which is found in all pDCs. Hence, CD11c<sup>+</sup> MHCII<sup>-</sup> Siglec H<sup>-</sup> CCR9<sup>+</sup> cells were not classified as pDCs due to the absence of Siglec H. CD11c<sup>+</sup> MHCII<sup>-</sup> Siglec H<sup>+</sup> cells expressed CCR9 but lack MHCII. Hence, they were considered as precursors of CCR9<sup>low</sup> pDC like-cells or Siglec H<sup>+</sup> pre-DCs. The analysis of cell fates was focused only on CD11c<sup>+</sup> MHCII<sup>+</sup> cells that contained DCs of all subtypes.

CD11c<sup>+</sup>MHCII<sup>+</sup> cells were then further divided into two categories based on their Siglec H expression as CD11c<sup>+</sup>MHCII<sup>+</sup> Siglec H<sup>+</sup> cells and CD11c<sup>+</sup> MHCII<sup>+</sup> Siglec H<sup>-</sup> cells. CCR9<sup>+</sup> pDCs were defined as CD11c<sup>+</sup> MHCII<sup>+</sup> Siglec H<sup>+</sup> CCR9<sup>high</sup> and/or Siglec H<sup>high</sup>. In contrast, CCR9<sup>low</sup> pDC-like cells were defined as CD11c<sup>+</sup> MHCII<sup>+</sup> Siglec H<sup>+</sup> CCR9<sup>+</sup>, with neither high expression of Siglec H nor CCR9. cDCs were defined as CD11c<sup>+</sup>MHCII<sup>+</sup> Siglec H<sup>-</sup> with the possibility to upregulate CD11c or MHCII.

By filtering cells based on solely their surface marker expression, we observed that Siglec H signal occurred in the majority of CD11c<sup>+</sup>MHCII<sup>+</sup> cells (91.6%). Timing of Siglec H onset differed between daughter cells. A minor population, 8.4% of CD11c<sup>+</sup>MHCII<sup>+</sup> cells, did not show any Siglec H expression over time suggesting that these cells could be cDCs. Indeed, 25.9% of CD11c<sup>+</sup> MHCII<sup>+</sup> Siglec H<sup>-</sup> cells expressed high levels of MHCII indicating a cDC phenotype. Within this group, CCR9 or CD11c high expression was not observed.

CD11c<sup>+</sup> MHCII<sup>+</sup> Siglec H<sup>+</sup> cells were further filtered. Almost all of the cells in this group expressed CCR9 at different time points (hereafter called pDCs). 8.6 % of pDCs had a very high signal for Siglec H (CD11c<sup>+</sup> MHCII<sup>+</sup> Siglec H<sup>+</sup> and Siglec H<sup>high</sup>), 23.6% of pDCs upregulated CCR9, and together with Siglec H<sup>high</sup> cells contributed to the group of differentiated CCR9<sup>+</sup> pDCs. CCR9 upregulation occurred around day 3 (63.8 h  $\pm$  12.8 h) whereas Siglec H upregulation was observed at later time points (83.3 h  $\pm$  9.6 h). 66.7% of CD11c<sup>+</sup> Siglec H<sup>+</sup> MHCII<sup>+</sup> CCR9<sup>+</sup> cells did not show any CCR9 or Siglec H high expression and they were categorized as CCR9<sup>low</sup> pDC like cells (Fig. 11). The CCR9<sup>low</sup> pDC-like cell phenotype was maintained for 66.1  $\pm$  24.5 h in these pedigrees.

	<b>%Parent</b>
<b>CD11c<sup>+</sup>MHCII<sup>+</sup></b>	<b>49.5%</b>
<b>CD11c<sup>+</sup>MHCII<sup>+</sup>SiglecH<sup>+</sup></b>	<b>91.6%</b>
CD11c <sup>+</sup> MHCII <sup>+</sup> SiglecH <sup>+</sup> CCR9 <sup>+</sup>	<b>98.6%</b>
CD11c <sup>+</sup> MHCII <sup>+</sup> SiglecH <sup>+</sup> CCR9 <sup>+</sup> AND CCR9 up.	<b>23.6%</b>
CD11c <sup>+</sup> MHCII <sup>+</sup> SiglecH <sup>+</sup> CCR9 <sup>+</sup> AND SiglecH up.	<b>8.6%</b>
CD11c <sup>+</sup> MHCII <sup>+</sup> SiglecH <sup>+</sup> CCR9 <sup>+</sup> NO CCR9&SiglecH up.	<b>66.7%</b>
CD11c <sup>+</sup> MHCII <sup>+</sup> SiglecH <sup>+</sup> CCR9 <sup>-</sup>	<b>1.4%</b>
<b>CD11c<sup>+</sup>MHCII<sup>+</sup>SiglecH<sup>-</sup></b>	<b>8.4%</b>
CD11c up.	<b>0%</b>
CCR9 up.	<b>0%</b>
MHCII up.	<b>25.9%</b>
<b>CD11c<sup>+</sup> MHCII<sup>-</sup></b>	<b>38.2%</b>
<b>CD11c<sup>+</sup> MHCII<sup>-</sup> SiglecH<sup>+</sup></b>	<b>66.5%</b>
<b>CD11c<sup>+</sup> MHCII<sup>-</sup> SiglecH<sup>-</sup></b>	<b>33.5%</b>

**Fig. 11: Results of cell filter analysis of CDP and its progeny**

CDPs were cultured on EL08 cells for 5 days and tracked continuously using TTT software. The imaging data was analyzed using staTTTs software. Cell filters were created for progeny of the CDP. The percentages of all cells fulfilling the indicated properties at any time point during the experiment time (1-120 h) are shown.

On the basis of my observations, I conclude that commitment to a unique and specific lineage could occur at any time during development. In 13 pedigrees with CCR9<sup>+</sup> pDC fate, lineage commitment to CCR9<sup>+</sup> pDCs occurred in a step-wise manner via CCR9<sup>low</sup> pDC-like cells. CCR9<sup>low</sup> pDC-like cells upregulate CCR9 and/or Siglec H and develop into CCR9<sup>+</sup> pDCs. Upregulation of CCR9 or Siglec H in the majority of the cases occurred in the presence of the respective markers. The transition time from first occurrence of the CCR9 signal until the upregulation of CCR9 varied greatly ranging from < 10 h to > 35 h. Immediate upregulation of CCR9 and expression of Siglec H (direct commitment) from the CDP was observed rarely (5 cells in 2 pedigrees).

It can be concluded from these observations that the majority of pDCs develop from CDPs via a transitory stage characterized by expression of CD11c, MHCII and Siglec H, but lack of or lower expression of CCR9. This transitory stage can be very short or can take longer.

#### 4.1.5 CDPs are heterogeneous and imprinted to give rise to pDCs or cDCs

End point FACS analysis of lineage output confirmed the live cell imaging observations to a large extent. As shown in Fig. 12A, CDPs gave rise to large numbers of CD11c<sup>+</sup> cells. 14% of CD11c<sup>+</sup> cells expressed MHCII surface marker at higher levels and were Siglec H negative (cDCs). 17% of CD11c<sup>+</sup> cells were Siglec H<sup>+</sup> and MHCII<sup>+</sup>. MHCII expression was lower in these cells than in cDCs. Cells with pDC phenotype contained 62% CCR9<sup>high</sup> pDCs and 30% CCR9<sup>low</sup> pDC-like cells. FACS analysis at the end of the experiment showed that, CDPs gave rise to a higher number of CD11c<sup>+</sup> MHCII<sup>high</sup> cDCs than the number of cDCs, which were identified by live cell imaging. MHCII signal intensity was only weakly detectible by live cell imaging. This may lead to underestimate the number of cDCs, which were generated and to overestimate the number of undifferentiated pre-DCs (CD11c<sup>+</sup> MHCII<sup>-</sup>). The number of CCR9<sup>+</sup> pDCs may also have been underestimated, as only pDCs with very high intensity of the CCR9 signal and/or very high Siglec H signal in the imaging analysis were counted as definitive CCR9<sup>+</sup> pDCs.

Heterogeneity is more pronounced when looking at the lineage output at the single cell level (Fig. 12B). Within 5 days, CDPs gave rise to pedigrees with either pDC or cDC differentiation. Pedigrees containing both cell fates (CCR9<sup>+</sup> pDCs and cDCs) were not observed during this time. The majority of CDPs generated only CCR9<sup>low</sup> pDC-like cells (18 of 20 CCR9<sup>low</sup> pDC-like pedigrees). In addition, CCR9<sup>low</sup> pDC-like cells were found together with cDCs in 2 pedigrees. Live cell imaging observations suggested, many undifferentiated

cells (pre-DC, CD11c<sup>+</sup> MHCII<sup>-</sup> Siglec H<sup>+</sup>), which retained their division capacity, could differentiate at later time points than 120 h, but this was not investigated. Pedigrees, which were defined as undifferentiated could still retain their potential to differentiate into pDCs or cDCs but could not be further evaluated due to the limitations of live cell imaging. Similarly, it cannot be excluded that in pedigrees, which contain CCR9<sup>low</sup> pDC-like cells as final differentiated stage, differentiation into cDCs could have been observed after the 120 h time point.

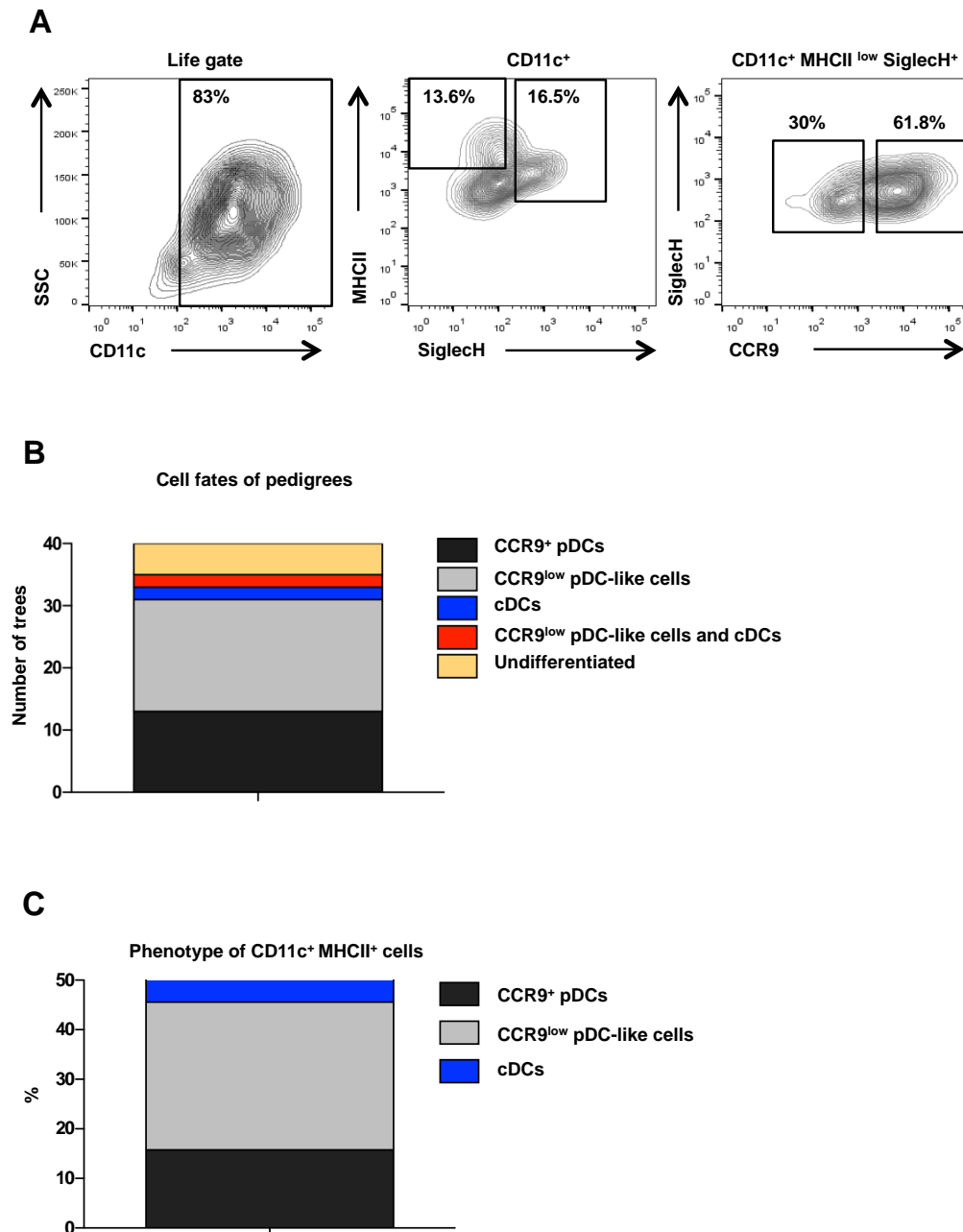


**Fig. 12: End point FACS analysis of CDP**

(A) CDPs were cultured on EL08 cells for 5 days. After 5 days, CDP and its progeny were harvested from imaging slides by gentle pipetting. End point analysis was done by FACS. Prior to FACS, no additional staining was performed. Remnants of fluorescently labeled antibodies used for imaging were sufficient enough to detect signal. (B) CDPs were cultured and tracked continuously over time for 5 days. Pedigrees were segregated according to their cell fate choices as pedigrees either with CCR9<sup>+</sup> pDCs (n=13) or CCR9<sup>low</sup> pDC-like cells (n=18), pedigrees with cDCs (n=2), pedigrees with cDCs and CCR9<sup>low</sup> pDC-like cells (n=2) and undifferentiated pedigrees (n=5) are shown. Undifferentiated pedigrees refer to pre-DCs and are shown in yellow bars. (C) Similarly, the phenotype of distinct cells derived from the CDP between 1-120 h is shown.

---

#### 4.1.6 Analysis of transcription factor Id2 expression during differentiation of individual CDPs into pDCs and cDCs

Id2 is a transcription factor, member of helix-loop-helix transcription factor family. It has been shown that Id2 is upregulated during DC development in vitro and is required for development of the CD8 $\alpha$ <sup>+</sup> DC subset in vivo (Hacker, Kirsch et al. 2003). To get more insight into transcriptional regulation of DC development and the role of Id2 at the single cell level, we used Id2 eGFP reporter mice, in which endogenous Id2 expression can be detected as green fluorescence in DCs.

##### 4.1.6.1 Expression of Id2 in DC subpopulations

It has been reported that the ID2<sup>eGFP/eGFP</sup> mouse is indistinguishable from C57BL/6 controls in hematopoietic compartments. It was reported that Id2 is expressed at very low levels in pDCs, pre-cDCs, CDPs and earlier progenitors whereas it is highly expressed in cDCs (Jackson, Hu et al. 2011). To delineate endogenous Id2 expression in BM-DCs, BM cells of ID2<sup>eGFP/eGFP</sup> and ID2<sup>eGFP/+</sup> mice were analyzed by FACS. In heterozygous mice, pDCs, defined as CD11c<sup>+</sup> B220<sup>high</sup> BST2<sup>high</sup>, expressed low levels of GFP, whereas CD11c<sup>+</sup> B220<sup>-</sup> BST2<sup>low</sup> cDCs expressed high levels of GFP. In homozygous mice, GFP fluorescence intensity was not changed in pDCs, but was higher in cDCs (Fig. 13).

Further validation of Id2 expression was done in Flt3L-cultured BM-DCs. Total BM cells were cultured in the presence of 20 ng/ml Flt3L for 12 days and expression of Id2 was measured by FACS analysis in pDCs, cDCs and pDC subsets. In accordance with previous findings, among all DC subsets, cDCs (CD11c<sup>high</sup> MHCII<sup>high</sup> B220<sup>-</sup>) expressed high levels of GFP. Unexpectedly, CCR9<sup>+</sup> pDCs and CCR9<sup>low</sup> pDC-like cells also expressed GFP, which was considered “low expression”, compared with cDCs (Fig. 14). A small percentage of CCR9<sup>low</sup> pDC-like cells expressed higher levels of Id2-GFP.



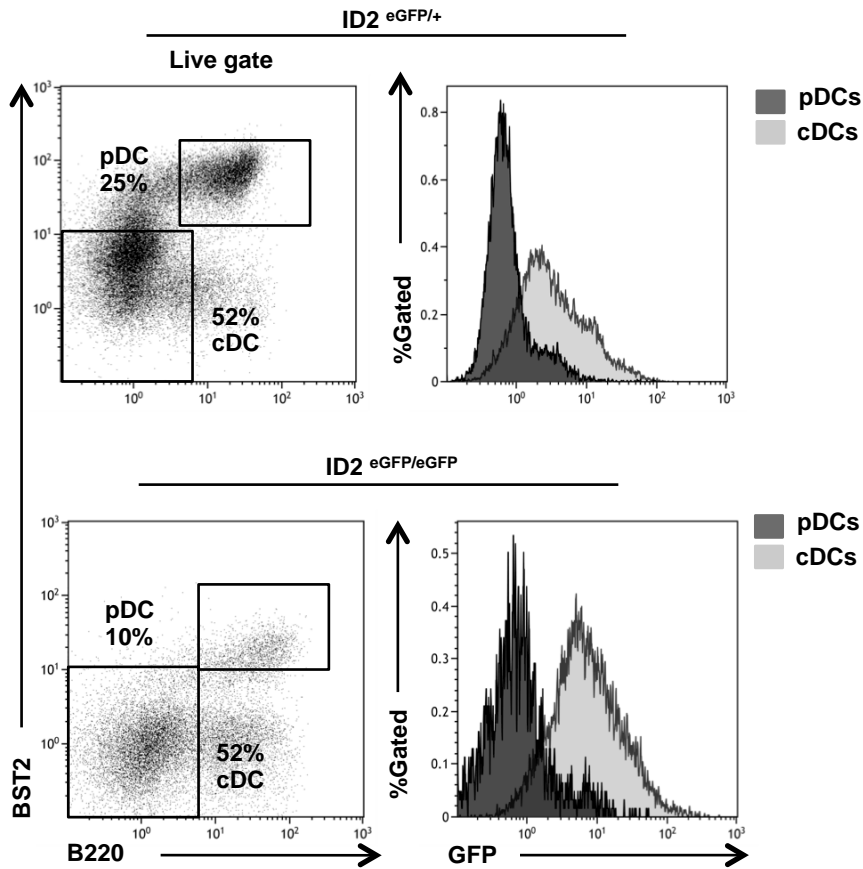


**Fig. 13: Id2-GFP expression in DCs**

Id2-GFP expression was analyzed in  $B220^{high} BST2^{high}$  pDCs and  $B220^{-} BST2^{-}$  cDCs in the BM of Id2 heterozygous and homozygous mice by FACS analysis. Results of one representative of two experiments are shown.

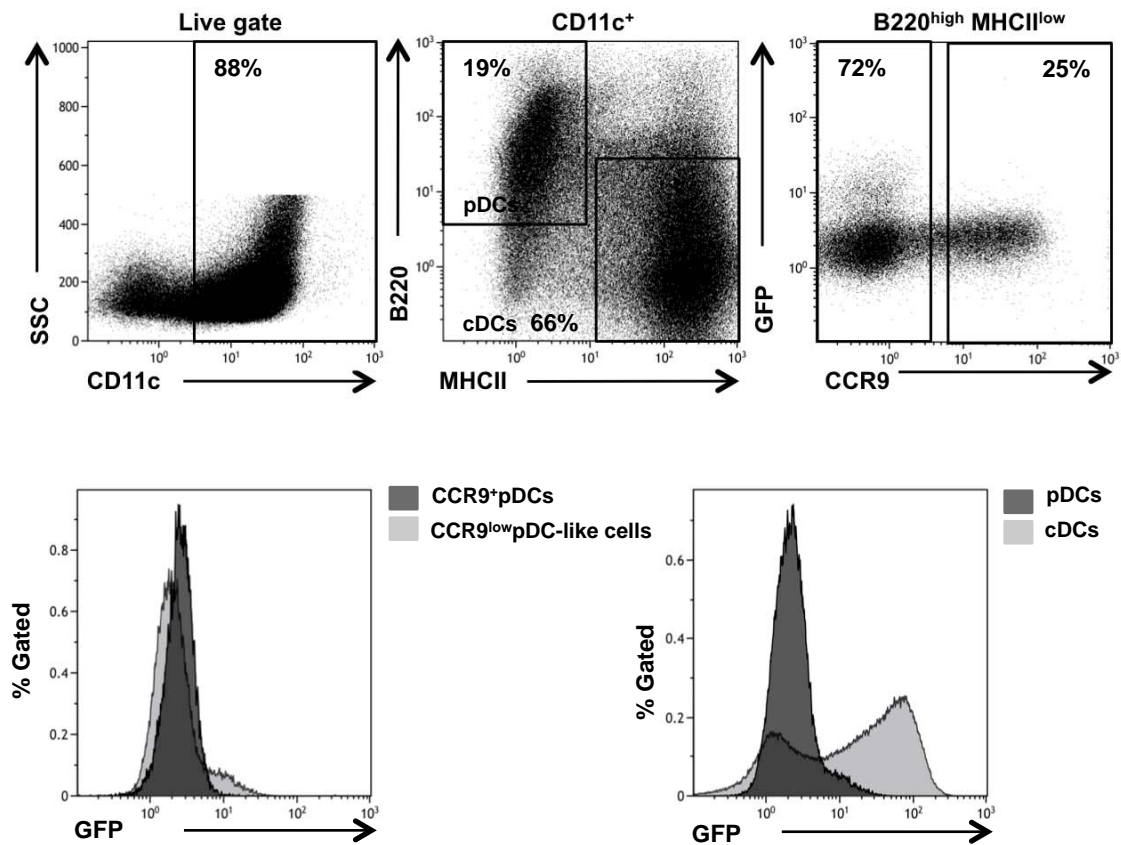


**Fig. 14: Id2-GFP expression in BM derived DC subsets**

Total BM cells were isolated from Id2<sup>eGFP/eGFP</sup> mice and cultured in the presence of 20 ng/ml Flt3L for 12 days. Id2-GFP expression was analyzed in BM derived CD11c<sup>+</sup> MHCII<sup>high</sup> B220<sup>-</sup> cDCs, CD11c<sup>+</sup> MHCII<sup>low</sup> B220<sup>+</sup> pDCs and in pDC subsets. The result of one representative experiment is shown.

Expression of Id2 was analyzed in CDP progeny. CDPs from the ID2<sup>eGFP/eGFP</sup> mouse were sorted to high purity and co-cultured with EL08 feeder cells as described in 3.2.5.1. GFP expression was measured in CDP-derived DC subsets by FACS analysis after 3 days. As previously reported, CDPs did not show any remarkable GFP expression (Jackson, Hu et al. 2011) (data not shown). When CDPs were cultured with EL08 feeder cells, among all DC subsets, cDCs expressed higher levels of GFP compared to pDCs and pDC-like cells (Fig. 15A).

At last, expression of Id2-GFP was validated by confocal microscopy. CDPs were purified from ID2<sup>eGFP/eGFP</sup> BM cells and incubated with Siglec H antibody labeled with Alexa-647. CDPs were maintained in the same conditions as in live cell imaging experiments. After 120 h incubation with Siglec H antibody, cells that expressed high levels of GFP were not stained with Siglec H antibody indicating a cDC phenotype. The majority of the cells that were stained with Siglec H exhibited low levels of GFP. Furthermore, the results confirm that cells, which internalize Siglec H antibody, do not develop into cDCs expressing high levels of Id2 (Fig. 15B)

Taken together, Id2-GFP expression can be faithfully detected in developing DCs and the Id2-GFP reporter system is suitable for live cell imaging experiments.

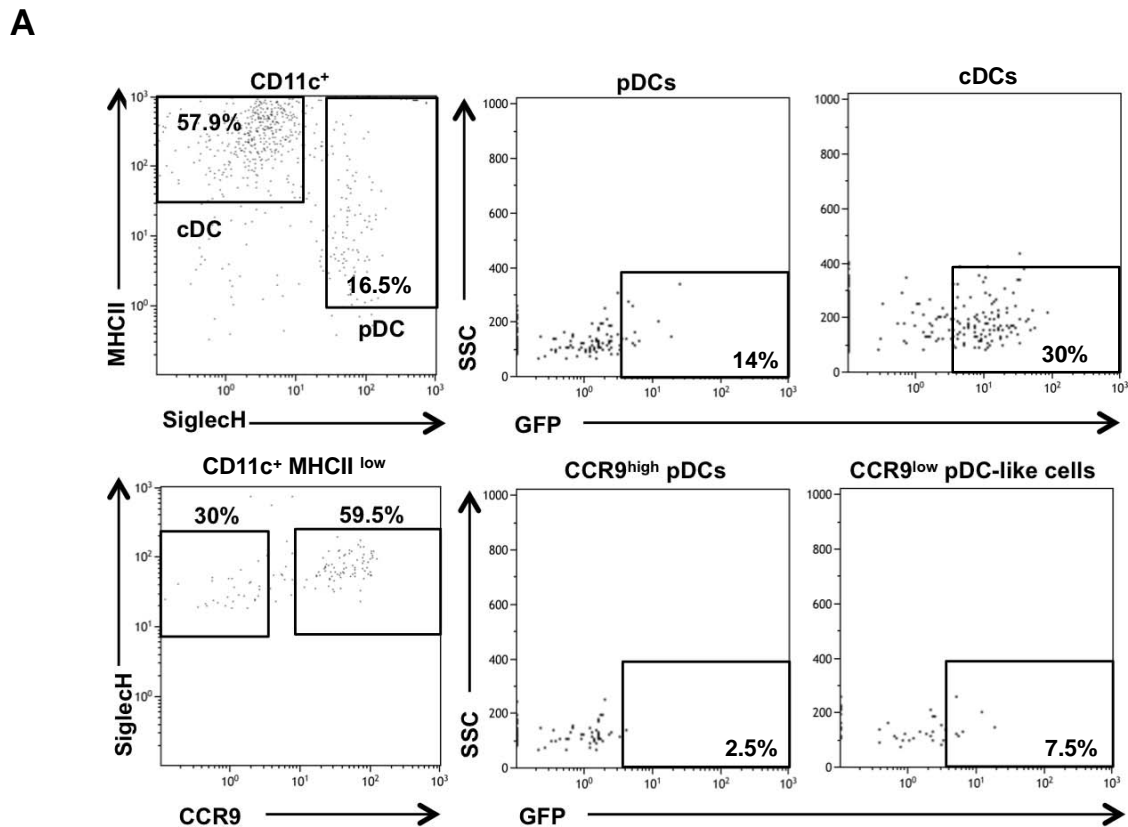


**Fig. 15: Id2-GFP expression in DCs derived from CDP**

**(A)** CDPs were isolated from BM of  $ID2^{eGFP/eGFP}$  mice and cultured in the presence of 20 ng/ml Flt3L on EL08 feeder cells for 3 days. CDP-derived DCs were analyzed by flow cytometry for GFP expression in cDCs and pDC subsets. Result of one representative experiment is shown. **(B)** CDPs were sorted from  $ID2^{eGFP/eGFP}$  mice and cultured in the presence of Siglec H-A647 antibody for 120 h. Subsequently, cells were imaged with the confocal microscope. Two representative images are shown.

#### 4.1.6.2 Tracing *Id2*-GFP expression in CDP progeny at the single cell level

The live-cell imaging approach used in this study described the development and phenotypic behavior of the CDP and their progeny over time at the single cell level. Heterogeneity within CDPs and their progeny was more than previously thought. To extend our findings to the level of transcriptional regulation, *Id2*-GFP reporter mice were used to study cell fate decisions and the role of *Id2* in DC differentiation.

Isolation and sorting of CDPs was performed as described before in 3.2.5.1. The FITC channel was occupied with GFP, therefore CD11c, Siglec H and CCR9 antibodies were used for in culture staining at very low concentrations as shown in **Table 7**.

As previously described, DC subtypes were distinguished by creating cell filters (see Fig. 4). Lacking MHCII surface marker in the imaging panel, DC of all subtypes including pre-DCs were identified based on their CD11c expression. Of note, in almost all progeny the GFP signal was detectable by fluorescence microscopy at early time points. CD11c<sup>+</sup> GFP<sup>+</sup> cells were further divided into two main groups based on presence or absence of Siglec H. Moreover, Siglec H was used to confirm the pDC phenotype. CCR9<sup>+</sup> pDCs were further defined by their high expression of CCR9 and/or Siglec H whereas cells fulfilling pDC criteria but expressing low levels of CCR9 and Siglec H were defined as CCR9<sup>low</sup> pDC-like cells. cDCs were identified as CD11c<sup>+</sup> GFP<sup>high</sup> Siglec H<sup>-</sup>. CD11c<sup>+</sup> cells with low GFP signal and absence of Siglec H signal were considered undifferentiated DC precursors (pre-DCs). Results of cell filter analysis can be seen in Fig. 16. Definition of DC subsets combining several surface markers is shown in Table 9.

Marker	CDP	pre-DC	cDC	CCR9 <sup>+</sup> pDCs	CCR9 <sup>low</sup> pDC-like cell
GFP	-	+/low	high	low	low
CD11c	-	-	high	+	+
Siglec H	-	+/-	-	+ or high	+
CCR9	-	-	-	high	+

**Table 9: Definition of DC subsets in time-lapse imaging experiments performed with cells from *Id2*-GFP reporter mice**

		<b>%Parent</b>
<b>CD11c<sup>+</sup></b>		<b>74%</b>
<b>CD11c<sup>+</sup> GFP<sup>+</sup></b>		<b>99.3%</b>
<b>CD11c<sup>+</sup> GFP<sup>+</sup> SiglecH<sup>+</sup></b>		<b>38.4%</b>
CD11c <sup>+</sup> GFP <sup>+</sup> SiglecH <sup>+</sup> CCR9 <sup>+</sup>		<b>99.1%</b>
CD11c <sup>+</sup> GFP <sup>+</sup> SiglecH <sup>+</sup> CCR9 <sup>+</sup> AND SiglecH up.		<b>15%</b>
<b>GFP upregulation</b>		<b>0%</b>
CD11c <sup>+</sup> GFP <sup>+</sup> SiglecH <sup>+</sup> CCR9 <sup>+</sup> AND CCR9 up.		<b>16.5%</b>
<b>GFP upregulation</b>		<b>0%</b>
CD11c <sup>+</sup> GFP <sup>+</sup> SiglecH <sup>+</sup> CCR9 <sup>+</sup> NO CCR9 up.&SiglecH up.		<b>60%</b>
<b>GFP upregulation</b>		<b>0%</b>
CD11c <sup>+</sup> GFP <sup>+</sup> SiglecH <sup>+</sup> CCR9 <sup>-</sup>		<b>0.9%</b>
<b>CD11c<sup>+</sup> GFP<sup>+</sup> SiglecH<sup>-</sup></b>		<b>61.6%</b>
CD11c <sup>+</sup> GFP <sup>+</sup> SiglecH <sup>-</sup> AND GFP up.		<b>40.9%</b>
CD11c <sup>+</sup> GFP <sup>+</sup> SiglecH <sup>-</sup> NO GFP up.		<b>59.1%</b>
<b>CD11c<sup>+</sup> GFP<sup>-</sup></b>		<b>0.7%</b>

**Fig. 16: Results of cell filter analysis of ID2-GFP CDP and its progeny**

CDPs were cultured on EL08 cells with Flt3L for 5 days and progeny of the CDP were tracked continuously using TTT software. The cell filters were created to analyze the tracking results. The percentage of cells with specific marker combinations occurring between 1-120 hours of experiment time is shown.

The majority of the CDP and their progeny were faithfully tracked though some were lost to tracking. In line with previous observations, CDP and their progeny proliferated and survived well when cultured with EL08 stromal cells leading to only 2% apoptotic cells (Fig. 17A). Among not lost cells, 65% were dividing. Detection of surface molecules is exemplified in Fig. 18.

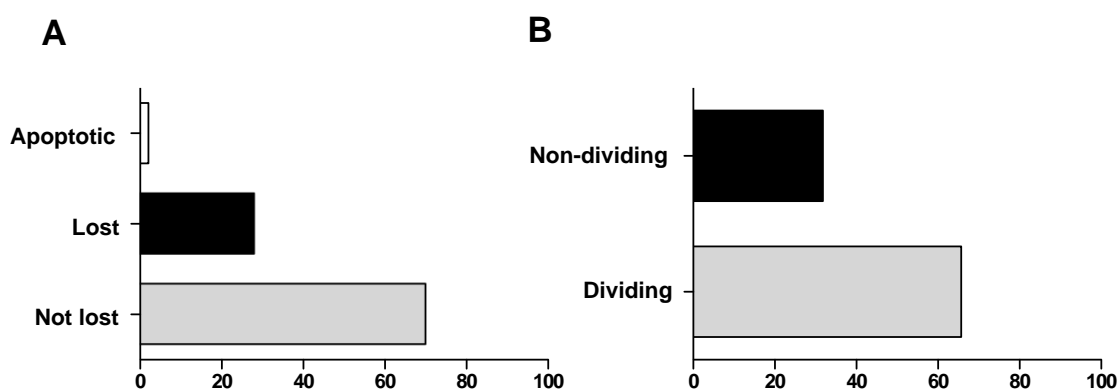


**Fig. 17: Quantitative analysis of Id2<sup>eGFP/eGFP</sup> CDP and its progeny by single cell tracking**  
**(A)** CDPs were cultured with EL08 cells with 20ng/ml Flt3L for 5 days and progeny of the CDPs were continuously monitored by time-lapse imaging. The percentage of apoptotic, lost and continuously tracked (not lost) cells until the end of the experiment time among all progeny is shown. **(B)** The percentage of dividing and non-dividing cells among not lost cells is shown.

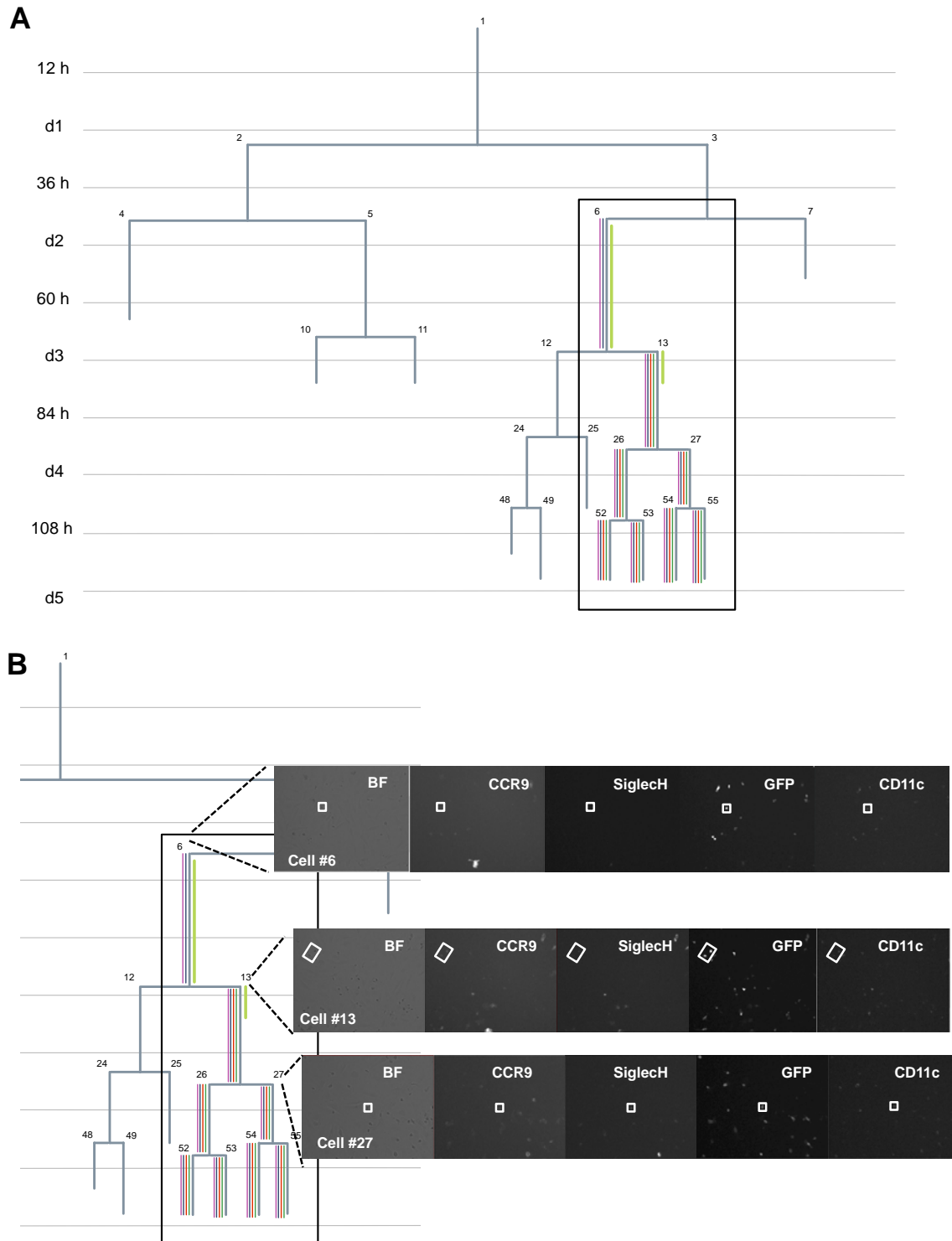


**Fig. 18: Detection of surface molecules using fluorescently labelled antibodies in ID2<sup>eGFP/eGFP</sup> CDP**

**(A)** A representative pedigree of a single CDP and its progeny is shown. CDPs were cultured on EL08 feeder cells for 5 days. Fluorescently labeled antibodies against Siglec H, CCR9 and CD11c were added at the start of the experiment. CDPs and their progeny were monitored continuously by time-lapse imaging. All relevant information was recorded annotated in colored lines (red: Siglec H; blue: GFP; pink: CD11c; green: CCR9). Bold lines denote upregulation of certain fluorescent marker (Here, bold green line indicates GFP upregulation). **(B)** Bright field and fluorescent images of indicated cells are shown.



The first occurrence of each fluorescent marker was assessed in pedigrees. The GFP was detected earlier than other markers in all pedigrees (Fig. 19A). On the other hand, when looking at dividing CDPs and their progeny in all pedigrees, GFP expression occurred simultaneously with CD11c expression in most of the cells whereas CCR9 and Siglec H were expressed later. The GFP onset was followed by first CD11c and then by Siglec H and CCR9 onset (Fig. 19B).

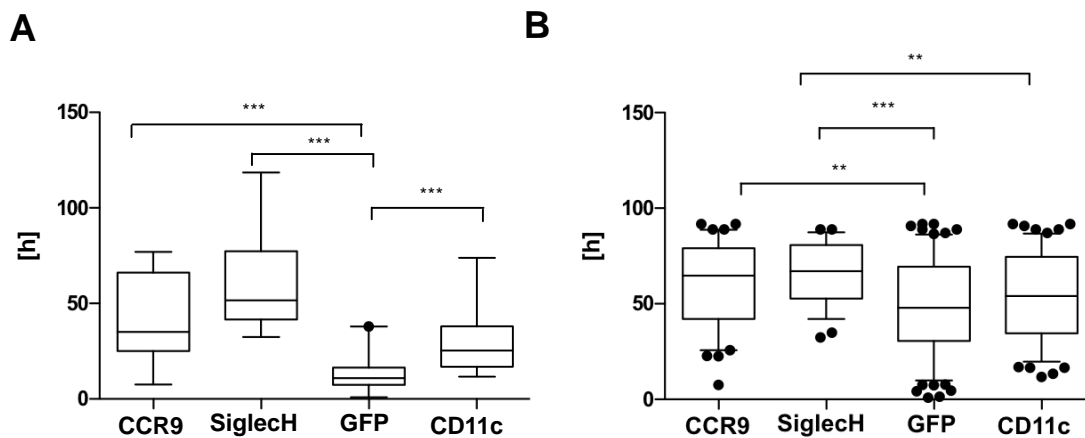


**Fig. 19: The time point of occurrence of fluorescent markers**

CDPs were cultured on EL08 cells with 20 ng/ml Flt3L for 5 days. Progeny of CDPs were tracked and single cell imaging results were analyzed quantitatively. **(A)** The time of first occurrence of fluorescent markers is shown in all pedigrees (n=20). **(B)** The time of first occurrence of fluorescent markers is shown in all dividing cells among CDP progeny (CCR9, n=81; Siglec H, n=55; GFP, n=173; CD11c, n=132). Statistical analysis was performed using Kruskal-Wallis and Dunn's multiple comparison tests (\*\* p ≤ 0.01; \*\*\* p ≤ 0.001).

---

By using the Id2-GFP reporter system we sought to distinguish cDCs with their unique GFP expression by fluorescence microscopy. Unexpectedly, GFP expression was found in almost all CD11c<sup>+</sup> cells and was not only restricted to the cDC lineage. Although GFP expression was evident for 99% of the cells and started early, high expression of GFP was observed later and only 25% of the pedigrees. Before pDC lineage commitment (CCR9<sup>high</sup> and/or Siglec H<sup>high</sup>), GFP expression was downregulated, and high expression of GFP was not observed in cells with pDC phenotype. GFP upregulation in CD11c<sup>+</sup> SiglecH<sup>-</sup> cells was seen around 50 hours (48.36 h ± 19.74 h).

In line with the previous experiment performed with cells from wildtype mice, CCR9<sup>+</sup> pDC progenitors went through a transient stage expressing low levels of CCR9 and Siglec H at earlier times. CCR9 upregulation occurred around day 3 (84 h ± 25.71 h) in CD11c<sup>+</sup> GFP<sup>+</sup> Siglec H<sup>+</sup> CCR9<sup>low</sup> cells. Direct development of CCR9<sup>high</sup> pDCs from CDPs or CD11c<sup>+</sup> Siglec H<sup>-</sup> precursors was a rare event.

End point FACS analysis confirmed that, majority of the cells were CD11c<sup>+</sup> GFP<sup>+</sup> (Fig. 20A). Observations at the single cell resolution confirmed heterogeneity within the CDP as previously reported. CDP and their progeny generated pedigrees with pDC or cDC fate (Fig. 20B). After 5 days of culture, a great amount of cells were still undifferentiated DC precursors expressing low levels of CD11c and GFP and lack Siglec H. Progeny of CD11c<sup>+</sup> GFP<sup>+</sup> cells were composed of pDCs and cDCs (Fig. 20C).

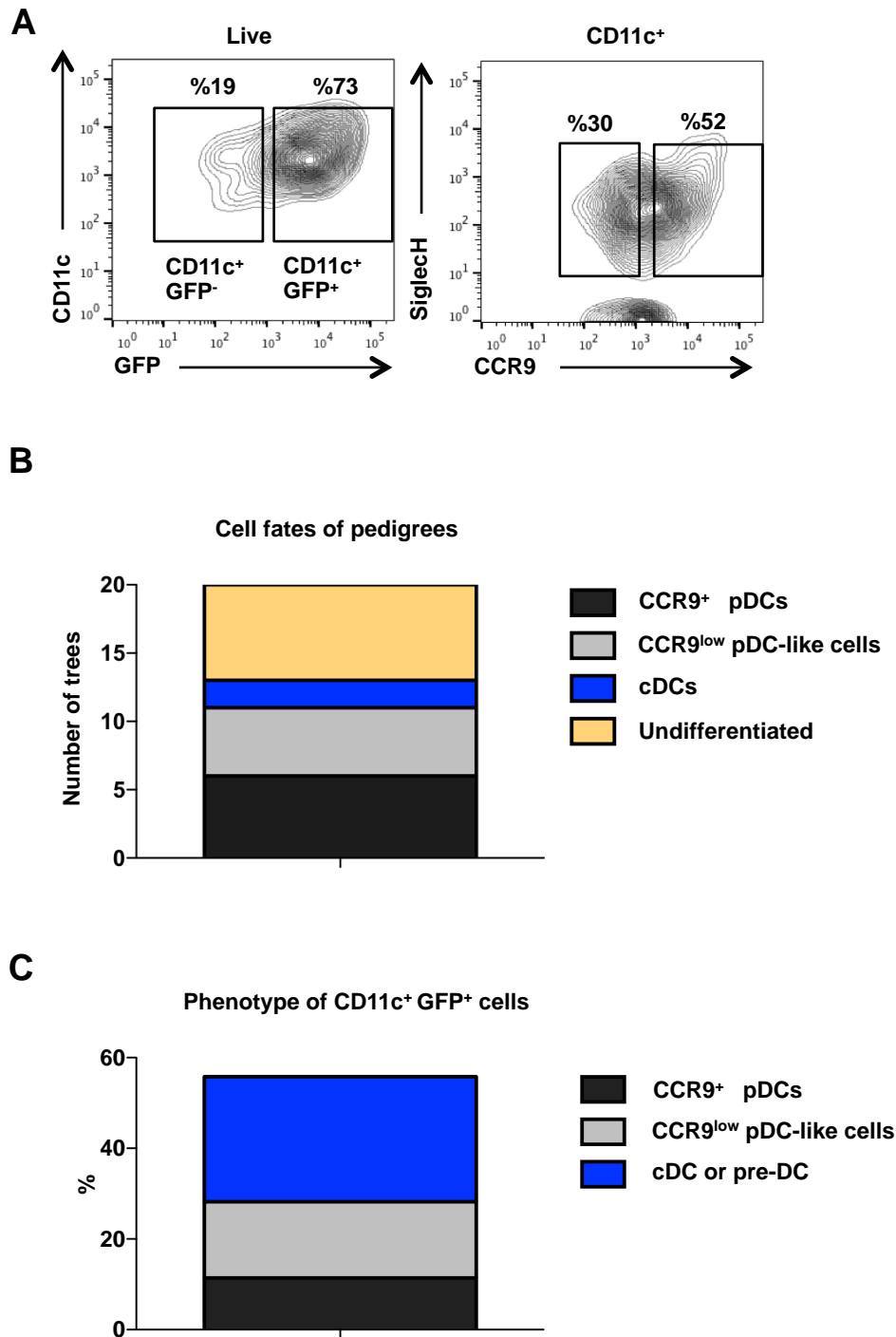


**Fig. 20: End point analysis of Id2<sup>eGFP/eGFP</sup> CDP and its progeny**

(A) CDPs were cultured on EL08 cells for 5 days with Flt3L and fluorescently labeled antibodies and were continuously imaged. CDP and its progeny harvested from the Ibidi  $\mu$ -slides and end point analysis was done by flow cytometry. No additional staining was performed prior FACS analysis. After gating CD11c<sup>+</sup> cells, pDC subsets were defined based on low or high expression of CCR9 and presence of Siglec H. (B) The number of trees with distinct cell fates is shown. (C) Progeny of CD11c<sup>+</sup> GFP<sup>+</sup> cells with indicated cell fate choices are shown.

---

#### 4.1.7 Internalization of recombinant antibodies

One of the obstacles of live cell imaging is long-term detection of surface molecules. The “in-culture staining” approach used in this study was sufficient to detect surface markers in living cells for 120 h. Nonetheless, it raised some concerns regarding veracity of the signal. It is known that antibodies when bound to the cell surface may induce receptor-mediated endocytosis and can be internalized by the cell. An internalized antibody can give a positive signal in time-lapse fluorescence microscopy, which may not reflect the surface expression of the marker at that point.

To measure internalization, splenocytes were cultured in the presence of biotinylated  $\alpha$ -Siglec H antibody up to 2 h and surface expression of Siglec H was measured by Streptavidin-APC staining by FACS analysis in pDCs at the indicated time points. As shown in Fig. 21A, within one hour, Siglec H antibody was internalized and surface expression of Siglec H was reduced to more than half and remained stable at this level thereafter. Internalization of Siglec H was further confirmed by confocal imaging in Flt3L-derived BM cells. Flt3L-derived BM cells were cultured with Siglec H-A647 antibody for 1 h or 120 h. After 1 h, Siglec H antibody was found in vesicles where it colocalized with LysoTracker (red). Following 120 h of incubation with Siglec H-A647 antibody, FITC conjugated Siglec H was added to culture medium shortly before imaging to determine antibody binding on the cell surface. As shown in Fig. 21B, although Siglec H antibody was mostly internalized, Siglec H could be detected on the cell surface.

We concluded that Siglec H antibody used for live cell imaging experiments was efficiently internalized by endocytosis in most of the cells and this enhanced the signal intensity, however Siglec H was still detectable on the surface of the same cells which had internalized the Siglec H antibody.

Previous confocal analysis of the “in culture” staining signal for Siglec H in CDP progeny from Id2-GFP reporter mice (Fig. 15B) showed that, high GFP expression characteristic of cDCs did not coincide with Siglec H signal confirming pDC specificity of the staining.

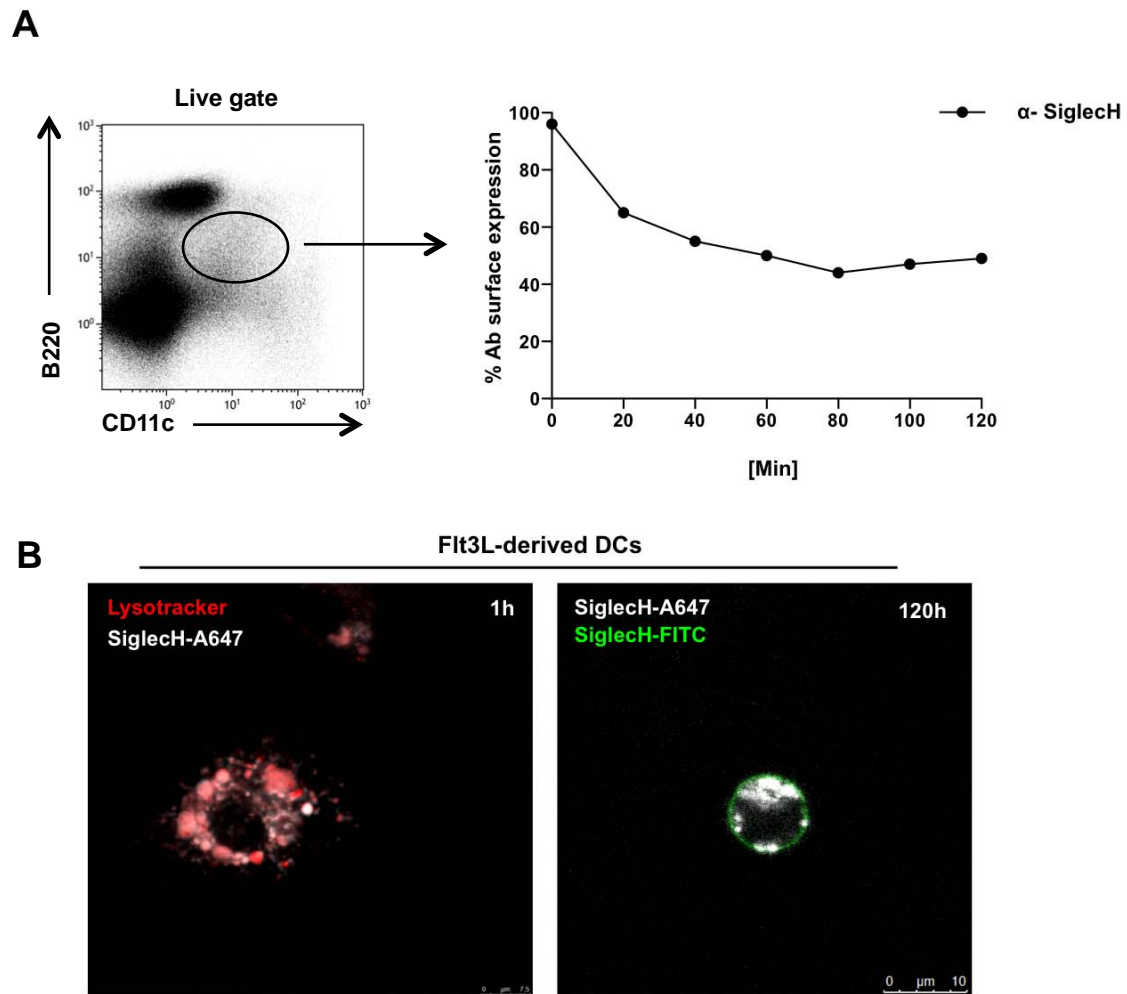


**Fig. 21: Internalization of Siglec H antibody**

**(A)** Splenocytes were incubated with  $\alpha$ -Siglec H antibody at 37°C. At indicated time points cells were stained with CD11c, B220 and Streptavidin-APC and surface expression of Siglec H was measured in CD11c<sup>+</sup> B220<sup>+</sup> pDCs by FACS analysis. **(B)** Flt3L-derived BM cells were incubated with Siglec H-A647 antibody at 37°C for 1 h or 120 h. Following incubation, cells were stained with LysoTracker (red) shown on the left or Siglec H-FITC shown on the right and analyzed with the confocal microscope.

---

## 4.2 Plasticity of CCR9<sup>+</sup> pDCs and CCR9<sup>low</sup> pDC-like precursors in inflammation

It has been shown recently that in the steady state CCR9<sup>low</sup> pDC-like cells are immediate precursors that can give rise to fully differentiated CCR9<sup>+</sup> pDCs and may also generate CD11b<sup>+</sup> MHC<sup>high</sup> cDCs under the influence of the tissue microenvironment in vivo (Schlitzer, Heiseke et al. 2012). We hypothesized that regulation of immune responses can be altered at the DC differentiation level and influenced by local tissue microenvironment under inflammatory conditions. It has been reported that production of GM-CSF by Th cells influences the disease course in EAE (Codarri, Gyulveszi et al. 2011). Therefore, we proposed that differentiation of CCR9<sup>low</sup> pDC-like precursors, which can enter the CNS via the blood-brain-barrier (BBB), could be influenced by cytokines in the inflamed brain including GM-CSF. Therefore, the objective was to examine differentiation of pDC-like precursors and their contribution to inflammatory responses in the EAE model of CNS inflammation.

To determine the frequency and phenotype of CCR9<sup>+</sup> pDCs and CCR9<sup>low</sup> pDC-like precursors, which migrate into the inflamed brain, adoptive transfer experiments were performed. Naïve BM contains about 3% of cells expressing CD11c and pDC markers (Siglec H and BST2), which include CCR9<sup>+</sup> pDCs and CCR9<sup>low</sup> pDC-like cells. To obtain sufficient numbers of cells for transfer experiments, DCs were expanded in vivo by flank injection of Flt3L expressing B16 melanoma cells in CD45.1 congenic mice. Subsequently, BM cells were isolated from these mice after 7 days and CD11c<sup>+</sup> B220<sup>high</sup> SiglecH<sup>+</sup> BST2<sup>+</sup> cells were sorted into CCR9<sup>low</sup> and CCR9<sup>high</sup> subsets with high purity (Fig. 22 B and C). In contrast to previous experiments (Schlitzer, Heiseke et al. 2012), anti-B220 antibody was included in the staining panel for sorting and both populations were sorted as B220<sup>high</sup> cells. These pDC populations were transferred into mice with active EAE, which had been induced by MOG peptide immunization 16 days earlier. Experimental workflow explained in details in Fig. 22A.

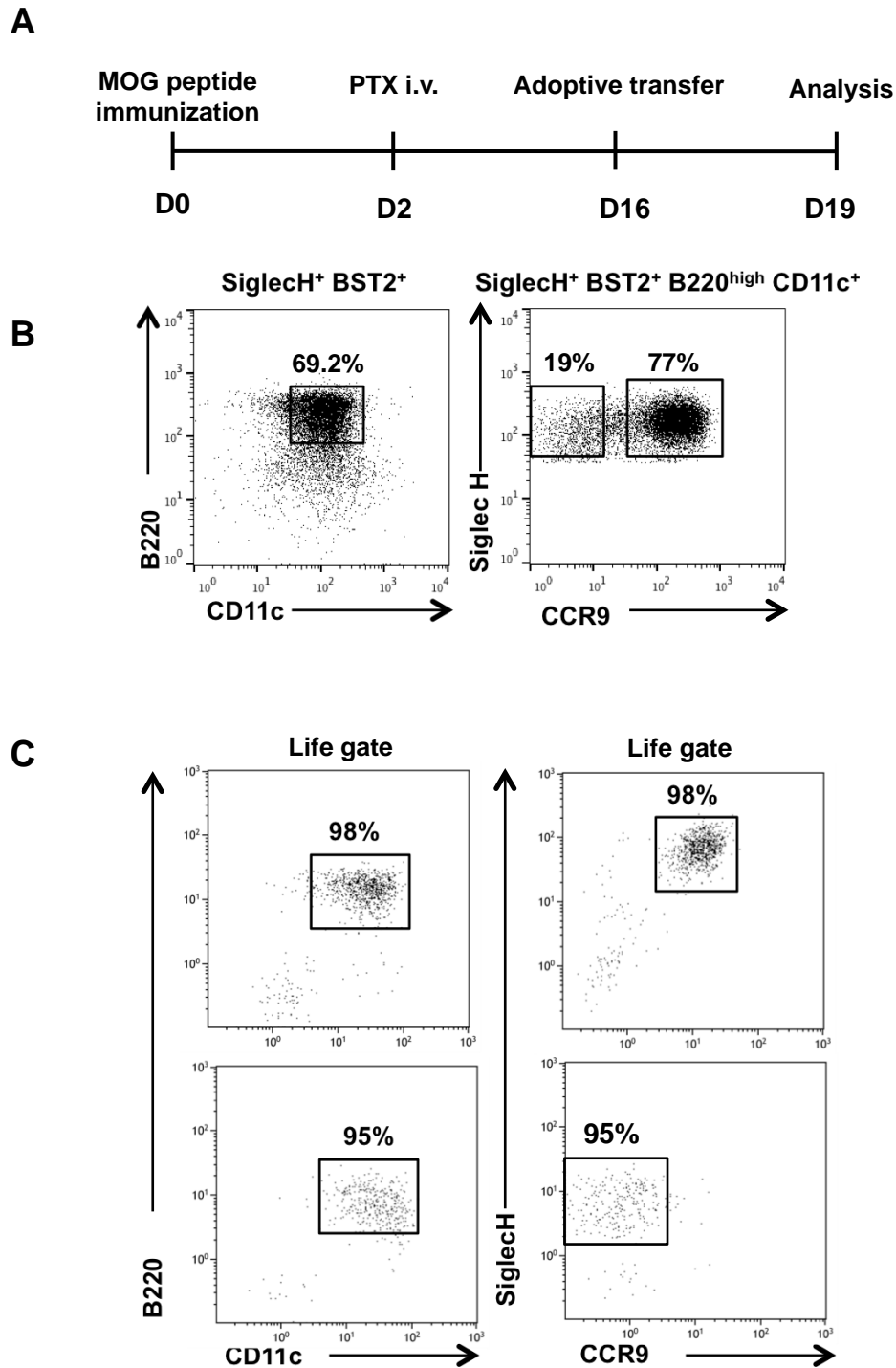


**Fig. 22: Outline of EAE experiment setup and FACS sorting of pDC subsets from BM**

**(A)** Adoptive transfer of pDC subsets into EAE mice was performed at peak disease (D16) following immunization by MOG peptide. Phenotype and fate of the transferred cells were analyzed 3 days after transfer. **(B)** Prior to sort experiments, mice were injected with Flt3L secreting melanoma, which resulted in expansion of DCs within 7 days. Subsequently, BM cells were isolated from CD45.1<sup>+</sup> CD45.2<sup>-</sup> mice. Cells were stained with fluorescently labeled antibodies against CD11c, B220, BST2, Siglec H and CCR9. After gating Siglec H<sup>high</sup> BST2<sup>high</sup> CD11c<sup>+</sup> B220<sup>high</sup> pDCs, pDC subsets were further segregated by presence or absence of CCR9 expression. **(C)** Quality control was done by FACS analysis after cell sorting. The results of one representative of three experiments are shown.

#### 4.2.1 Accumulation of CCR9<sup>+</sup> pDCs and CCR9<sup>low</sup> pDC-like cells in CNS under inflammatory conditions

Transfer experiments were performed at the peak time in EAE (day 16) while the blood brain barrier was opened. Animals with comparable EAE scores ( $3 \pm 0.128$ ) were selected as recipient mice. B220<sup>high</sup> CCR9<sup>+</sup> pDCs and B220<sup>high</sup> CCR9<sup>low</sup> pDC-like cells were injected into C57BL/6 recipients. Transferred cells were distinguished from host cells by using congenic fluorescence markers (CD45.1<sup>+</sup> CD45.2<sup>-</sup>). Disease activity was assessed using the clinical EAE score (Table 6). At the end point of the experiment 3 days after transfer, all mice had partially recovered at normal pace and there was no difference in clinical scores between the two groups (EAE score 3 days after transfer, CCR9<sup>+</sup> recipients:  $2,5 \pm 0.408$ ; CCR9<sup>low</sup> recipients:  $2,625 \pm 0.144$ ).

CNS recruitment and phenotypic changes in the transferred cells were assessed by FACS analysis. Immune cell infiltrates were isolated from the CNS and the spleen 3 days after adoptive transfer and the frequency of the transferred cells within the total leucocyte population was determined (Fig. 23). The recovery of transferred cells in the spleen was lower than in CNS, which may be due to lower inflammation in the spleen compared to the CNS at this time point (data not shown).

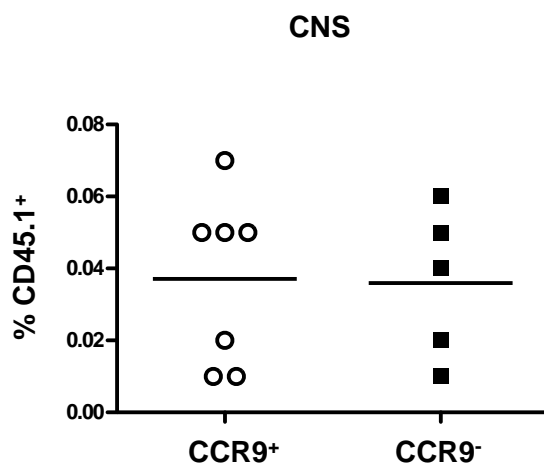


**Fig. 23: The frequency of CD45.1<sup>+</sup> infiltrates in CNS**

Mice were immunized with MOG peptide. Adoptive transfer of pDC subsets into EAE mice was performed at peak time (D16). The percentage of CD45.1<sup>+</sup> infiltrates in CNS was shown. Pooled results of two independent experiments are shown (n=5-7 mice).



In both groups the transferred cells largely maintained their pDC phenotype and only a minor fraction downregulated pDC markers (BST2, Siglec H) in the CNS and in the spleen (Fig. 24). CCR9<sup>low</sup> pDC-like cells gave rise to a very small fraction of cells with cDC phenotype in vivo (data not shown). These were detected by downregulation of pDC markers and upregulation of CD11b and/or CD103.

In conclusion, within the CD11c<sup>+</sup> B220<sup>high</sup> Siglec H<sup>+</sup> BST2<sup>+</sup> cells in the BM, the great majority of both CCR9<sup>+</sup> and CCR9<sup>low</sup> pDC populations maintained their pDC phenotype even in highly inflammatory conditions such as EAE. This was surprising given the fact that in our previous studies the CCR9<sup>low</sup> pDC-like cells had the plasticity to differentiate into cDCs after transfer even in the absence of inflammation. In these studies however B220 was not included in the staining panel for sorting the CCR9<sup>low</sup> pDC-like cells from BM.

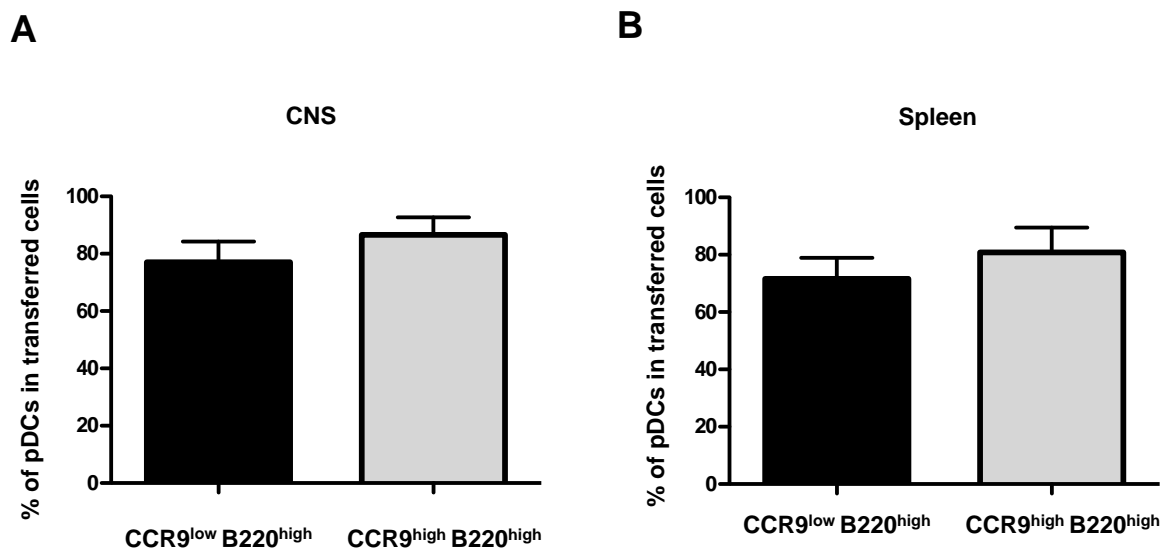


**Fig. 24: The percentage of BST2<sup>+</sup> pDCs in CCR9<sup>low</sup> B220<sup>high</sup> and CCR9<sup>high</sup> B220<sup>high</sup> transferred groups**

EAE was induced and adoptive transfer of pDC subsets into EAE mice was performed at peak disease (D16). Phenotype and fate of the transferred cells were analyzed 3 days after transfer by FACS in CNS and spleen using antibodies against CD45.1, CD45.2, BST2, Siglec H, CD11b, CD103, CD8, CD64, CD11b, CD11c and Lineage cocktail which contains CD3e, NK1.1, Ly6G and CD19. The percentage of CD45.1<sup>+</sup> pDCs in CNS (**A**) and the spleen (**B**) were shown. Error bars represent standard deviation. Pooled results of two independent experiments are shown (n=5-7 mice).

#### 4.2.2 B220<sup>low</sup> CCR9<sup>low</sup> pDC-like cells differentiate into cDCs in the inflamed CNS

The BM pDC subset sort panel, including antibodies against Siglec H, BST2, CD11c, CCR9 and B220 was revisited. The CD11c<sup>+</sup> fraction contains two populations based on their Siglec H expression: Siglec H<sup>+</sup> B220<sup>low/high</sup> cells and Siglec H<sup>-</sup> B220<sup>-</sup> cells, which contain cDCs and Siglec H<sup>-</sup> pre-DCs. Siglec H<sup>+</sup> cells that express low levels of B220 exhibited low levels of CCR9 expression. The majority of B220<sup>high</sup> Siglec H<sup>+</sup> cells are differentiated CCR9<sup>high</sup> pDCs but a smaller population of CCR9<sup>low</sup> cells is also contained in that fraction (Fig. 25). Thus, by including B220 as marker, the CCR9<sup>low</sup> pDC-like cells in murine BM can be separated into B220<sup>high</sup> and B220<sup>low</sup> subsets.

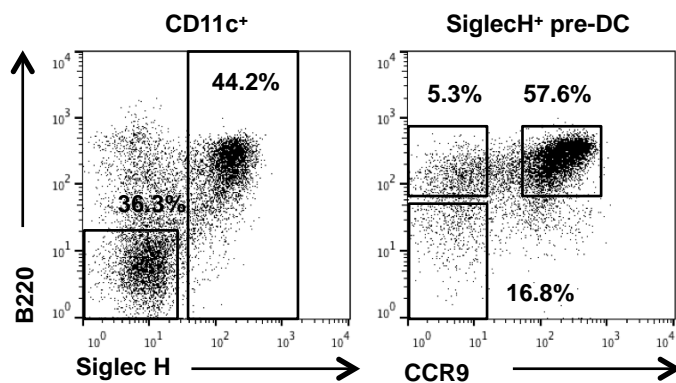
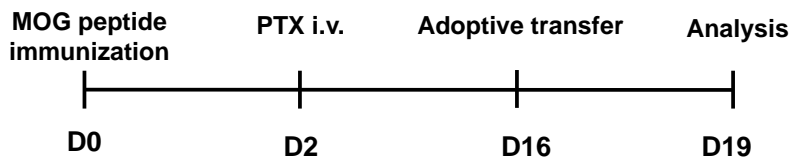


**Fig. 25: Staining of pre-DCs and pDCs in the BM**

BM cells were isolated from WT mice and stained with anti-CD11c Pe Cy7, anti-Siglec H Alexa 488, anti-BST2 Alexa 647, anti-CCR9 PE and anti-B220 Pe Cy5. After gating CD11c<sup>+</sup> cells, BM cells were further divided based on absence or presence of Siglec H expression that represent Siglec H<sup>+</sup> and Siglec H<sup>-</sup> pre-DCs. Siglec H<sup>+</sup> pre-DCs were further gated on based on their high or low CCR9 expression. Results of one representative experiment are shown.

We postulated that the low percentage of cDCs, which were generated from CCR9<sup>low</sup> pDC-like cells in previous experiments, was due to the exclusion of B220<sup>low</sup> cells from the sort gate. Therefore, B220<sup>high</sup> CCR9<sup>low</sup> as well as B220<sup>low</sup> CCR9<sup>low</sup> pDC-like cell subsets were sorted from the BM cells and transferred into mice with ongoing EAE (day 16 after MOG-peptide immunization). The purity of the population was greater than 90%. The phenotype of the transferred cells isolated from the CNS, was analyzed 3 days after transfer. Experimental workflow and sorting strategy are explained in details in Fig. 26.

A



B

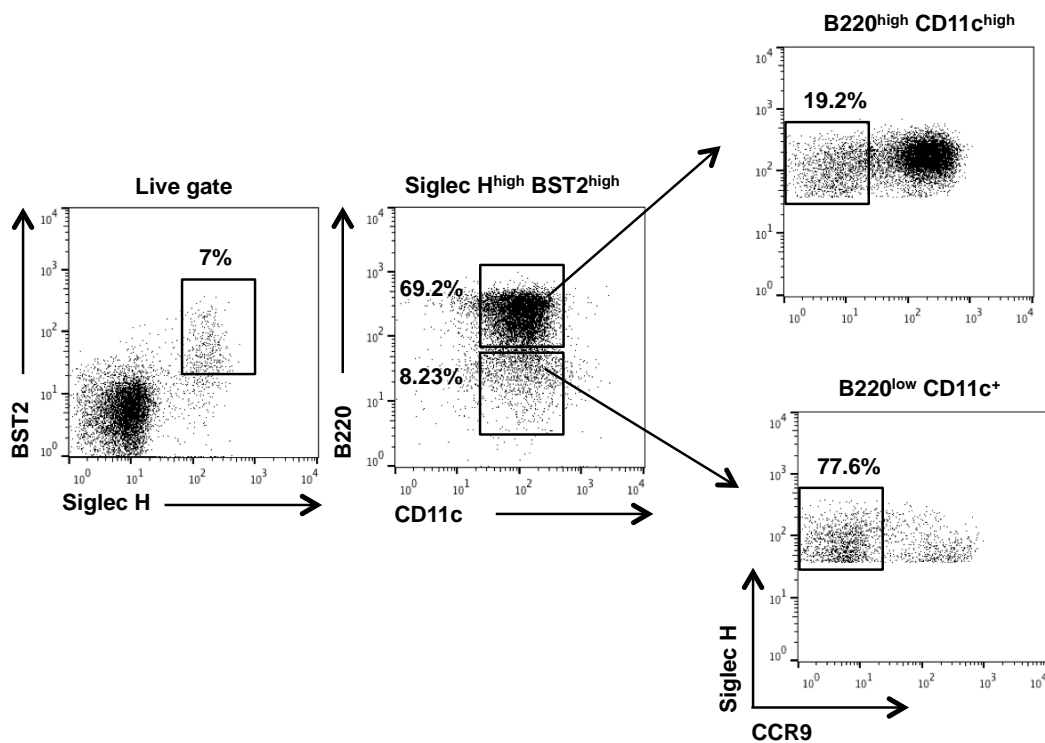


### Fig. 26: Sorting strategy of pDC subsets

**(A)** Mice were immunized by MOG peptide to induce EAE. Adoptive transfer of pDC subsets into EAE mice was performed at peak disease (D16). Phenotype and fate of the transferred cells were analyzed 3 days after transfer. **(B)** Seven days prior to sort experiments, CD45.1 congenic mice were injected s.c. with Flt3L secreting melanoma cells, which resulted in expansion of DCs. Subsequently BM cells were isolated and stained for sorting. After gating on Siglec H<sup>high</sup> BST2<sup>high</sup>, cells were further segregated based on their high or low expression of B220. CD11c<sup>high</sup> B220<sup>high</sup> CCR9<sup>low</sup> and CD11c<sup>+</sup> B220<sup>low</sup> CCR9<sup>low</sup> pDC subsets were sorted. Sorting strategy of pDC subsets is shown.

Leucocyte infiltrates were recovered from the CNS of both transferred groups 3 days after transfer. Within the  $CD45.2^+ CD45.1^-$  Leucocyte infiltrate of the recipient mice (Fig. 27, lower panels). DCs were gated as  $CD64^-$  Lineage $^-$  cells and then divided into  $BST2^+ CD11b^-$  pDCs and  $BST2^-$  cDCs. cDCs could be further characterized by their  $CD11b$  versus  $CD103$  expression. These results clearly show that pDCs and cDC subsets infiltrate the CNS during EAE. Within the  $CD45.2^- CD45.1^+$  fraction of transferred cells infiltrating the CNS both cells with pDC phenotype and cells with cDC phenotype, could be detected using same gating strategy (Fig. 27, upper panels).

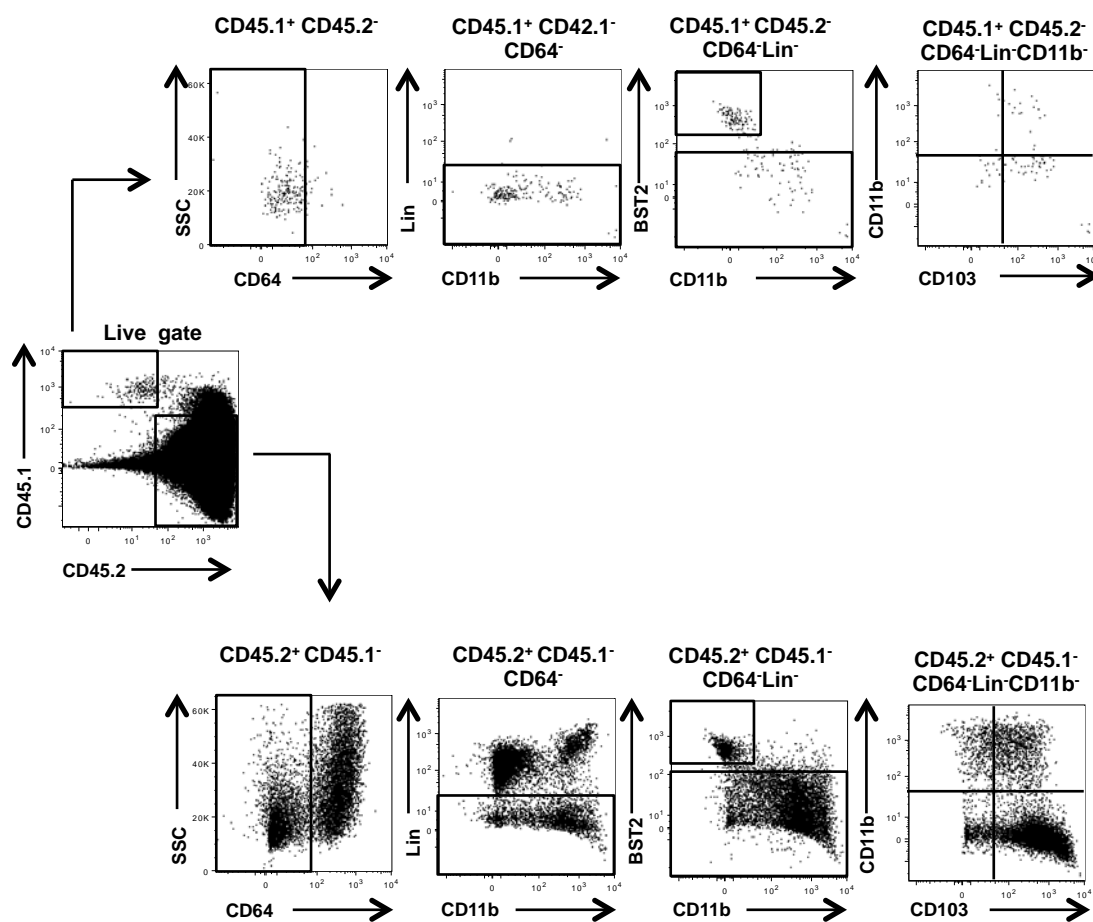


**Fig. 27: CNS gating exemplified in EAE induced mice**

Leucocytes were isolated from brain and spinal cord tissue of each recipient mice. Pooled brain and spinal cord leucocyte fractions were analyzed by FACS. After gating on live cells and excluding autofluorescent signals, transferred cells were distinguished from recipient leucocytes using congenic markers  $CD45.1$  and  $CD45.2$ . Gates were set on recipient leucocytes (lower panel) as shown and the same gates were used for analysis of the transferred cells (upper panel). Macrophages, microglial cells, T cells, B cells and NK cells were excluded by gating on  $CD64^-$  Lin $^-$  ( $CD3e$ ,  $CD19$ ,  $NK1.1$ ) cells.

---

Consistent with previous experiments, transferred B220<sup>high</sup> CCR9<sup>low</sup> pDC-like cells maintained their pDC phenotype to a high extent ( $\geq 80\%$  BST2<sup>+</sup> CD11b<sup>-</sup> phenotype, Fig. 28 A) However, a large percentage of B220<sup>low</sup> CCR9<sup>low</sup> pDC-like cells downregulated the pDC marker BST2, and gave rise to cDCs expressing CD103 and/or CD11b (Fig. 28A). In control experiments it was verified that transferred cells which downregulated BST2 also downregulated Siglec H expression (data not shown). Within the fraction of transferred cells, which had lost the pDC phenotype a clear population of CD103<sup>+</sup> cDCs could be observed some of which also expressed CD11b. The majority of CD103<sup>-</sup> cDCs expressed CD11b, but a smaller percentage was negative for both markers (Fig. 28A). In Fig. 28B, the results of three experiments are summarized (data from the experiments shown in Fig. 24 and Fig. 27 are included).

In conclusion, compared to B220<sup>high</sup> CCR9<sup>low</sup> pDC-like cells, B220<sup>low</sup> CCR9<sup>low</sup> pDC-like retained higher plasticity to differentiate into cells with cDC phenotype in inflammatory conditions. Thus, the CD11c<sup>+</sup> Siglec H<sup>+</sup> BST2<sup>+</sup> B220<sup>low</sup> CCR9<sup>low</sup> fraction of murine BM cells has properties of pre-DCs with the capacity to differentiate into all DC subtypes. Upregulation of B220 in cells expressing CD11c and pDC markers indicates stronger commitment to the pDC lineage.

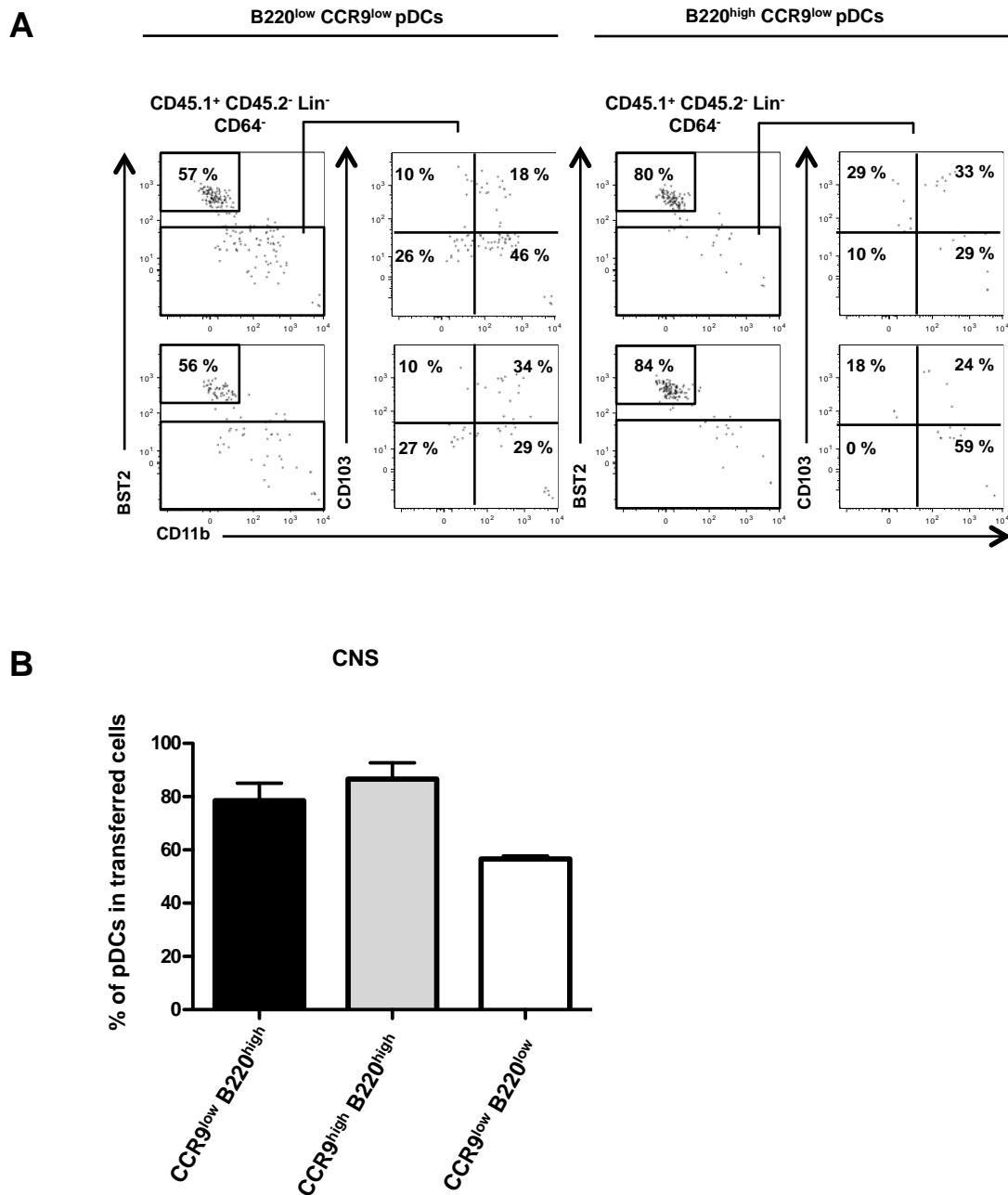


**Fig. 28: Composition of CD45.1<sup>+</sup> infiltrates in CNS**

(A) EAE was induced by MOG peptide immunization and adoptive transfer experiments were performed as described in Fig. 26. Phenotype and fate of the transferred cells were analyzed 3 days after adoptive transfer experiments. The phenotype of CD45.1<sup>+</sup> infiltrates in CNS is shown. (B) pDC subsets were sorted as B220<sup>high</sup> CCR9<sup>low</sup>, B220<sup>high</sup> CCR9<sup>high</sup> and CCR9<sup>low</sup> B220<sup>low</sup> cells. The percentage of BST2<sup>+</sup>CD11b<sup>-</sup> pDCs within transferred cells recovered from CNS is shown. Error bars indicate standard deviation. Cumulative results from three independent experiments are shown.

## 5 Discussion

Functional heterogeneity within the progenitor pool in the BM has been shown to influence cell fate decisions. It is known that self-renewal and maintenance of DC progenitors within the niche is orchestrated by cell intrinsic transcription factors as well as cell extrinsic signals such as cytokines and growth factors. Although the hematopoietic system is one of the most well understood systems, the mechanisms that regulate the fate of progenitor cells remain poorly understood.

In recent years, methods required for HSC isolation have been improved and access to the hematopoietic system has become quite easy. However, hematopoiesis is often analyzed in bulk populations of cells and due to diversity within populations, studies can only reflect the average behavior of the population, but not of the single cells. Moreover, studies done by transferring HSCs or progenitor cells into mice often underestimated the role of niches and cell-cell interactions. Finding a suitable microenvironment for the development of a diversity of subsets is crucial for studying progenitor cell fate decisions *in vitro*. In this study, we demonstrated that EL08 cell line, derived from murine embryonic liver cells, could be used as a feeder layer wherein the development of CDPs into pDCs and cDCs can be studied in long term cultures at the single cell level.

In comparison to the steady state, the tissue microenvironment changes dramatically under inflammatory conditions. Anti-inflammatory cytokines released by stroma can influence the fate of progenitors by influencing their phenotype. In this study, we examined the fate of CCR9<sup>low</sup> pDC-like cells, immediate precursors of pDCs, and CCR9<sup>+</sup> pDCs *in vivo* by using a mouse model of multiple sclerosis.

### 5.1 EL08 co-culture system to study DC development

Stromal cells derived from ontogenically different hematopoietic microenvironments such as aorta gonad mesonephros (AGM), yolk sac and liver can support the differentiation of HSC *in vitro* (Durand, Robin et al. 2007). In this study, we established a co-culture system with EL08 stromal cells, derived from livers of murine embryos, to study cell fate decisions of pDCs and cDCs derived from CDPs *in vitro*. Previously, we tried to culture CDPs without feeder cells on surfaces coated with extracellular matrix proteins (gelatin or fibronectin), but CDPs failed to

differentiate on both surfaces. Obviously, CDPs are dependent on feeder cells for their survival and differentiation.

It has been reported that, the EL08 stromal cell line supported differentiation of human CD34<sup>+</sup>Lin<sup>-</sup>CD38<sup>-</sup> umbilical cord blood cells into CD56<sup>-</sup> NK cells in vitro (McCullar, Oostendorp et al. 2008). Murine studies performed with Lin<sup>-</sup> BM cells confirmed supportive role of EL08 cells in vitro (Buckley, Ulloa-Montoya et al. 2011). When the differentiation potential of CDPs was tested in co-culture with total BM cells and compared with stromal cells, we found that EL08 stromal cells were similarly effective as total BM cells in supporting pDC and cDC development in vitro. It has been previously shown that supportive capacity of EL08 cells is enhanced when progenitors are cultured in direct contact with the murine feeder cells (McCullar, Oostendorp et al. 2008). Consistent with these findings, CDP differentiation was only possible when CDPs were cultured on feeder cells. Conditioned medium derived from EL08 cell culture did not support survival and differentiation of CDPs. One explanation could be that EL08 stromal cells show characteristics of vascular smooth muscle cells (Dennis and Charbord 2002) as well as osteoblastic cells (Calvi, Adams et al. 2003), which resemble the main stromal cell type involved in hematopoiesis in the BM.

Importantly, murine cytokines that can be secreted by EL08 stromal cells may also contribute to the development of progenitors. For instance, in a study, which compared distinct embryo-derived stromal cells, EL08 uniquely supported the differentiation of human hematopoietic progenitors without further addition of cytokines (Kusadasi, Oostendorp et al. 2002). This study posed the question whether cytokines with activity on murine CDPs are secreted by these stromal cells. We tested for several murine cytokines, including GM-CSF and M-CSF, which may affect differentiation potential of CDPs. However, neither GM-CSF nor M-CSF were detectable in the supernatants of CDP-EL08 co-cultures. Using EL08 stromal cells did not just provide a suitable microenvironment; their flat morphology also enabled us to distinguish sorted CDPs from the feeder layer by their smaller size and round shape without using congenic markers for imaging experiments. The co-culture systems of CDPs with OP9 cell line and other cell lines are also effective and have been reported in several studies (Naik, Sathe et al. 2007, Onai, Kurabayashi et al. 2013). The cell density is very important in maintenance of OP9 cell line. If the cells overgrow, the OP9 cell line can easily lose its supportive capacity and differentiate into adipocytes (Wolins, Quaynor et al. 2006). Thus, the EL08 cell line used in this study was better suitable for long-term CDP co-culture experiments.



CDPs were sorted using the previously established sort strategy as Lin<sup>-</sup> CD135<sup>+</sup> CD117<sup>low</sup> CD115<sup>+</sup> CD11c<sup>-</sup> and MHCII<sup>-</sup> (here after CD115<sup>+</sup> CDP). Recently, Onai et.al, have identified CD115<sup>-</sup> progenitors (here after CD115<sup>-</sup> CDP) in the BM, which is more biased to give rise pDCs than CDPs (Onai, Kurabayashi et al. 2013). We focused on CD115<sup>+</sup> fraction, which is upstream of the CD115<sup>-</sup> CDP and is better characterized. In this study, we could show that CD115<sup>+</sup> CDP can give rise to pDCs and cDCs very efficiently in Flt3L supplemented co-cultures with total BM cells or with EL08 stromal cells.

Taken together, these experiments demonstrated that the EL08 cell line can be used to study murine DC differentiation and is a highly supportive environment for the maintenance of CDPs in long-term cultures.

## **5.2 Graded commitment of CDPs to CCR9<sup>low</sup> pDC-like cells and to CCR9<sup>+</sup> pDCs**

As recently described by Schlitzer et al., cells with pDC phenotype in the BM are heterogeneous and can be further divided based on their CCR9 expression into two populations; CCR9<sup>+</sup> differentiated pDCs and CCR9<sup>low</sup> pDC-like cells (Schlitzer, Loschko et al. 2011). Here, we studied pDC development from CDPs by time-lapse microscopy in the EL08 co-culture system to gain insight into the development of CCR9<sup>low</sup> pDC-like cells and CCR9<sup>+</sup> pDCs from progenitors on the single cell level. My aim was to understand if CCR9<sup>low</sup> pDC-like cells develop in parallel with CCR9<sup>+</sup> pDCs from CDPs or if pDCs go through a defined CCR9<sup>low</sup> stage before differentiating into mature CCR9<sup>+</sup> pDCs.

All CDPs were tracked continuously until the end of the experiment (120 h), unless they died or were lost to tracking before 36 hours of experiment time. It has been shown that instructive versus selective effects of cytokines can be distinguished by recording the frequency of cell death events in pedigrees (Rieger, Hoppe et al. 2009). In the culture system described here, Flt3L was the only cytokine added at the beginning of the culture. Nevertheless, early apoptotic events (before 36 hours) were rare and almost all CDPs were dividing. We postulated that Flt3L has an instructive and not a selective effect on CDPs, and early cell death, which occurred rarely, can be explained by post-sort stress.

Hematopoiesis is often described as a series of hierarchy levels. All mature cells are generated from progenitors during hematopoiesis and the lineage potential is reduced in

---

each differentiation step, when divergence to a specific lineage occurs. Continuous tracking of CDPs led to genealogies with the probability of homogeneous pedigrees with either pDC or cDC development as well as heterogeneous pedigrees with both pDC and cDC potential. In accordance with published results of clonal assays, most pedigrees contained either pDCs or cDCs and not both at the same time. Only in 2 of 40 pedigrees, cDCs and CCR9<sup>low</sup> pDC-like cells developed from the same CDP. The low number of pedigrees with clearly identifiable cDC fate, which were tracked, may explain why CDPs giving rise to both mature pDCs and cDCs were not observed.

Consistent with recent reports (Schlitzer, Loschko et al. 2011, Onai, Kurabayashi et al. 2013), CDPs gave rise to CD11c<sup>+</sup> MHCII<sup>+</sup> SiglecH<sup>+</sup> CCR9<sup>high</sup> and/or Siglec H<sup>high</sup> pDCs via a CCR9<sup>low</sup> precursor stage with variable duration. CCR9 upregulation occurred around day 3 whereas Siglec H upregulation was observed at later time points. These data indicate that shortly before day 3 could be the time window when CCR9<sup>low</sup> pDC-like cells differentiation into mature CCR9<sup>+</sup> pDCs occurs. In many pedigrees CDPs gave rise only to CCR9<sup>low</sup> pDC-like cells (Siglec H<sup>+</sup> CD11c<sup>+</sup> CCR9<sup>low</sup> MHCII<sup>+</sup>) and no CCR9<sup>+</sup> pDCs or cDCs were generated during the experiment time. In these pedigrees the onset of the CCR9 signal was delayed compared to pedigrees giving rise to CCR9<sup>+</sup> pDCs. It is unclear if these cells further differentiate at later time points or maintain their CCR9<sup>low</sup> pDC-like phenotype.

The CDP cultures could not be maintained and imaged continuously in an “untouched” system for more than 120 h due to high cell densities and consumption of nutrients and growth factors. Methods allowing replacement of medium and growth factors without disturbance and cultures with lower cell densities need to be developed to allow single cell tracking of CDP progeny for longer time-periods. Another approach would be the culture and tracking of single CDPs in separate culture chambers for longer times.

Around 40% of the CD11c<sup>+</sup> cells observed during 120 hours of culture did not exhibit MHCII expression detectable by imaging using in culture staining method. Naik and colleagues studied development of pDCs and cDCs from precursor cells and defined CD11c<sup>+</sup> MHCII<sup>-</sup> cells as pre-DCs (Naik, Sathe et al. 2007). Interestingly, CD11c<sup>+</sup> MHCII<sup>-</sup> cells that were tracked also expressed Siglec H and CCR9 at low levels. Some cells transiently upregulated CCR9 as well. We postulated that CD11c<sup>+</sup> MHCII<sup>-</sup> cells are “undifferentiated” or they are early DCs with MHCII expression below the detection limit of our imaging method. The method could be further improved by enhancement of the MHCII signal or by inclusion of an

additional marker, which allows distinguishing pre-DCs from cDCs such as Zbtb46 and Clec9.

In our imaging panel B220 could not be included as additional surface marker, because only four fluorescence channels were available. For further characterization of the cells with pDC phenotype, B220 would be an interesting candidate since among the CCR9<sup>low</sup> pDC-like cells B220<sup>low</sup> and B220<sup>high</sup> cells with different differentiation potential can be distinguished (see chapter 4.2.2).

### 5.3 Id2-GFP mouse model to study the role of intrinsic regulators in DC development

Live-cell imaging of CDPs derived from wildtype C57BL6 mice provided insight into pDC development at the single cell level in real time. But cDCs could not be clearly distinguished from CD11c<sup>+</sup> MHCII<sup>+</sup> Siglec H<sup>-</sup> pre-cDCs. To understand the complex network between DC subtypes, we used CDPs isolated from BM of Id2-GFP reporter mice, which enabled us to track endogenous GFP expression of the Id2 locus in individual cells.

Id2-GFP is expressed in a variety of cDC subsets, with highest expression in CD8α<sup>+</sup> and CD103<sup>+</sup> cDCs, and is silenced in pDCs. This was confirmed using the Id2-eGFP reporter mice. Moreover, Id2 expression was evaluated in the progenitor cell compartment and its expression in CDPs as well as pre-cDCs was very low as detected on mRNA level using the Id2-eGFP reporter mouse (Jackson, Hu et al. 2011). We hypothesized that Id2 expression is closely regulated in DCs and high expression of Id2-eGFP would indicate divergence of the pDC and cDC lineages. The Id2-eGFP reporter mouse generated by Gabrielle Belz's group, which was used in this study, is an Id2-IRES-eGFP mouse, which allows to faithfully detect onset and upregulation of Id2 mRNA expression (Jackson, Hu et al. 2011). Although it was reported that eGFP expression correlated precisely with Id2 transcription in several cell types in this reporter mouse, it has to be taken into consideration, that eGFP protein downregulation may be delayed compared with actual Id2 protein downregulation due to the long half-life of eGFP. Nevertheless, in some pedigrees we observed transient high eGFP expression, which may reflect an even shorter phase of high Id2 expression in some CDP progeny.

Interestingly, when we sorted and cultured CDPs isolated from Id2<sup>eGFP/eGFP</sup> reporter mice on EL08 cells, we found that not only cDCs, but also CCR9<sup>low</sup> pDC-like cells expressed Id2-

eGFP, but only at low levels. Recently, it has been reported that loss of *Mtg16*, a member of ETO proteins, impaired differentiation and functionality of pDCs. The defect in pDC development was associated with aberrant induction of *Id2*, detected by qRT-PCR in *SiglecH*<sup>+</sup> *CCR9*<sup>-</sup> pre-DCs in BM and spleen of *Mtg16*<sup>-/-</sup> mice (Ghosh, Ceribelli et al. 2014).

In my study, continuous single cell imaging of CDPs revealed that GFP was the first signal to be detected in all developing DCs. Even in some pedigrees with pDC fate high *Id2*-GFP expression was observed in the pre-DC stage at earlier time points. In these pedigrees *Id2*-GFP was downregulated at the onset of *Siglec H* expression, well before upregulation of *Siglec H*, suggesting that differentiation of *Id2* expressing pre-DCs into pDCs requires *Id2* repression.

Transcription factors are one of the most important determinants in developing DC progenitors to branch into pDC or cDC lineages. Within the DC lineage *E2-2* is preferentially expressed in pDCs and drives the development and maintenance of pDCs (Cisse, Caton et al. 2008, Ghosh, Cisse et al. 2010). The activity of E proteins is antagonized in a dose-dependent manner by ID proteins, which prevents E proteins binding to DNA (Kee 2009) Balance between E and ID proteins one of the main mediators in cell fate choices. These findings raised the hypothesis that CDP-derived DC precursors, which develop into pDCs, downregulate *Id2* and as a consequence *E2-2* driven branching to the pDC lineage occurs. In contrast, cells which have cDC fate upregulate *Id2* and maintain high *Id2* expression, thus suppressing *E2-2* activity and preventing further upregulation of *E2-2* expression, which is required for a stable pDC phenotype (Ghosh, Cisse et al. 2010). The interplay between *E2-2* and *Id2* at the branching point between pDCs and cDCs requires further investigation by single cell imaging using CDPs from mice reporting *E2-2* and *Id2* expression simultaneously.

#### **5.4 In vitro live cell imaging as a tool to study cell fate decisions**

In recent years, continuous in vitro long-term imaging has re-awakened interest in defining the mechanisms of lineage commitment. It is obvious that studying heterogeneous populations such as HSCs requires continuous observation of individual cells and their progeny rather than population snapshots or clonal assay using single isolated progenitor cells. In this study, we established for the first time a co-culture system, where CDP development into pDCs and cDCs can be observed continuously at the single cell level. This allowed us to study the behavior of single CDPs and their progeny over time in the presence of master regulator, *Flt3L*, during DC development.

“In culture” antibody staining used in this study allowed simultaneous detection of several surface markers in CDP progeny in long-term cultures. This approach has been proven before to detect surface markers in endothelial cells and hematopoietic cell types (Eilken, Nishikawa et al. 2009). Although, very low concentrations of antibodies were used in this study, surface staining was sufficient to detect a signal by fluorescence microscopy for 5 days, as well as by FACS analysis when harvesting cells after 5 days of culture. On the other hand, there is no single surface molecule, which unambiguously marks pDCs or cDCs. Lack of clear lineage characterization is one of the disadvantages of in culture antibody staining. This can be achieved by using transgenic mice, which express fluorescent proteins under the control of specific promoters (Nutt, Metcalf et al. 2005, Olme, Finnon et al. 2013). Here, we used the Id2-GFP reporter system to track endogenous Id2 expression during DC differentiation at the single cell level. Importantly, because eGFP was used in this study, the combination of surface markers that could be used for imaging purposes was limited. Therefore, an expansion of the number of fluorescence channels, which can be used simultaneously for time-lapse imaging, would be beneficial.

Live cell imaging is a trade-off between how best to image your cells and stress factors, which need to be minimized to maintain good cell viability. In microscopy, one of the stress factors is phototoxicity. It is known that long exposure to excitation light might cause cell death (Hoebe, Van Oven et al. 2007). In this study, to reduce phototoxicity we extended time intervals between fluorescent imaging up to 3 hours, which still allowed us to observe changes in fluorescence intensity at high temporal resolution in single cells.

To culture CDPs under conditions that resemble the actual situation in their BM niche, we used EL08 cells as feeder layer. One problem for the analysis was that most of the CDPs were in contact with stromal cells and they were quite motile. Not to lose identity of the tracked progenitors, we chose short time intervals (2 min for phase contrast) to capture individual cell movements by time-lapse imaging. Still, continuous observation of single CDPs was challenging and losing cells while tracking due to migration under the stromal cell layer, migration out of the imaging position or high cell density at the later time points was inevitable. The best solution for this problem would be to image cells seeded at low density on surfaces coated with extracellular matrix proteins, which can also restrict movement of the cells, but this approach was not successful for CDP cultures.

One of the crucial parts of live-cell imaging experiments is analyzing the primary imaging data. All studies published so far of continuous imaging used manual tracking and analysis of

the imaging data (Ravin, Hoepfner et al. 2008, Costa, Ortega et al. 2011), which is also one of the biggest disadvantages in these experiments. Also TTT software (Timm's Tracking Tool) used in this study is not an automated tracking program. All relevant information (division kinetics, marker onsets, cell behaviors...etc.) are logged manually by the researcher into the tracking program. In other words, data interpretation highly depends on researcher's assessment and might have a great risk of missing relevant information. Nevertheless, long-term single cell imaging has already contributed answers to many long-standing questions in the stem cell field (Mossadegh-Keller, Sarrazin et al. 2013, Thalheimer, Wingert et al. 2014, Walter, Lier et al. 2015).

In my experiments, the tracking results for some of the pedigrees were checked by a second investigator and comparable results were obtained, thus excluding a strong bias of the individual investigator. Using the barcoding technique with in vivo progenitor cell transfer, a graded commitment of progenitor cells to the DC lineage has been observed (Perie, Hodgkin et al. 2014). Our results from in vitro single cell imaging experiments are consistent with these findings as they also show great heterogeneity at the progenitor level and a graded commitment at different stages of differentiation. This consistency further supports the validity of the method described here.

## **5.5 Plasticity of pDC precursors under inflammatory conditions**

PDCs have been shown to inhibit immune responses by promoting Tregs or by reducing pathogenic effector T cell responses in mouse model of EAE (Bailey-Bucktrout, Caulkins et al. 2008, Irla, Kupfer et al. 2010). Moreover, it has been shown that delivery of MOG-peptide antigen to pDCs before EAE induction reduces disease severity by reducing the induction of autoreactive MOG specific Th1 and Th17 cells (Loschko, Heink et al. 2011). Nevertheless, the role of pDCs in CNS autoimmunity, especially in the effector phase, is still under debate. In this study, we investigated the frequency and phenotype of CCR9<sup>+</sup> pDCs and CCR9<sup>low</sup> pDC-like cells infiltrating the inflamed brain and their contribution to immune responses in the MOG-peptide induced mouse model of EAE.

Analysis of the leucocyte infiltrates derived from the recipient mice showed that pDCs were recruited to the CNS during EAE. This is consistent with the observation by Galicia-Rosas et al., that pDCs are actively recruited to the inflamed CNS around day 10 after EAE induction following the entry of T cells into the brain (Galicia-Rosas, Pikor et al. 2012).

The majority of transferred B220<sup>high</sup> CCR9<sup>low</sup> pDCs as well as B220<sup>high</sup> CCR9<sup>+</sup> pDCs homed to the inflamed brain during ongoing EAE. However, it is not clear how pDCs were attracted to the inflamed brain. In addition to inflammatory chemokines, which may attract pDCs to the inflamed CNS, growth factors may play an important role. The intracranial injection of Flt3L induces pDC recruitment (Curtin, King et al. 2006) whereas intracranial injection of GM-CSF attracts monocytes and DCs (Hesske, Vincenzetti et al. 2010). It has been shown that both Th1 and Th17 cells during EAE can secrete GM-CSF, which is essential for their pathogenic function (Codarri, Gyulveszi et al. 2011, El-Behi, Ciric et al. 2011). Therefore, we speculated that pDCs and pDC-like precursors could be attracted by chemokines as well as growth factors secreted by effector T cells or other innate immune cells in the CNS during EAE.

Despite highly inflammatory conditions, both B220<sup>high</sup> populations (CCR9<sup>low</sup> and CCR9<sup>high</sup>) largely maintained their phenotype and did not differentiate or convert into other DC subpopulations in considerable numbers. Schlitzer et al. reported that differentiation of CCR9<sup>low</sup> pDC-like cells is subject to the local tissue microenvironment. It was also shown that CCR9<sup>low</sup> pDCs retain the ability to develop into cDC-like cells with higher antigen presentation capacity under the influence of environmental factors including GM-CSF (Schlitzer, Loschko et al. 2011). We speculated that high amounts of GM-CSF or other soluble factors produced by Th1 and Th17 cells during inflammation could influence the differentiation of pDC-like cells and promote their differentiation into cDCs. However, data presented in this thesis showed that the phenotype of B220<sup>high</sup> CCR9<sup>low</sup> pDC-like cells was mostly stable for at least 3 days even under inflammatory conditions almost as stable as the phenotype of B220<sup>high</sup> CCR9<sup>high</sup> pDCs.

In contrast, almost half of the B220<sup>low</sup> CCR9<sup>low</sup> pDC-like cells downregulated their pDC markers and gave rise to cDC-like cells in vivo within 3 days after transfer. CCR9<sup>low</sup> pDC-like cells defined by Schlitzer et al. (CD11c<sup>+</sup> BST2<sup>+</sup> Siglec H<sup>+</sup> CCR9<sup>low</sup>) contained both B220<sup>high</sup> and B220<sup>low</sup> fractions and showed similar plasticity as observed here, even after transfer into steady state mice (Schlitzer, Heiseke et al. 2012). It can be concluded from the preliminary results presented here that CD11c<sup>+</sup> BST2<sup>+</sup> Siglec H<sup>+</sup> CCR9<sup>low</sup> precursors in the BM, which express high levels of B220, are further advanced and more committed to pDC differentiation than the more abundant population of CCR9<sup>low</sup> pDC-like precursors, which express low levels of B220. Therefore, I propose that upregulation of B220 indicates a stronger commitment to the pDC lineage and subsequent upregulation of CCR9 then indicates further differentiation into pDCs. These findings are consistent with a model of stepwise “graded” commitment of progenitor and precursor cells to the pDC and cDC lineages, which allows for plasticity within

the DC compartment until late stages of differentiation. This is likely to be relevant in fine-tuning innate and adaptive immune responses during infections and in inflammatory or autoimmune diseases.

Recently, it was shown that pre-DCs identified as Lineage negative (B220<sup>-</sup>, NKp46<sup>-</sup>) Sca1<sup>-</sup> CD105<sup>-</sup> MHCII<sup>-</sup> CD135<sup>+</sup> CD117<sup>low</sup> cells in murine BM contained 40-50 % Siglec H positive cells. A subset of these Siglec H<sup>+</sup> pre-DCs also expressed Zbtb46 and gave rise only to cDCs, whereas the Siglec H<sup>+</sup> Zbtb46<sup>-</sup> subset gave rise to pDCs and cDCs (Satpathy, Wu et al. 2012). In a recent publication pre-DCs defined as Lineage negative (CD3<sup>-</sup>, CD19<sup>-</sup>, Ter119, Ly6G<sup>-</sup>, B220<sup>-</sup>) CD135<sup>+</sup> CD11c<sup>+</sup> MHCII<sup>-</sup> SIRP $\alpha$ <sup>low</sup> BST2<sup>low</sup> cells in murine BM were also shown to contain 40-50 % Siglec H<sup>+</sup> CCR9<sup>-/low</sup> cells capable of generating both CCR9<sup>+</sup> pDCs and cDCs in vitro (Ghosh, Ceribelli et al. 2014). Thus, the pDC-like precursors described in our study as CD11c<sup>+</sup> BST2<sup>+</sup> Siglec H<sup>+</sup> B220<sup>low</sup> CCR9<sup>low</sup> cells in the BM (which are also Lineage negative and express MHCII, SIRP $\alpha$  and BST2 at low levels) are overlapping with the Siglec H<sup>+</sup> pre-DCs described in these studies. From the preliminary results presented here, I propose, that the Siglec H<sup>+</sup> B220<sup>high</sup> CCR9<sup>low</sup> subset contains the immediate precursor of CCR9<sup>+</sup> pDCs, the pre-pDC.

Neither CCR9<sup>+</sup> pDCs nor CCR9<sup>low</sup> pDC-like cells (B220<sup>high</sup> and B220<sup>low</sup> fraction), when transferred during ongoing EAE influenced the disease activity. This can be partially explained by the low numbers of precursor cells used in adoptive transfer experiments. Although, DCs and DC precursors were expanded by injection of Flt3L secreting melanoma cells prior to sort experiments, the number of sorted cells was quite low. In addition, the time period of 3 days may have been too short to observe changes in the disease course and transfer at the peak of disease activity may have been too late to observe any influence on the disease activity. Increasing the number of transferred cells and testing different time points for the pDC transfer and observing the mice for longer time periods may give a better understanding about the role of pDCs in CNS autoimmunity in the future.



## 6 Summary

Functionally distinct dendritic cell (DC) populations, plasmacytoid DCs (pDCs) and conventional DCs (cDCs) develop from common DC progenitors (CDP) defined by coexpression of Fms-like tyrosine kinase 3 ligand (Flt3L) and macrophage-colony stimulation factor receptor (M-CSFR) and lack of lineage markers. Although it was shown *in vitro* that CDPs gave rise to pDCs and cDCs in the presence of Flt3L, the exact developmental steps and the sequence of the events were unclear. In this study, using the live-cell imaging and single cell tracking approach, developmental steps of CDP-derived pDCs have been studied for the first time at the single cell level.

In this study, an *in vitro* culture system wherein CDP development into pDCs and cDCs were continuously monitored by time-lapse microscopy was established using EL08 stromal cells. Moreover, “*in culture* antibody staining” used in this study provided long-term detection of fluorescent markers in living cells. The data presented in this study provided evidence for a sequential development of CDPs into CCR9<sup>low</sup> pDC-like cells, which further differentiate into CCR9<sup>+</sup> pDCs. Direct differentiation of CDPs into pDCs expressing simultaneously Siglec H and high levels of CCR9 was observed rarely. Most CCR9<sup>+</sup> pDCs, which were tracked, differentiated from a CD11c<sup>+</sup> Siglec H<sup>+</sup> CCR9<sup>low</sup> precursor stage.

Inhibitor of DNA-binding 2 (Id2) is a repressor of E2-2, and is critical for cDC development. Conversely, Id2 repression allowing E2-2 expression and activity is required for pDC development. Using Id2-eGFP reporter mice, which coexpress green fluorescent protein (GFP) controlled by the Id2 promoter, the expression of Id2 was traced by assessing GFP fluorescence in CDP progeny by continuous single cell tracking. In this analysis Id2-eGFP was found to be expressed early on in the majority of CDP progeny at low levels. Id2-eGFP upregulation was observed in several pedigrees at the CD11c<sup>+</sup> Siglec H<sup>+</sup> precursor stage. In some pedigrees with CCR9<sup>+</sup> pDC differentiation, Id2-eGFP was transiently expressed at high levels and then downregulated, suggesting that active repression of Id2 is required for pDC development from precursors. This is consistent with a branching model in which Id2 repression in pre-DCs indicates pDC cell fate decision, whereas continued expression of Id2 indicates cDC cell fate decision.

Furthermore, the *in vivo* fate of CCR9<sup>low</sup> pDC-like precursors (B220<sup>high</sup> and B220<sup>low</sup> CCR9<sup>low</sup> fraction) and B220<sup>high</sup> CCR9<sup>+</sup> pDCs were analyzed in the mouse model of experimental autoimmune encephalomyelitis (EAE). Even under highly inflammatory conditions, the

phenotype of B220<sup>high</sup> CCR9<sup>+</sup> pDCs as well as B220<sup>high</sup> CCR9<sup>low</sup> pDC-like cells was quite stable, whereas B220<sup>low</sup> CCR9<sup>low</sup> pDC-like cells, which overlap with Siglec H<sup>+</sup> pre-DCs in the BM, retained their plasticity and were capable of giving rise to cDCs. These results suggest that B220<sup>low</sup> CCR9<sup>low</sup> pDC-like cells are pre-DCs with pDC and cDC potential and B220<sup>high</sup> CCR9<sup>low</sup> pDC-like cells are pDC-committed precursors (pre-pDCs), which give rise mainly to pDCs. Conversion of B220<sup>high</sup> CCR9<sup>+</sup> pDCs to cDCs at significant frequency was not observed even under highly inflammatory conditions in the inflamed CNS. The contribution of pDCs and pDC-like precursors to the immune response during EAE remains to be determined.

In conclusion, the findings of this study are consistent with a model of stepwise “graded” commitment of progenitor and precursor cells to the pDC or cDC lineages, which allows for plasticity within the DC compartment until late stages of differentiation. Thus, the frequency of functionally distinct subpopulations of DCs can be adapted to the local tissue microenvironment and situation during infections and inflammatory or autoimmune responses.

---

## REFERENCES

- Adolfsson, J., O. J. Borge, D. Bryder, K. Theilgaard-Monch, I. Astrand-Grundstrom, E. Sitnicka, Y. Sasaki and S. E. Jacobsen (2001). "Upregulation of Flt3 expression within the bone marrow Lin(-)Sca1(+)c-kit(+) stem cell compartment is accompanied by loss of self-renewal capacity." *Immunity* **15**(4): 659-669.
- Allan, R. S., J. Waithman, S. Bedoui, C. M. Jones, J. A. Villadangos, Y. Zhan, A. M. Lew, K. Shortman, W. R. Heath and F. R. Carbone (2006). "Migratory dendritic cells transfer antigen to a lymph node-resident dendritic cell population for efficient CTL priming." *Immunity* **25**(1): 153-162.
- Anderson, K. L., H. Perkin, C. D. Surh, S. Venturini, R. A. Maki and B. E. Torbett (2000). "Transcription factor PU.1 is necessary for development of thymic and myeloid progenitor-derived dendritic cells." *J Immunol* **164**(4): 1855-1861.
- Bailey-Bucktrout, S. L., S. C. Caulkins, G. Goings, J. A. Fischer, A. Dzionek and S. D. Miller (2008). "Cutting edge: central nervous system plasmacytoid dendritic cells regulate the severity of relapsing experimental autoimmune encephalomyelitis." *J Immunol* **180**(10): 6457-6461.
- Bedoui, S., P. G. Whitney, J. Waithman, L. Eidsmo, L. Wakim, I. Caminschi, R. S. Allan, M. Wojtasiak, K. Shortman, F. R. Carbone, A. G. Brooks and W. R. Heath (2009). "Cross-presentation of viral and self antigens by skin-derived CD103+ dendritic cells." *Nat Immunol* **10**(5): 488-495.
- Belz, G. T., G. M. N. Behrens, C. M. Smith, J. F. A. P. Miller, C. Jones, K. Lejon, C. G. Fathman, S. N. Mueller, K. Shortman, F. R. Carbone and W. R. Heath (2002). "The CD8+ Dendritic Cell Is Responsible for Inducing Peripheral Self-Tolerance to Tissue-associated Antigens." *Journal of Experimental Medicine* **196**(8): 1099-1104.
- Bjorck, P., H. X. Leong and E. G. Engleman (2011). "Plasmacytoid dendritic cell dichotomy: identification of IFN-alpha producing cells as a phenotypically and functionally distinct subset." *J Immunol* **186**(3): 1477-1485.
- Bogunovic, M., F. Ginhoux, J. Helft, L. Shang, D. Hashimoto, M. Greter, K. Liu, C. Jakubzick, M. A. Ingersoll, M. Leboeuf, E. R. Stanley, M. Nussenzweig, S. A. Lira, G. J. Randolph and M. Merad (2009). "Origin of the lamina propria dendritic cell network." *Immunity* **31**(3): 513-525.
- Breton, G., J. Lee, Y. J. Zhou, J. J. Schreiber, T. Keler, S. Puhr, N. Anandasabapathy, S. Schlesinger, M. Caskey, K. Liu and M. C. Nussenzweig (2015). "Circulating precursors of human CD1c+ and CD141+ dendritic cells." *J Exp Med* **212**(3): 401-413.
- Buckley, S. M., F. Ulloa-Montoya, D. Abts, R. A. Oostendorp, E. Dzierzak, S. C. Ekker and C. M. Verfaillie (2011). "Maintenance of HSC by Wnt5a secreting AGM-derived stromal cell line." *Exp Hematol* **39**(1): 114-123.e111-115.
- Calvi, L. M., G. B. Adams, K. W. Weibrecht, J. M. Weber, D. P. Olson, M. C. Knight, R. P. Martin, E. Schipani, P. Divieti, F. R. Bringhurst, L. A. Milner, H. M. Kronenberg and D. T. Scadden (2003). "Osteoblastic cells regulate the haematopoietic stem cell niche." *Nature* **425**(6960): 841-846.
- Carotta, S., A. Dakic, A. D'Amico, S. H. Pang, K. T. Greig, S. L. Nutt and L. Wu (2010). "The transcription factor PU.1 controls dendritic cell development and Flt3 cytokine receptor expression in a dose-dependent manner." *Immunity* **32**(5): 628-641.

- Chen, Y. L., T. T. Chen, L. M. Pai, J. Wesoly, H. A. Bluysen and C. K. Lee (2013). "A type I IFN-Flt3 ligand axis augments plasmacytoid dendritic cell development from common lymphoid progenitors." *J Exp Med* **210**(12): 2515-2522.
- Chicha, L., D. Jarrossay and M. G. Manz (2004). "Clonal type I interferon-producing and dendritic cell precursors are contained in both human lymphoid and myeloid progenitor populations." *J Exp Med* **200**(11): 1519-1524.
- Cisse, B., M. L. Caton, M. Lehner, T. Maeda, S. Scheu, R. Locksley, D. Holmberg, C. Zweier, N. S. den Hollander, S. G. Kant, W. Holter, A. Rauch, Y. Zhuang and B. Reizis (2008). "Transcription factor E2-2 is an essential and specific regulator of plasmacytoid dendritic cell development." *Cell* **135**(1): 37-48.
- Codarri, L., G. Gyulveszi, V. Tosevski, L. Hesse, A. Fontana, L. Magnenat, T. Suter and B. Becher (2011). "RORgammat drives production of the cytokine GM-CSF in helper T cells, which is essential for the effector phase of autoimmune neuroinflammation." *Nat Immunol* **12**(6): 560-567.
- Costa, M. R., F. Ortega, M. S. Brill, R. Beckervordersandforth, C. Petrone, T. Schroeder, M. Gotz and B. Berninger (2011). "Continuous live imaging of adult neural stem cell division and lineage progression in vitro." *Development* **138**(6): 1057-1068.
- Curtin, J. F., G. D. King, C. Barcia, C. Liu, F. X. Hubert, C. Guillonneau, R. Josien, I. Anegon, P. R. Lowenstein and M. G. Castro (2006). "Fms-like tyrosine kinase 3 ligand recruits plasmacytoid dendritic cells to the brain." *J Immunol* **176**(6): 3566-3577.
- De Smedt, T., B. Pajak, E. Muraille, L. Lespagnard, E. Heinen, P. De Baetselier, J. Urbain, O. Leo and M. Moser (1996). "Regulation of dendritic cell numbers and maturation by lipopolysaccharide in vivo." *J Exp Med* **184**(4): 1413-1424.
- den Haan, J. M., S. M. Lehar and M. J. Bevan (2000). "CD8(+) but not CD8(-) dendritic cells cross-prime cytotoxic T cells in vivo." *J Exp Med* **192**(12): 1685-1696.
- Dennis, J. E. and P. Charbord (2002). "Origin and differentiation of human and murine stroma." *Stem Cells* **20**(3): 205-214.
- Dudziak, D., A. O. Kamphorst, G. F. Heidkamp, V. R. Buchholz, C. Trumpfheller, S. Yamazaki, C. Cheong, K. Liu, H. W. Lee, C. G. Park, R. M. Steinman and M. C. Nussenzweig (2007). "Differential antigen processing by dendritic cell subsets in vivo." *Science* **315**(5808): 107-111.
- Durand, C., C. Robin, K. Bollerot, M. H. Baron, K. Ottersbach and E. Dzierzak (2007). "Embryonic stromal clones reveal developmental regulators of definitive hematopoietic stem cells." *Proc Natl Acad Sci U S A* **104**(52): 20838-20843.
- Edelson, B. T., W. Kc, R. Juang, M. Kohyama, L. A. Benoit, P. A. Klekotka, C. Moon, J. C. Albring, W. Ise, D. G. Michael, D. Bhattacharya, T. S. Stappenbeck, M. J. Holtzman, S. S. Sung, T. L. Murphy, K. Hildner and K. M. Murphy (2010). "Peripheral CD103+ dendritic cells form a unified subset developmentally related to CD8alpha+ conventional dendritic cells." *J Exp Med* **207**(4): 823-836.
- Eilken, H. M., S. Nishikawa and T. Schroeder (2009). "Continuous single-cell imaging of blood generation from haemogenic endothelium." *Nature* **457**(7231): 896-900.

- El-Behi, M., B. Ciric, H. Dai, Y. Yan, M. Cullimore, F. Safavi, G. X. Zhang, B. N. Dittel and A. Rostami (2011). "The encephalitogenicity of T(H)17 cells is dependent on IL-1- and IL-23-induced production of the cytokine GM-CSF." *Nat Immunol* **12**(6): 568-575.
- Fancke, B., M. Suter, H. Hochrein and M. O'Keeffe (2008). "M-CSF: a novel plasmacytoid and conventional dendritic cell poietin." *Blood* **111**(1): 150-159.
- Fogg, D. K., C. Sibon, C. Miled, S. Jung, P. Aucouturier, D. R. Littman, A. Cumano and F. Geissmann (2006). "A clonogenic bone marrow progenitor specific for macrophages and dendritic cells." *Science* **311**(5757): 83-87.
- Galicia-Rosas, G., N. Pikor, J. A. Schwartz, O. Rojas, A. Jian, L. Summers-Deluca, M. Ostrowski, B. Nüsslein-Hildesheim and J. L. Gommerman (2012). "A sphingosine-1-phosphate receptor 1-directed agonist reduces central nervous system inflammation in a plasmacytoid dendritic cell-dependent manner." *J Immunol* **189**(7): 3700-3706.
- Gautier, E. L., T. Shay, J. Miller, M. Greter, C. Jakubzick, S. Ivanov, J. Helft, A. Chow, K. G. Elpek, S. Gordonov, A. R. Mazloom, A. Ma'ayan, W. J. Chua, T. H. Hansen, S. J. Turley, M. Merad and G. J. Randolph (2012). "Gene-expression profiles and transcriptional regulatory pathways that underlie the identity and diversity of mouse tissue macrophages." *Nat Immunol* **13**(11): 1118-1128.
- Ghosh, H. S., M. Ceribelli, I. Matos, A. Lazarovici, H. J. Bussemaker, A. Lasorella, S. W. Hiebert, K. Liu, L. M. Staudt and B. Reizis (2014). "ETO family protein Mtg16 regulates the balance of dendritic cell subsets by repressing Id2." *J Exp Med* **211**(8): 1623-1635.
- Ghosh, H. S., B. Cisse, A. Bunin, K. L. Lewis and B. Reizis (2010). "Continuous expression of the transcription factor e2-2 maintains the cell fate of mature plasmacytoid dendritic cells." *Immunity* **33**(6): 905-916.
- Ginhoux, F., K. Liu, J. Helft, M. Bogunovic, M. Greter, D. Hashimoto, J. Price, N. Yin, J. Bromberg, S. A. Lira, E. R. Stanley, M. Nussenzweig and M. Merad (2009). "The origin and development of nonlymphoid tissue CD103+ DCs." *J Exp Med* **206**(13): 3115-3130.
- Ginhoux, F., F. Tacke, V. Angeli, M. Bogunovic, M. Loubreau, X. M. Dai, E. R. Stanley, G. J. Randolph and M. Merad (2006). "Langerhans cells arise from monocytes in vivo." *Nat Immunol* **7**(3): 265-273.
- Greter, M., J. Helft, A. Chow, D. Hashimoto, A. Mortha, J. Agudo-Cantero, M. Bogunovic, E. L. Gautier, J. Miller, M. Leboeuf, G. Lu, C. Aloman, B. D. Brown, J. W. Pollard, H. Xiong, G. J. Randolph, J. E. Chipuk, P. S. Frenette and M. Merad (2012). "GM-CSF controls nonlymphoid tissue dendritic cell homeostasis but is dispensable for the differentiation of inflammatory dendritic cells." *Immunity* **36**(6): 1031-1046.
- Hacker, C., R. D. Kirsch, X. S. Ju, T. Hieronymus, T. C. Gust, C. Kuhl, T. Jorgas, S. M. Kurz, S. Rose-John, Y. Yokota and M. Zenke (2003). "Transcriptional profiling identifies Id2 function in dendritic cell development." *Nat Immunol* **4**(4): 380-386.
- Hadeiba, H., K. Lahl, A. Edalati, C. Oderup, A. Habtezion, R. Pachynski, L. Nguyen, A. Ghodsi, S. Adler and E. C. Butcher (2012). "Plasmacytoid dendritic cells transport peripheral antigens to the thymus to promote central tolerance." *Immunity* **36**(3): 438-450.
- Hambleton, S., S. Salem, J. Bustamante, V. Bigley, S. Boisson-Dupuis, J. Azevedo, A. Fortin, M. Haniffa, L. Ceron-Gutierrez, C. M. Bacon, G. Menon, C. Trouillet, D. McDonald, P. Carey, F. Ginhoux, L. Alsina, T. J. Zumwalt, X. F. Kong, D. Kumararatne, K. Butler, M. Hubeau, J. Feinberg, S. Al-Muhsen, A. Cant, L. Abel, D. Chaussabel, R. Doffinger, E. Talesnik, A. Grumach, A. Duarte, K. Abarca, D. Moraes-Vasconcelos, D. Burk, A.

- 
- Berghuis, F. Geissmann, M. Collin, J. L. Casanova and P. Gros (2011). "IRF8 mutations and human dendritic-cell immunodeficiency." N Engl J Med **365**(2): 127-138.
- Hesske, L., C. Vincenzetti, M. Heikenwalder, M. Prinz, W. Reith, A. Fontana and T. Suter (2010). "Induction of inhibitory central nervous system-derived and stimulatory blood-derived dendritic cells suggests a dual role for granulocyte-macrophage colony-stimulating factor in central nervous system inflammation." Brain **133**(Pt 6): 1637-1654.
- Hoebe, R. A., C. H. Van Oven, T. W. Gadella, Jr., P. B. Dhonukshe, C. J. Van Noorden and E. M. Manders (2007). "Controlled light-exposure microscopy reduces photobleaching and phototoxicity in fluorescence live-cell imaging." Nat Biotechnol **25**(2): 249-253.
- Idoyaga, J., N. Suda, K. Suda, C. G. Park and R. M. Steinman (2009). "Antibody to Langerin/CD207 localizes large numbers of CD8alpha+ dendritic cells to the marginal zone of mouse spleen." Proc Natl Acad Sci U S A **106**(5): 1524-1529.
- Inaba, K., M. Inaba, N. Romani, H. Aya, M. Deguchi, S. Ikehara, S. Muramatsu and R. M. Steinman (1992). "Generation of large numbers of dendritic cells from mouse bone marrow cultures supplemented with granulocyte/macrophage colony-stimulating factor." J Exp Med **176**(6): 1693-1702.
- Irla, M., N. Kupfer, T. Suter, R. Lissilaa, M. Benkhoucha, J. Skupsky, P. H. Lalive, A. Fontana, W. Reith and S. Hugues (2010). "MHC class II-restricted antigen presentation by plasmacytoid dendritic cells inhibits T cell-mediated autoimmunity." J Exp Med **207**(9): 1891-1905.
- Iwakoshi, N. N., M. Pypaert and L. H. Glimcher (2007). "The transcription factor XBP-1 is essential for the development and survival of dendritic cells." J Exp Med **204**(10): 2267-2275.
- Jackson, J. T., Y. Hu, R. Liu, F. Masson, A. D'Amico, S. Carotta, A. Xin, M. J. Camilleri, A. M. Mount, A. Kallies, L. Wu, G. K. Smyth, S. L. Nutt and G. T. Belz (2011). "Id2 expression delineates differential checkpoints in the genetic program of CD8alpha+ and CD103+ dendritic cell lineages." EMBO J **30**(13): 2690-2704.
- Jego, G., A. K. Palucka, J. P. Blanck, C. Chalouni, V. Pascual and J. Banchereau (2003). "Plasmacytoid dendritic cells induce plasma cell differentiation through type I interferon and interleukin 6." Immunity **19**(2): 225-234.
- Karrich, J. J., M. Balzarolo, H. Schmidlin, M. Libouban, M. Nagasawa, R. Gentek, S. Kamihira, T. Maeda, D. Amsen, M. C. Wolkers and B. Blom (2012). "The transcription factor Spi-B regulates human plasmacytoid dendritic cell survival through direct induction of the antiapoptotic gene BCL2-A1." Blood **119**(22): 5191-5200.
- Karsunky, H., M. Merad, A. Cozzio, I. L. Weissman and M. G. Manz (2003). "Flt3 ligand regulates dendritic cell development from Flt3+ lymphoid and myeloid-committed progenitors to Flt3+ dendritic cells in vivo." J Exp Med **198**(2): 305-313.
- Kee, B. L. (2009). "E and ID proteins branch out." Nat Rev Immunol **9**(3): 175-184.
- Korn, T., J. Reddy, W. Gao, E. Bettelli, A. Awasthi, T. R. Petersen, B. T. Backstrom, R. A. Sobel, K. W. Wucherpfennig, T. B. Strom, M. Oukka and V. K. Kuchroo (2007). "Myelin-specific regulatory T cells accumulate in the CNS but fail to control autoimmune inflammation." Nat Med **13**(4): 423-431.

- 
- Krug, A., R. Uppaluri, F. Facchetti, B. G. Dorner, K. C. Sheehan, R. D. Schreiber, M. Cella and M. Colonna (2002). "IFN-producing cells respond to CXCR3 ligands in the presence of CXCL12 and secrete inflammatory chemokines upon activation." J Immunol **169**(11): 6079-6083.
- Kueh, H. Y., A. Champhekar, S. L. Nutt, M. B. Elowitz and E. V. Rothenberg (2013). "Positive feedback between PU.1 and the cell cycle controls myeloid differentiation." Science **341**(6146): 670-673.
- Kusadasi, N., R. A. Oostendorp, W. J. Koevoet, E. A. Dzierzak and R. E. Ploemacher (2002). "Stromal cells from murine embryonic aorta-gonad-mesonephros region, liver and gut mesentery expand human umbilical cord blood-derived CAFc(week6) in extended long-term cultures." Leukemia **16**(9): 1782-1790.
- Lee, J., G. Breton, T. Y. Oliveira, Y. J. Zhou, A. Aljoufi, S. Pühr, M. J. Cameron, R. P. Sekaly, M. C. Nussenzweig and K. Liu (2015). "Restricted dendritic cell and monocyte progenitors in human cord blood and bone marrow." J Exp Med **212**(3): 385-399.
- Liu, K., G. D. Victora, T. A. Schwickert, P. Guermonprez, M. M. Meredith, K. Yao, F. F. Chu, G. J. Randolph, A. Y. Rudensky and M. Nussenzweig (2009). "In vivo analysis of dendritic cell development and homeostasis." Science **324**(5925): 392-397.
- Liu, Y. J. (2005). "IPC: professional type 1 interferon-producing cells and plasmacytoid dendritic cell precursors." Annu Rev Immunol **23**: 275-306.
- Loschko, J., S. Heink, D. Hackl, D. Dudziak, W. Reindl, T. Korn and A. B. Krug (2011). "Antigen targeting to plasmacytoid dendritic cells via Siglec-H inhibits Th cell-dependent autoimmunity." J Immunol **187**(12): 6346-6356.
- Lund, J. M., M. M. Linehan, N. Iijima and A. Iwasaki (2006). "Cutting Edge: Plasmacytoid dendritic cells provide innate immune protection against mucosal viral infection in situ." J Immunol **177**(11): 7510-7514.
- Mach, N., S. Gillessen, S. B. Wilson, C. Sheehan, M. Mihm and G. Dranoff (2000). "Differences in dendritic cells stimulated in vivo by tumors engineered to secrete granulocyte-macrophage colony-stimulating factor or Flt3-ligand." Cancer Res **60**(12): 3239-3246.
- Manfra, D. J., S. C. Chen, K. K. Jensen, J. S. Fine, M. T. Wiekowski and S. A. Lira (2003). "Conditional Expression of Murine Flt3 Ligand Leads to Expansion of Multiple Dendritic Cell Subsets in Peripheral Blood and Tissues of Transgenic Mice." The Journal of Immunology **170**(6): 2843-2852.
- Manz, M. G., D. Traver, K. Akashi, M. Merad, T. Miyamoto, E. G. Engleman and I. L. Weissman (2001). "Dendritic cell development from common myeloid progenitors." Ann N Y Acad Sci **938**: 167-173; discussion 173-164.
- Maraskovsky, E., E. Daro, E. Roux, M. Teepe, C. R. Maliszewski, J. Hoek, D. Caron, M. E. Lebsack and H. J. McKenna (2000). "In vivo generation of human dendritic cell subsets by Flt3 ligand." Blood **96**(3): 878-884.
- Martin-Gayo, E., E. Sierra-Filardi, A. L. Corbi and M. L. Toribio (2010). "Plasmacytoid dendritic cells resident in human thymus drive natural Treg cell development." Blood **115**(26): 5366-5375.
- McCullar, V., R. Oostendorp, A. Panoskaltsis-Mortari, G. Yun, C. T. Lutz, J. E. Wagner and J. S. Miller (2008). "Mouse fetal and embryonic liver cells differentiate human umbilical cord blood progenitors into CD56-negative natural killer cell precursors in the absence of interleukin-15." Exp Hematol **36**(5): 598-608.

- McKenna, H. J., K. L. Stocking, R. E. Miller, K. Brasel, T. De Smedt, E. Maraskovsky, C. R. Maliszewski, D. H. Lynch, J. Smith, B. Pulendran, E. R. Roux, M. Teepe, S. D. Lyman and J. J. Peschon (2000). "Mice lacking flt3 ligand have deficient hematopoiesis affecting hematopoietic progenitor cells, dendritic cells, and natural killer cells." Blood **95**(11): 3489-3497.
- Merad, M., F. Ginhoux and M. Collin (2008). "Origin, homeostasis and function of Langerhans cells and other langerin-expressing dendritic cells." Nat Rev Immunol **8**(12): 935-947.
- Merad, M., M. G. Manz, H. Karsunky, A. Wagers, W. Peters, I. Charo, I. L. Weissman, J. G. Cyster and E. G. Engleman (2002). "Langerhans cells renew in the skin throughout life under steady-state conditions." Nat Immunol **3**(12): 1135-1141.
- Merad, M., P. Sathe, J. Helft, J. Miller and A. Mortha (2013). "The dendritic cell lineage: ontogeny and function of dendritic cells and their subsets in the steady state and the inflamed setting." Annu Rev Immunol **31**: 563-604.
- Meredith, M. M., K. Liu, G. Darrasse-Jeze, A. O. Kamphorst, H. A. Schreiber, P. Guermonprez, J. Idoyaga, C. Cheong, K. H. Yao, R. E. Niec and M. C. Nussenzweig (2012). "Expression of the zinc finger transcription factor zDC (Zbtb46, Btbd4) defines the classical dendritic cell lineage." J Exp Med **209**(6): 1153-1165.
- Mossadegh-Keller, N., S. Sarrazin, P. K. Kandalla, L. Espinosa, E. R. Stanley, S. L. Nutt, J. Moore and M. H. Sieweke (2013). "M-CSF instructs myeloid lineage fate in single haematopoietic stem cells." Nature **497**(7448): 239-243.
- Naik, S. H., D. Metcalf, A. van Nieuwenhuijze, I. Wicks, L. Wu, M. O'Keeffe and K. Shortman (2006). "Intrasplenic steady-state dendritic cell precursors that are distinct from monocytes." Nat Immunol **7**(6): 663-671.
- Naik, S. H., P. Sathe, H. Y. Park, D. Metcalf, A. I. Proietto, A. Dakic, S. Carotta, M. O'Keeffe, M. Bahlo, A. Papenfuss, J. Y. Kwak, L. Wu and K. Shortman (2007). "Development of plasmacytoid and conventional dendritic cell subtypes from single precursor cells derived in vitro and in vivo." Nat Immunol **8**(11): 1217-1226.
- Naik, S. H., T. N. Schumacher and L. Perie (2014). "Cellular barcoding: a technical appraisal." Exp Hematol **42**(8): 598-608.
- Nestle, F. O., C. Conrad, A. Tun-Kyi, B. Homey, M. Gombert, O. Boyman, G. Burg, Y. J. Liu and M. Gilliet (2005). "Plasmacytoid predendritic cells initiate psoriasis through interferon-alpha production." J Exp Med **202**(1): 135-143.
- Nutt, S. L., D. Metcalf, A. D'Amico, M. Polli and L. Wu (2005). "Dynamic regulation of PU.1 expression in multipotent hematopoietic progenitors." J Exp Med **201**(2): 221-231.
- Ohl, L., M. Mohaupt, N. Czeloth, G. Hintzen, Z. Kiafard, J. Zwirner, T. Blankenstein, G. Henning and R. Forster (2004). "CCR7 governs skin dendritic cell migration under inflammatory and steady-state conditions." Immunity **21**(2): 279-288.
- Olme, C. H., R. Finnon, N. Brown, S. Kabacik, S. D. Bouffler and C. Badie (2013). "Live cell detection of chromosome 2 deletion and Sfp1/PU1 loss in radiation-induced mouse acute myeloid leukaemia." Leuk Res **37**(10): 1374-1382.



- Onai, N., K. Kurabayashi, M. Hosoi-Amaiike, N. Toyama-Sorimachi, K. Matsushima, K. Inaba and T. Ohteki (2013). "A clonogenic progenitor with prominent plasmacytoid dendritic cell developmental potential." *Immunity* **38**(5): 943-957.
- Onai, N., A. Obata-Onai, M. A. Schmid, T. Ohteki, D. Jarrossay and M. G. Manz (2007). "Identification of clonogenic common Flt3+M-CSFR+ plasmacytoid and conventional dendritic cell progenitors in mouse bone marrow." *Nat Immunol* **8**(11): 1207-1216.
- Oostendorp, R. A., K. N. Harvey, N. Kusadasi, M. F. de Bruijn, C. Saris, R. E. Ploemacher, A. L. Medvinsky and E. A. Dzierzak (2002). "Stromal cell lines from mouse aorta-gonads-mesonephros subregions are potent supporters of hematopoietic stem cell activity." *Blood* **99**(4): 1183-1189.
- Oostendorp, R. A., A. J. Medvinsky, N. Kusadasi, N. Nakayama, K. Harvey, C. Orelia, K. Ottersbach, T. Covey, R. E. Ploemacher, C. Saris and E. Dzierzak (2002). "Embryonal subregion-derived stromal cell lines from novel temperature-sensitive SV40 T antigen transgenic mice support hematopoiesis." *J Cell Sci* **115**(Pt 10): 2099-2108.
- Paul, F. and I. Amit (2014). "Plasticity in the transcriptional and epigenetic circuits regulating dendritic cell lineage specification and function." *Curr Opin Immunol* **30**: 1-8.
- Perie, L., P. D. Hodgkin, S. H. Naik, T. N. Schumacher, R. J. de Boer and K. R. Duffy (2014). "Determining lineage pathways from cellular barcoding experiments." *Cell Rep* **6**(4): 617-624.
- Randolph, G. J., J. Ochando and S. Partida-Sanchez (2008). "Migration of dendritic cell subsets and their precursors." *Annu Rev Immunol* **26**: 293-316.
- Ravin, R., D. J. Hoepfner, D. M. Munno, L. Carmel, J. Sullivan, D. L. Levitt, J. L. Miller, C. Athaide, D. M. Panchision and R. D. McKay (2008). "Potency and fate specification in CNS stem cell populations in vitro." *Cell Stem Cell* **3**(6): 670-680.
- Rieger, M. A., P. S. Hoppe, B. M. Smejkal, A. C. Eitelhuber and T. Schroeder (2009). "Hematopoietic cytokines can instruct lineage choice." *Science* **325**(5937): 217-218.
- Rothbauer, U., K. Zolghadr, S. Tillib, D. Nowak, L. Schermelleh, A. Gahl, N. Backmann, K. Conrath, S. Muyldermans, M. C. Cardoso and H. Leonhardt (2006). "Targeting and tracing antigens in live cells with fluorescent nanobodies." *Nat Methods* **3**(11): 887-889.
- Satpathy, A. T., W. Kc, J. C. Albring, B. T. Edelson, N. M. Kretzer, D. Bhattacharya, T. L. Murphy and K. M. Murphy (2012). "Zbtb46 expression distinguishes classical dendritic cells and their committed progenitors from other immune lineages." *J Exp Med* **209**(6): 1135-1152.
- Satpathy, A. T., X. Wu, J. C. Albring and K. M. Murphy (2012). "Re(de)fining the dendritic cell lineage." *Nat Immunol* **13**(12): 1145-1154.
- Schepers, K., E. Swart, J. W. van Heijst, C. Gerlach, M. Castrucci, D. Sie, M. Heimerikx, A. Velds, R. M. Kerkhoven, R. Arens and T. N. Schumacher (2008). "Dissecting T cell lineage relationships by cellular barcoding." *J Exp Med* **205**(10): 2309-2318.

- Schiavoni, G., F. Mattei, P. Sestili, P. Borghi, M. Venditti, H. C. Morse, 3rd, F. Belardelli and L. Gabriele (2002). "ICSBP is essential for the development of mouse type I interferon-producing cells and for the generation and activation of CD8alpha(+) dendritic cells." *J Exp Med* **196**(11): 1415-1425.
- Schlitzer, A., A. F. Heiseke, H. Einwachter, W. Reindl, M. Schiemann, C. P. Manta, P. See, J. H. Niess, T. Suter, F. Ginhoux and A. B. Krug (2012). "Tissue-specific differentiation of a circulating CCR9- pDC-like common dendritic cell precursor." *Blood* **119**(25): 6063-6071.
- Schlitzer, A., J. Loschko, K. Mair, R. Vogelmann, L. Henkel, H. Einwachter, M. Schiemann, J. H. Niess, W. Reindl and A. Krug (2011). "Identification of CCR9- murine plasmacytoid DC precursors with plasticity to differentiate into conventional DCs." *Blood* **117**(24): 6562-6570.
- Schmid, M. A., D. Kingston, S. Boddupalli and M. G. Manz (2010). "Instructive cytokine signals in dendritic cell lineage commitment." *Immunol Rev* **234**(1): 32-44.
- Schraml, B. U., J. van Blijswijk, S. Zelenay, P. G. Whitney, A. Filby, S. E. Acton, N. C. Rogers, N. Moncaut, J. J. Carvajal and C. Reis e Sousa (2013). "Genetic tracing via DNGR-1 expression history defines dendritic cells as a hematopoietic lineage." *Cell* **154**(4): 843-858.
- Schuler, G., N. Romani and R. M. Steinman (1985). "A comparison of murine epidermal Langerhans cells with spleen dendritic cells." *J Invest Dermatol* **85**(1 Suppl): 99s-106s.
- Scott, C. L., Z. M. Tfp, K. S. Beckham, G. Douce and A. M. Mowat (2014). "Signal regulatory protein alpha (SIRPalpha) regulates the homeostasis of CD103(+) CD11b(+) DCs in the intestinal lamina propria." *Eur J Immunol* **44**(12): 3658-3668.
- Serbina, N. V., T. P. Salazar-Mather, C. A. Biron, W. A. Kuziel and E. G. Pamer (2003). "TNF/iNOS-producing dendritic cells mediate innate immune defense against bacterial infection." *Immunity* **19**(1): 59-70.
- Sharma, M. D., B. Baban, P. Chandler, D. Y. Hou, N. Singh, H. Yagita, M. Azuma, B. R. Blazar, A. L. Mellor and D. H. Munn (2007). "Plasmacytoid dendritic cells from mouse tumor-draining lymph nodes directly activate mature Tregs via indoleamine 2,3-dioxygenase." *J Clin Invest* **117**(9): 2570-2582.
- Shortman, K. and Y. J. Liu (2002). "Mouse and human dendritic cell subtypes." *Nat Rev Immunol* **2**(3): 151-161.
- Sozzani, S., W. Vermi, A. Del Prete and F. Facchetti (2010). "Trafficking properties of plasmacytoid dendritic cells in health and disease." *Trends Immunol* **31**(7): 270-277.
- Spits, H., F. Couwenberg, A. Q. Bakker, K. Weijer and C. H. Uittenbogaart (2000). "Id2 and Id3 inhibit development of CD34(+) stem cells into predendritic cell (pre-DC)2 but not into pre-DC1. Evidence for a lymphoid origin of pre-DC2." *J Exp Med* **192**(12): 1775-1784.
- Steinman, R. M. and Z. A. Cohn (1973). "Identification of a novel cell type in peripheral lymphoid organs of mice. I. Morphology, quantitation, tissue distribution." *J Exp Med* **137**(5): 1142-1162.
- Suzuki, S., K. Honma, T. Matsuyama, K. Suzuki, K. Toriyama, I. Akitoyo, K. Yamamoto, T. Suematsu, M. Nakamura, K. Yui and A. Kumatori (2004). "Critical roles of interferon regulatory factor 4 in CD11bhighCD8alpha-dendritic cell development." *Proc Natl Acad Sci U S A* **101**(24): 8981-8986.

- 
- Swiecki, M., S. Gilfillan, W. Vermi, Y. Wang and M. Colonna (2010). "Plasmacytoid dendritic cell ablation impacts early interferon responses and antiviral NK and CD8(+) T cell accrual." *Immunity* **33**(6): 955-966.
- Tai, L. H., M. L. Goulet, S. Belanger, N. Toyama-Sorimachi, N. Fodil-Cornu, S. M. Vidal, A. D. Troke, D. W. McVicar and A. P. Makrigiannis (2008). "Positive regulation of plasmacytoid dendritic cell function via Ly49Q recognition of class I MHC." *J Exp Med* **205**(13): 3187-3199.
- Tamoutounour, S., S. Henri, H. Lelouard, B. de Bovis, C. de Haar, C. J. van der Woude, A. M. Woltman, Y. Reyal, D. Bonnet, D. Sichien, C. C. Bain, A. M. Mowat, C. Reis e Sousa, L. F. Poulin, B. Malissen and M. Guillemins (2012). "CD64 distinguishes macrophages from dendritic cells in the gut and reveals the Th1-inducing role of mesenteric lymph node macrophages during colitis." *Eur J Immunol* **42**(12): 3150-3166.
- Tamura, T., P. Taylor, K. Yamaoka, H. J. Kong, H. Tsujimura, J. J. O'Shea, H. Singh and K. Ozato (2005). "IFN regulatory factor-4 and -8 govern dendritic cell subset development and their functional diversity." *J Immunol* **174**(5): 2573-2581.
- Thalheimer, F. B., S. Wingert, P. De Giacomo, N. Haetscher, M. Rehage, B. Brill, F. J. Theis, L. Hennighausen, T. Schroeder and M. A. Rieger (2014). "Cytokine-regulated GADD45G induces differentiation and lineage selection in hematopoietic stem cells." *Stem Cell Reports* **3**(1): 34-43.
- Tsujimura, H., T. Tamura and K. Ozato (2003). "Cutting edge: IFN consensus sequence binding protein/IFN regulatory factor 8 drives the development of type I IFN-producing plasmacytoid dendritic cells." *J Immunol* **170**(3): 1131-1135.
- Varol, C., A. Vallon-Eberhard, E. Elinav, T. Aycheh, Y. Shapira, H. Luche, H. J. Fehling, W. D. Hardt, G. Shakhar and S. Jung (2009). "Intestinal lamina propria dendritic cell subsets have different origin and functions." *Immunity* **31**(3): 502-512.
- Walter, D., A. Lier, A. Geiselhart, F. B. Thalheimer, S. Huntscha, M. C. Sobotta, B. Moehle, D. Brocks, I. Bayindir, P. Kaschnig, K. Muedder, C. Klein, A. Jauch, T. Schroeder, H. Geiger, T. P. Dick, T. Holland-Letz, P. Schmezer, S. W. Lane, M. A. Rieger, M. A. Essers, D. A. Williams, A. Trumpp and M. D. Milsom (2015). "Exit from dormancy provokes DNA-damage-induced attrition in haematopoietic stem cells." *Nature* **520**(7548): 549-552.
- Waskow, C., K. Liu, G. Darrasse-Jeze, P. Guernonprez, F. Ginhoux, M. Merad, T. Shengelia, K. Yao and M. Nussenzweig (2008). "The receptor tyrosine kinase Flt3 is required for dendritic cell development in peripheral lymphoid tissues." *Nat Immunol* **9**(6): 676-683.
- Wolins, N. E., B. K. Quaynor, J. R. Skinner, A. Tzekov, C. Park, K. Choi and P. E. Bickel (2006). "OP9 mouse stromal cells rapidly differentiate into adipocytes: characterization of a useful new model of adipogenesis." *J Lipid Res* **47**(2): 450-460.
- Young, L. J., N. S. Wilson, P. Schnorrer, A. Proietto, T. ten Broeke, Y. Matsuki, A. M. Mount, G. T. Belz, M. O'Keefe, M. Ohmura-Hoshino, S. Ishido, W. Stoorvogel, W. R. Heath, K. Shortman and J. A. Villadangos (2008). "Differential MHC class II synthesis and ubiquitination confers distinct antigen-presenting properties on conventional and plasmacytoid dendritic cells." *Nat Immunol* **9**(11): 1244-1252.

## ACKNOWLEDGEMENT

First and foremost, I would like to thank **Prof. Dr. Anne Krug** for giving me the opportunity to conduct my PhD thesis in her laboratory. I would like to express my sincere gratitude for her constant support and guidance for the past 3 years. I'm grateful to her for all the time that she spent with me to discuss my project day and night, encouraging me to speak out as a woman scientist and for excellent technical possibilities that she provided throughout my work.

I would like to thank **Lynette Henkel** and **Prof. Dr. Matthias Schiemann** for their extraordinary efforts in assisting most difficult and crucial parts of my PhD work with their technical support and smile which never fades.

I would like to thank my excellent collaborators in Basel, D-BSSE, **Dr. Max Endeke and Prof. Dr. Timm Schroeder** for collaboration regarding live cell imaging experiments, especially **Max** for supporting this project and making all my TTT wishes come true. I would like to express my deep gratitude to **Christopher Sie**, for his excellent efforts in collaboration regarding EAE experiments, all the fruitful discussions we had and not just being a colleague but also a very good friend to me. I would like to also thank **Prof. Dr. Thomas Korn** for his collaboration and fruitful discussion of the project. I also would like to thank **Dr. Susanne Stutte** for her efforts in assisting confocal imaging experiments.

I would like to thank all the members, Katha, Alex, Ana-Marija, Yvonne, and former members; Silvia, Mona and Livia, of AG Krug for assisting me in the laboratory at any time when I needed it, for their fair criticism and their kind and every-day support. Very special thanks to **Anamarija Markota**, for being not just a great colleague but also for supporting me in long experiments, for very valuable advice that she gave and her every day smile. I am also truly glad to **Andrea Musumeci** and **Lisa Jandl** for their support, their friendship and being available whenever I had something to discuss and for showing always the bright side of science.

I'm also thankful to **Dr. Katrin Offe** and **Desislava Zlatanova** for their extraordinary support in administrative issues.

I want to say very special thanks to **René Rüttgers**, being right next to me whenever I need, for being extremely patience, for believing in me and making Munich "home" for me.

Lastly, I would like to thank to my parents, **Fusun Dursun** and **Adnan Dursun**, my first teachers in life, who gave me my wings and taught how to fly far away. Without your love and every day support, this work would never have been possible.

# CURRICULUM VITAE

## EZGI DURSUN

### Personal details

Date of birth: 29.01.1985

Place of birth: Istanbul, Turkey

Nationality: Turkish

Adress: Clemensstraße 29, 80803, München

### Scientific Education

- |                   |  |
|-------------------|--|
| Since 5/2012      | PhD Thesis in the laboratory of Prof. Dr. Anne Krug,<br>II.Medical Department, Klinikum Rechts der Isar<br>Technical University Munich, Germany          |
| 10/2011 - 4/2012  | Research assistant in the laboratory of<br>PD. Dr. rer.nat Harald Lahm<br>Department of Experimental Surgery<br>German Hearth Center, Munich, Germany    |
| 09/2007 - 09/2010 | Master studies, in the laboratory of Prof. Dr. Isil Tekmen<br>Histology & Embryology Department<br>Dokuz Eylul University Medical Faculty, Izmir, Turkey |
| 09/2003 - 06/2007 | Study of Biology, Uludag University, Bursa, Turkey   |

### Education

- |           |                                 |
|-----------|---------------------------------|
| 1991-1996 | Primary School, Izmir, Turkey   |
| 1996-1999 | Secondary School, Izmir, Turkey |
| 1999-2003 | High School, Izmir, Turkey      |

### Publications

Keles, D., B. Arslan, C. Terzi, I. Tekmen, E. Dursun, O. Altungoz and G. Oktay (2014).  
"Expression and activity levels of matrix metalloproteinase-7 and in situ localization of  
caseinolytic activity in colorectal cancer." Clin Biochem 47(13-14): 1265-1271.

**Congress abstracts**

**13<sup>th</sup> International Congress on Dendritic Cells, Tours, Loire Valley, France (14.08.2014-18.08.2014)**

Dursun Ezgi, Endele Max, Musumeci Andrea, Schroeder Timm, Krug Anne. Common DC progenitor differentiation characterized at the single cell level (poster).

**4<sup>th</sup> International Workshop on plasmacytoid Dendritic Dells, Institute Pasteur, Paris, France (9.12.2013 - 10.12.2013)**

Dursun Ezgi, Endele Max, Musumeci Andrea, Schroeder Timm, Krug Anne. Common DC progenitor commitment to the plasmacytoid DC lineage at the single cell level (poster)

**Travel grants**

4<sup>th</sup> International Workshop on plasmacytoid Dendritic Cells, Paris, France

13<sup>th</sup> Interational Congress on Dendritic Cells, Tours, France